CRCLEME
Cooperative Research Centre for
Landscape Evolution & Mineral Exploration

CSIRO
EXPLORATION AND MINING

AMIRA
Australian Mineral Industries Research Association Limited ACN 004 448 266

OPEN FILE REPORT SERIES

THE DISTRIBUTION OF GOLD AND OTHER ELEMENTS IN SOILS AND VEGETATION AT PANGLO, WESTERN AUSTRALIA

M.J. Lintern and K.M. Scott

CRC LEME OPEN FILE REPORT 44

October 1998

(CSIRO Division of Exploration Geoscience Report 129R, 1990
Second impression, 1998)

AMIRA
Australian Mineral Industries Research Association Limited ACN 004 448 266

CRCLEME
Cooperative Research Centre for Landscape Evolution & Mineral Exploration

CSIRO
EXPLORATION AND MINING

THE DISTRIBUTION OF GOLD AND OTHER ELEMENTS IN SOIL AND VEGETATION AT PANGLO, WESTERN AUSTRALIA

M.J. Lintern and K.M. Scott

CRC LEME OPEN FILE REPORT 44

October 1998

(CSIRO Division of Exploration Geoscience Report 129R, 1990.
Second impression 1998))

CRC LEME is an unincorporated joint venture between The Australian National University,
University of Canberra, Australian Geological Survey Organisation and CSIRO Exploration and Mining
Headquarters: CRC LEME c/o CSIRO Exploration and Mining, Private Bag, PO Wembley, Western Australia, 6014

RESEARCH ARISING FROM CSIRO/AMIRA REGOLITH GEOCHEMISTRY PROJECTS 1987-1993

In 1987, CSIRO commenced a series of multi-client research projects in regolith geology and geochemistry which were sponsored by companies in the Australian mining industry, through the Australian Mineral Industries Research Association Limited (AMIRA). The initial research program, "Exploration for concealed gold deposits, Yilgarn Block, Western Australia" (1987-1993) had the aim of developing improved geological, geochemical and geophysical methods for mineral exploration that would facilitate the location of blind, buried or deeply weathered gold deposits. The program included the following projects:

P240: Laterite geochemistry for detecting concealed mineral deposits (1987-1991). Leader: Dr R.E. Smith.
Its scope was development of methods for sampling and interpretation of multi-element laterite geochemistry data and application of multi-element techniques to gold and polymetallic mineral exploration in weathered terrain. The project emphasised viewing laterite geochemical dispersion patterns in their regolith-landform context at local and district scales. It was supported by 30 companies.

P241: Gold and associated elements in the regolith - dispersion processes and implications for exploration (1987-1991). Leader: Dr C.R.M. Butt.
The project investigated the distribution of ore and indicator elements in the regolith. It included studies of the mineralogical and geochemical characteristics of weathered ore deposits and wall rocks, and the chemical controls on element dispersion and concentration during regolith evolution. This was to increase the effectiveness of geochemical exploration in weathered terrain through improved understanding of weathering processes. It was supported by 26 companies.

These projects represented "an opportunity for the mineral industry to participate in a multi-disciplinary program of geoscience research aimed at developing new geological, geochemical and geophysical methods for exploration in deeply weathered Archaean terrains". This initiative recognised the unique opportunities, created by exploration and open-cut mining, to conduct detailed studies of the weathered zone, with particular emphasis on the near-surface expression of gold mineralisation. The skills of existing and specially recruited research staff from the Floreat Park and North Ryde laboratories (of the then Divisions of Minerals and Geochemistry, and Mineral Physics and Mineralogy, subsequently Exploration Geoscience and later Exploration and Mining) were integrated to form a task force with expertise in geology, mineralogy, geochemistry and geophysics. Several staff participated in more than one project. Following completion of the original projects, two continuation projects were developed.

P240A: Geochemical exploration in complex lateritic environments of the Yilgarn Craton, Western Australia (1991-1993). Leaders: Drs R.E. Smith and R.R. Anand.
The approach of viewing geochemical dispersion within a well-controlled and well-understood regolith-landform and bedrock framework at detailed and district scales continued. In this extension, focus was particularly on areas of transported cover and on more complex lateritic environments typified by the Kalgoorlie regional study. This was supported by 17 companies.

P241A: Gold and associated elements in the regolith - dispersion processes and implications for exploration. Leader: Dr. C.R.M. Butt.
The significance of gold mobilisation under present-day conditions, particularly the important relationship with pedogenic carbonate, was investigated further. In addition, attention was focussed on the recognition of primary lithologies from their weathered equivalents. This project was supported by 14 companies.

Although the confidentiality periods of the research reports have expired, the last in December 1994, they have not been made public until now. Publishing the reports through the CRC LEME Report Series is seen as an appropriate means of doing this. By making available the results of the research and the authors' interpretations, it is hoped that the reports will provide source data for future research and be useful for teaching. CRC LEME acknowledges the Australian Mineral Industries Research Association and CSIRO Division of Exploration and Mining for authorisation to publish these reports. It is intended that publication of the reports will be a substantial additional factor in transferring technology to aid the Australian Mineral Industry.

This report (CRC LEME Open File Report 44) is a Second impression (second printing) of CSIRO, Division of Exploration Geoscience Restricted Report 129R, first issued in 1990, which formed part of the CSIRO/AMIRA Project P241.

Copies of this publication can be obtained from:
The Publication Officer, c/- CRC LEME, CSIRO Exploration and Mining, PMB, Wembley, WA 6014, Australia. Information on other publications in this series may be obtained from the above or from http://leme.anu.edu.au/

Cataloguing-in-Publication:
Lintern, M.J.
The distribution of gold and other elements in soils and vegetation at Panglo, Western Australia
ISBN 0 642 28208 0
1. Soils 2. Weathering 3. Gold - Western Australia 4. Geochemistry.
I. Scott, K.M. II. Title
CRC LEME Open File Report 44.
ISSN 1329-4768

Preface

The CSIRO-AMIRA project "Exploration for Concealed Gold Deposits, Yilgarn Block, Western Australia" has as its overall aim the development of improved geological, geochemical and geophysical methods for mineral exploration that will facilitate the location of blind, concealed or deeply weathered gold deposits. This Report presents results of research conducted as part of Module 2 of this project (AMIRA Project 241): "Gold and Associated Elements in the Regolith - Dispersion Processes and Implications for Exploration".

The objectives of this module are, *inter alia*, to suggest improvements in techniques of sampling and data interpretation for gold exploration, and to increase knowledge of the properties and genesis of the regolith. This report describes the geochemistry of soils and vegetation of the Panglo gold deposit north of Kalgoorlie. The results contribute strongly to the objectives of the module by (i) providing further evidence (already demonstrated at Mt. Hope) of the strong association between Au and the alkaline earth metals, (ii) examining the distribution of other geochemical components of the regolith, (iii) sampling, analysing and interpreting geochemical results of vegetation and (iv) studying electron micrographs to elucidate the role of pedogenic carbonates in near-surface weathering processes. The work is of major significance to gold exploration as it has demonstrated that gold is preferentially concentrated in the soil carbonate horizon, even when the mineralization is concealed by leached saprolites and barren transported overburden. The research has also established that the phenomenon is of regional significance, having previously been documented at Mt. Hope, 250 km to the south-west. The principal conclusion is that it is essential to include the carbonate horizon, where present, in any soil sampling programme for gold exploration.

C.R.M. Butt,
Project Leader.
October, 1990.

Abstract

Shallow auger, surface, profile, trench, grab and vegetation samples were taken along two traverses at the Panglo gold deposit about 30 kilometres NNW of Kalgoorlie, Western Australia. Landscape and soil features were photographed, described and used to interpret geochemical information. The relationship between the geochemistry of soils and vegetation was explored with particular reference to Au. Detailed examination of weathering surface material was performed using SEM (scanning electron microscopy) techniques.

The results establish a widespread and strong association between Au and pedogenic carbonate. The most significant result was the presence of Au (up to several hundred ppb) in pedogenic carbonate occurring in transported overburden above mineralization. There was also a weak association between Au found in vegetation and that found in the soils. Other results indicated the strong association between landscape features, geochemistry and vegetation type. SEM studies revealed the importance of calcite in near-surface weathering processes.

The study demonstrates the importance of locating and sampling the pedogenic carbonate horizon if present. Augering and near-surface sampling appear to be the most successful exploration techniques whereas trench sampling may falsely locate or overlook the soil anomaly altogether. Vegetation sampling alone cannot be used to locate mineralization.

CONTENTS

4.METHODS

5.RESULTS and DISCUSSION

6.DISCUSSIONS and CONCLUSIONS

The Distribution of Gold and Other Elements of Soils and Vegetation at Panglo, Western Australia.

M.J. Lintern and K.M. Scott.

1. Introduction.

The Panglo gold deposit is situated approximately 30km kilometres NNW of Kalgoorlie between the Kalgoorlie-Leonora railway and adjacent Kalgoorlie-Meekatharra highway (Figure 1).

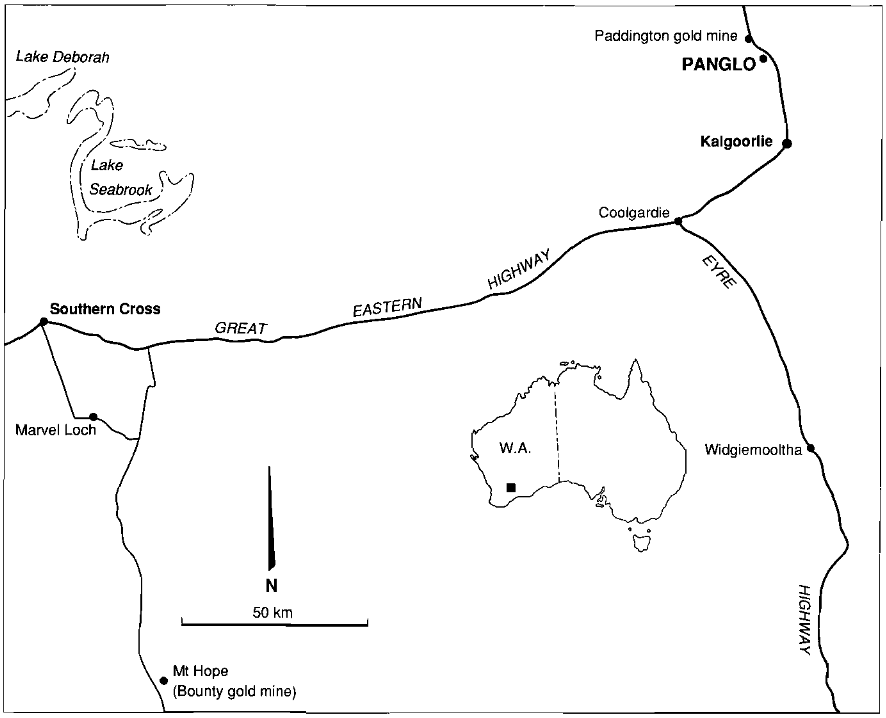

Figure 1: Map showing location of the Panglo deposit and the Bounty gold mine.

It was discovered in late 1986 by Pancontinental Mining Company Limited following routine soil sampling south of the Paddington mine. In 1989, a large test pit was excavated as part of mining evaluation procedures. The deposit comprises a mineable resource of 1 mt at 3.6 gpt and is due to start production shortly.

At the commencement of the study, the surface environment was relatively free from potential contamination and provided a favourable site for a detailed examination of the distribution of gold in soils.

The presence, at Panglo, of surface pedogenic carbonate is of particular importance. The studies at Mt Hope, situated over 250km to the south-west of Panglo (Figure 1), had indicated a strong association between soil carbonate and Au (Lintern, 1989). Demonstration of the same association in a different area has considerable implications for exploration as it overwhelmingly suggests that it is a regional phenomenon.

2. Scope of study.

The present study at Panglo includes a brief description of the relationships between the landscape, vegetation, soils and geology. A geochemical approach is used to relate these different aspects of the deposit to the weathering process. Particular attention is paid to soil geochemistry and mineralogy, and biogeochemistry on two traverses across supergene mineralization.

3. Site Description.

The Panglo deposit is situated to the west of an area of some salt scalding, a prominent surface feature that is clearly defined in aerial photographs by its light colour and diminished vegetation (Figure 2). The deposit itself is situated partly within, but mainly adjacent to, a broad, poorly-defined, highly saline ephemeral drainage channel. Towards the southern end of the mineralized zone, at 3700N, the drainage narrows to a relatively flat channel, approximately 100m wide confined by low steep slopes. The gradient of the drainage channel decreases from north to south (Figure 2).

There is little outcrop over mineralization but mineralized lithorelics of various sizes (ranging up to several centimetres) occur in a matrix of heavy clays within a few centimetres of the surface. The test pit reveals that bleached saprolitic clays are a prominent feature of the weathering profile. The depth of weathering is in excess of 60m. Economic grades of mineralization occur as a supergene deposit at a depth of about 40m, hosted by weathered shales and mafic volcanics within an 800m wide shear zone. Drilling indicates that the deposit is orientated SSW-NNE. Bedrock sources of gold mineralization have not been determined to date.

To the west and south-west of mineralization, a palaeodrainage of presumed Tertiary age has been defined (R. Howard, pers comm). It partially encroaches over the southern limit of mineralization, where its presence is indicated near the surface by loosely cemented lateritic gravels.

Soil development and character over the deposit and adjacent areas is broadly determined by geomorphology but locally determined by geology. In the drainage channels and broad flats, clay-rich soils dominate; on higher ground, soils are usually gravelly. Soils are often thin (generally <0.5m) and locally absent over outcropping barren undifferentiated sediments and siltstone/shale units to the west of mineralization. Generally, over mineralization, soils can be grouped into two classes: (i) the gravelly soils and (ii) the clay-rich soils.

(i) The gravelly soils occur in higher areas of the landscape and include those over the known southern limits of mineralization. They include those found in the palaeochannel. The soils consist of an organic-rich surface horizon containing Fe-rich gravels in a matrix of sandy material. Beneath this, the soil is characterized by unconsolidated, Fe-rich, rounded to sub-rounded ferruginous nodules varying in size from a few millimetres to several centimetres in diameter in a sandy to loamy matrix. Saprolite, at or near the surface in certain areas, limits soil depth to a few centimetres. Carbonate development occurs near the surface and continues to several tens of centimetres. Carbonate occurs as a) friable fragments and thin veneers in unconsolidated Fe-rich material and b) as coatings, up to several millimetres thick, on consolidated near-surface saprolite.

Figure 2: Aerial photograph with plan of the study area.

Air photograph probably taken by Kevron Air Surveys 15th Dec 1986, Photo 9115, published with permission of Goldfields Exploration Pty Ltd.

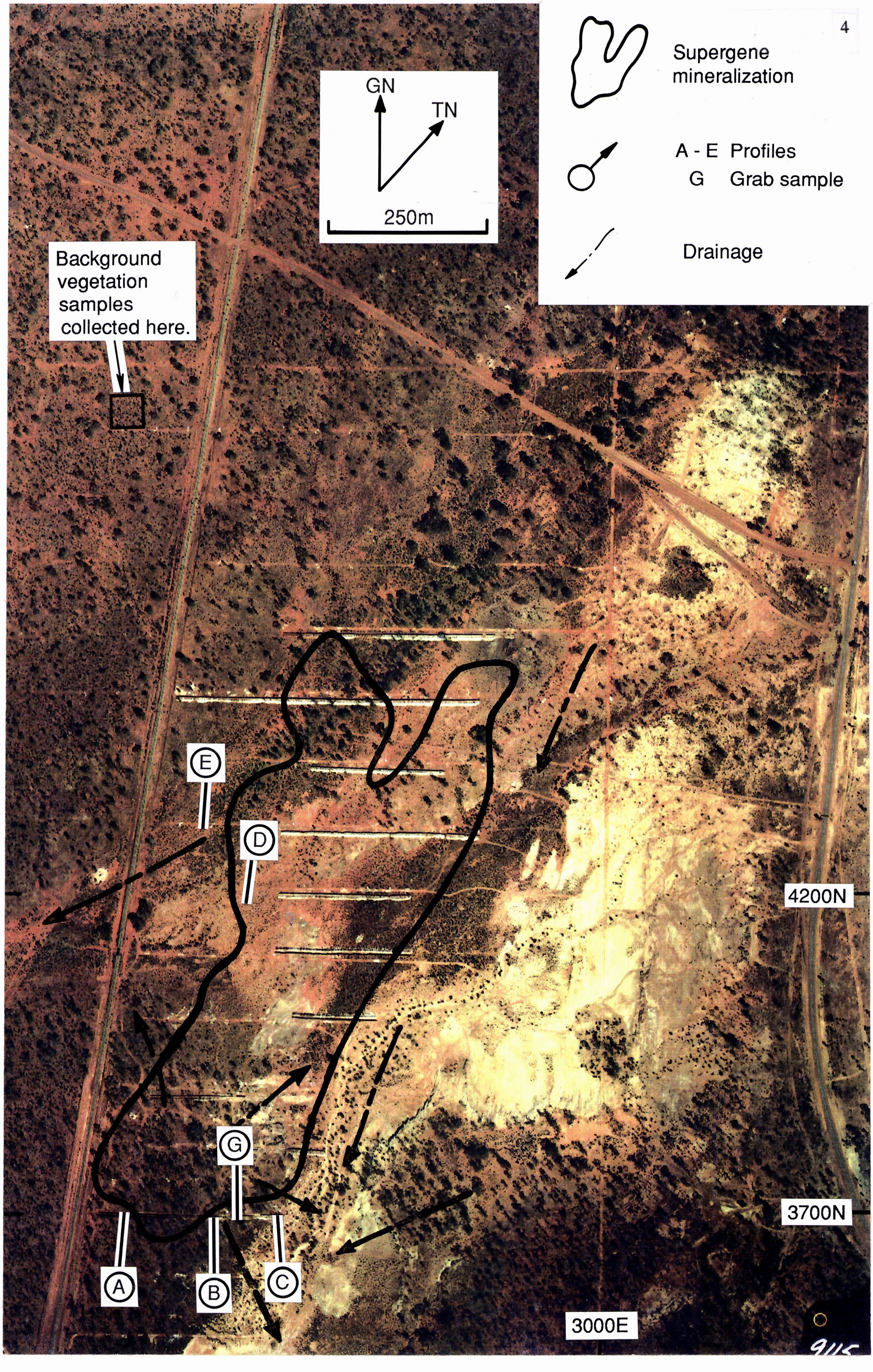
Supergene mineralization
A - E Profiles
G Grab sample
Drainage
GN
TN
250m
Background vegetation samples collected here.
E
D
G
A
B
C
4200N
3700N
3000E

9115

(ii) The clay-rich soils are dominant in the broad valley flats of the northern and central sections over the mineralized zone. They consist of a veneer of sand-rich material overlying pale grey to yellow fine homogeneous clays. Blocks of weathered rock are common within the soil profile and are either pale (clay-rich) or red (Fe-rich) coloured. Carbonate occurs within the profile as friable aggregates and veneers.

The diversity and abundance of the vegetation is determined by soil characteristics. Salt- and drought-tolerant species e.g. *Maeriana* spp. and *Atriplex* spp. (<0.5m in height) with minor *Eremophila* spp. (up to 2m) dominate the clay-rich soils of the broad valley floor to form an open heathland community. Where soils are thin, the vegetation is reduced to sporadic occurrences and the total biomass is low. Tall *Eucalyptus* spp. trees (up to 20m) with an under storey of *Eremophila* spp. (1-2m) form a medium dense woodland community over the gravelly soils. There is a sharp transition between the two vegetation communities reflecting the different soil types, although individual examples of plant species occur sporadically in both communities.

Figure 3: Photographs of the study area (overleaf).

a) Traverse 3700N looking east across the drainage channel.

b) Traverse 4200N looking west from 3000E across the drainage flat.

c) Traverse 3700N looking west from the weathered rock outcrop.

d) Traverse 3700N looking east from Profile A.

e) Large boulder of weathered rock.

f) Profile A.

g) Profile B.

h) Profile C.

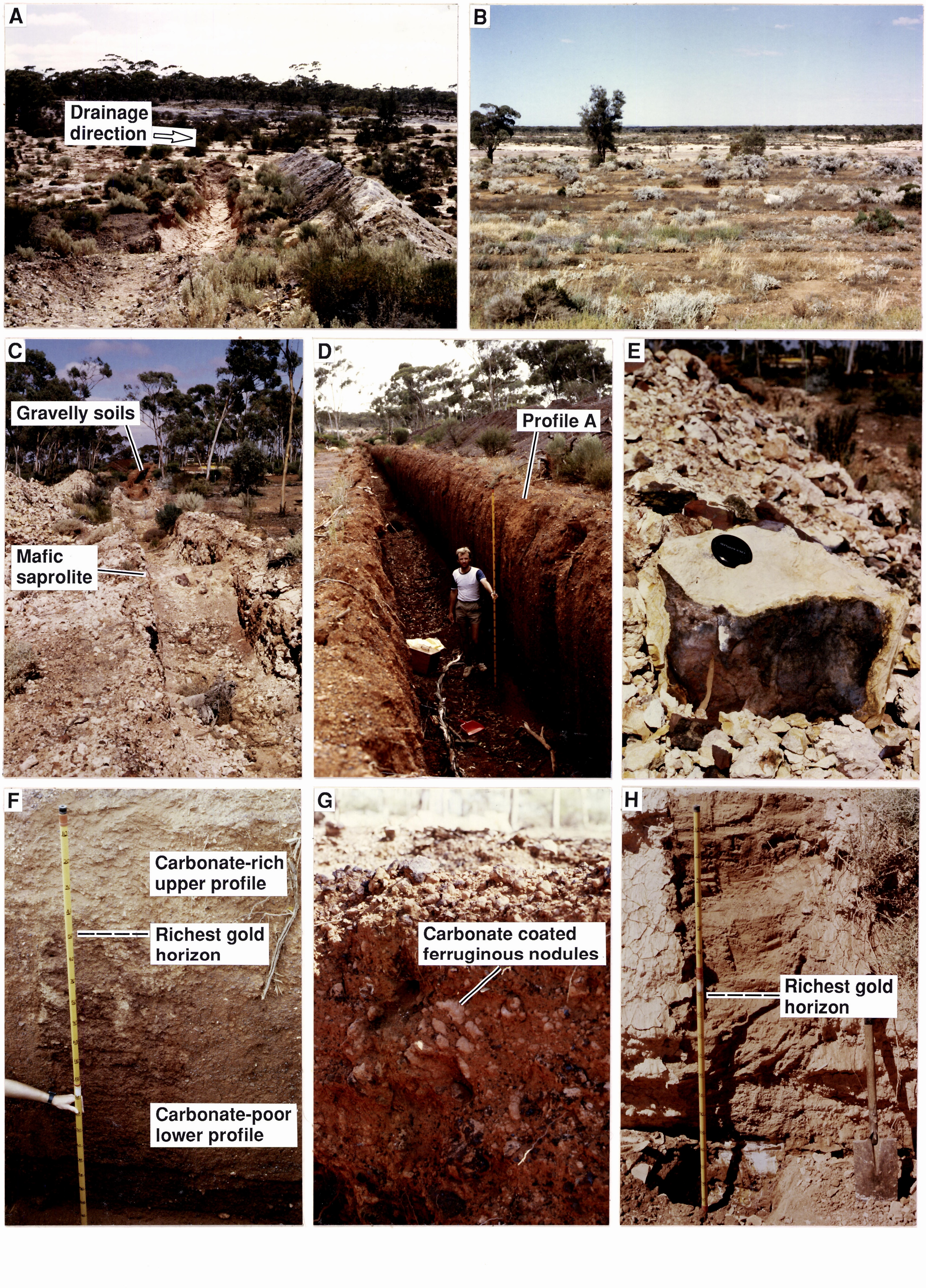
A
Drainage direction
B
C
Gravelly soils
Mafic saprolite
D
Profile A
E
F
Carbonate-rich upper profile
Richest gold horizon
Carbonate-poor lower profile
G
Carbonate coated ferruginous nodules
H
Richest gold horizon

4. Methods.

4.1. Sample collection.

Soil and vegetation samples were collected during winter 1988 and 1989. Pancontinental Ltd. provided surface soil, auger and trench samples for line 3700N and some surface soil samples from line 4200N (Table 1).

Sample Type	Northing sampled	Collected by
Profile	3700 4200 4300	CSIRO
Surface	3700 4200	CSIRO, Pancontinental
Auger	3700	Pancontinental
Trench	3700	Pancontinental
Vegetation	3700 4200 + others	CSIRO
Special		CSIRO

Table 1: Sample types, northings and collection summary.

Sample locations are shown in Figure 2. Lines 3700N and 4200N were chosen as the main sampling sites as they had the following attributes:
(i) Access was provided by trenching .
(ii) They occurred above mineralization.
(iii) Several lithologies and landscape features were represented.
(iv) Different vegetation communities were represented.

4.1.1. Profile.

Profiles were channel sampled in existing trenches and pits. Profiles were first cleaned to remove foreign material and photographed before sampling. Samples were obtained sequentially, from top to bottom, after benching of the profile using a geological hammer and rock chisels (where necessary). Samples were collected into a plastic pan before transferring to polyethylene bags. The benching technique ensured minimal cross-contamination from material higher up in the profile. Composite samples were generally collected over 10cm intervals but were varied according to the type of soil material being sampled.

4.1.2. Surface.

Decaying vegetation and/or foreign material if present were removed from the top 5cm and samples (about 1kg) collected by hand auger to 30cm depth, or refusal, along 3700N, and by hand from the top 10cm along 4200N. Subcropping weathered rock samples were taken from 4200N from about 30cm depth.

4.1.3. Power auger.

Composite auger sampling over 0 to 1.2m (one rod) was carried out using a vehicle-mounted power auger on 3700N.

4.1.4. Trench.

Samples were collected at a set height (about 0.5m or "knee-height") above the base of the trench. The depth of the trench was dependent upon penetration by the earth-moving equipment is thus of considerable importance. Over unconsolidated transported material, the trench is over 2m deep but over the weathered rock penetration was restricted to a few centimetres. The depth of the "knee-height" sampling method relative to the surface, therefore, resulted in different horizons of the soil profile being sampled. The north face of the trench at 3700N was sampled. Profiles in the trench (A, B and C) were sampled as described in 4.1.1 above.

4.1.5. Vegetation.

Vegetation sampling was restricted, where possible, to new growth. Samples were taken of leaves and some stems and broken off by hand or using secateurs. Vegetation samples were collected in plastic bags which were left open, to facilitate drying, before transfer to the laboratory.

4.1.6. Special samples.

Two grab samples were collected from locations near to Profile B for detailed geochemical studies.

4.2. Sample preparation.

Profile, near-surface and auger samples were dried, weighed, homogenized and split on a plastic sheet. Half the sample was bagged for reference and underwent no further treatment. Some near-surface material (500g sub-sample) underwent no further preparation prior to Au analysis by cyanide leaching.

Profile samples containing coarser material were crushed prior to splitting using a hydraulic press mounted with zirconia plates. Other samples containing coarser material (greater than 25 mm) were reduced in size using a Mn-steel jaw crusher. Approximately 50g of the split was incrementally extracted from the sample and ground to a nominal *minus* 75 μm in an agate ring mill. Self-supporting pressed discs were prepared for XRF analysis. Sub-samples were extracted for X-ray diffraction (XRD), inductively coupled plasma (ICP) and atomic absorption spectroscopy (AAS) analysis.

Sub-samples of carbonate and saprolite material from grab samples were obtained by percussion using a hand drill. Sub-samples were selected for polished sections and examination by scanning electron microscopy (SEM).

Vegetation samples, approximately 30g in weight, were placed in a plastic sieve and rinsed to remove soil material. The sample was then dried at 105°C for at least 24 hours to prevent smearing during milling.

The vegetation samples were passed through a four-bladed cross-beater mill twice - firstly without, and secondly with, a 1 mm mesh screen in place to ensure a suitably homogenized and macerated sample for instrumental analysis. Samples required no further preparation for instrumental neutron activation analysis (INAA) but required stepwise ashing up to 600^{o}C for 24 hours prior to other analyses by ICP and graphite furnace AAS. Samples were weighed before and after ashing so that data standardization could be made with the un-ashed samples sent for INAA.

4.3. Sample analysis.

Several analytical methods were used depending upon sample size, detection limits and instrument availability. In consequence, some elements were recorded by different methods. Standards were submitted with samples for each analytical batch to ensure results were consistent throughout the study. Satisfactory agreement was also found on selected elements using different analytical techniques on aliquots of the same sample. Only the most reliable data are reported upon. The instruments and methods used are listed below:

XRF - Pressed discs, prepared by the method of Norrish and Chappell (1977) were analysed for minor and trace elements using a Phillips PW 1200C XRF. Major elements were analysed using fused discs.

ICP - For soils, approximately 250 mg of sample was accurately weighed out and mixed with 1 g of lithium metaborate. The mix was fused at 1000°C in a furnace for one hour and the residue dissolved in 1N nitric acid. The solutions were analysed on either a Labtem or a Hilger E-100 ICP. For vegetation, the ashed sample (dry weight of 10g) was digested in *aqua regia*, diluted and analysed.

OES - 50mg of sample and buffer (LiF) was arced in a graphite anode and analysed by a Hilger Emission Spectrometer. Results are semi-quantitative as no matrix correction was applied.

ICP-MS - Soils were shaken with a solution of 0.2% KCN saturated with $Ca(OH)_2$ in the ratio of 1:2. The bottle, containing the sample and solution, was capped and agitated for a minimum of 24 hours. After standing to allow the clay particles to settle, at least 4mL of solution was collected by pipette and analysed directly for Au after 1:10 dilution at Sheen Laboratories, WA.

ICP-OES - Following mixed acid digestion samples were analysed by Genalysis, WA.

AAS - Samples were either digested in cyanide (CN) as for ICP-MS or by *aqua regia* (AR) and analysed for Au. The graphite furnace attachment was used for all samples.

INAA - Vegetation samples were pressed into discs, and soil and rock samples were accurately weighed (30g) in plastic containers prior to being sent for analysis at Becquerel Laboratories, NSW. Vegetation analysis using INAA was subject to considerable interference of Na on Au, resulting in unacceptably high detection limits. The problem was not resolved and an alternative *aqua regia* sample dissolution / graphite furnace AAS procedure adopted.

XRD - Homogenized powdered samples were packed and irradiated with CuKα radiation at 40kV using a Phillips PW1050 Diffractometer.

4.3.1. Profile.

ICP - SiO_2, TiO_2, Al_2O_3, Na_2O, Fe_2O_3, MgO, CaO, P_2O_5, Ba, Be, Co, and Cr.
XRF - S, Ce, Cu, Ga, Ge, Mn, Mo, Nb, Ni, Pb, Rb, Sr, V, Y, Zn and Zr.
INAA - As, Au (Profiles A, B and C), Br, Sb and W.
AAS - Au (CN, Profiles D and E)
XRD - On selected samples.

4.3.2. Surface.

ICP - Na_2O, Co, Cr, Cu, Ni, Pb (4200N soils), Sc, Sr, V, Y and Zn.
XRF - SiO_2, TiO_2, Al_2O_3, Fe_2O_3, S, MgO, CaO, P_2O_5, K_2O, As, Ba, Pb (4200N rocks) and Zr.
INAA - Au (4200N), Sb and W.
OES - Ag, B, Bi, Ga, Ge, Mo, Sn and Tl.
AAS - Au (CN, uncrushed soils)
XRD - On selected samples.

4.3.3. Auger.

ICP - SiO_2, TiO_2, Al_2O_3, Na_2O, Fe_2O_3, MgO, CaO, Co and Cr.
XRF - S, Ba, Ce, Cu, Mn, Ni, Nb, Pb, Rb, Sr, V, Y, Zn and Zr.
AAS - Au (AR).

4.3.4. Trench.

AAS - Au (AR).
ICP-OES - As.

4.3.5. Vegetation.

ICP - Si, Al, Mg, Ca, Ti, Na, P, Ba, Be, Co, Cr, Cu, Mn, Ni, V and Zr.

INAA - As, Br and Sb.

AAS - Au (AR).

4.3.6. Special.

ICP - SiO_2, Al_2O_3, Fe_2O_3, MgO, CaO, Na_2O, TiO_2, P_2O_5, Ba, Be, Co, Cu, Mn, Ni, V and Zr.

XRF - S, Ce, Ga, Ge, Mo, Nb, Pb, Rb, Sr, Y and Zn.

AAS - Au (CN).

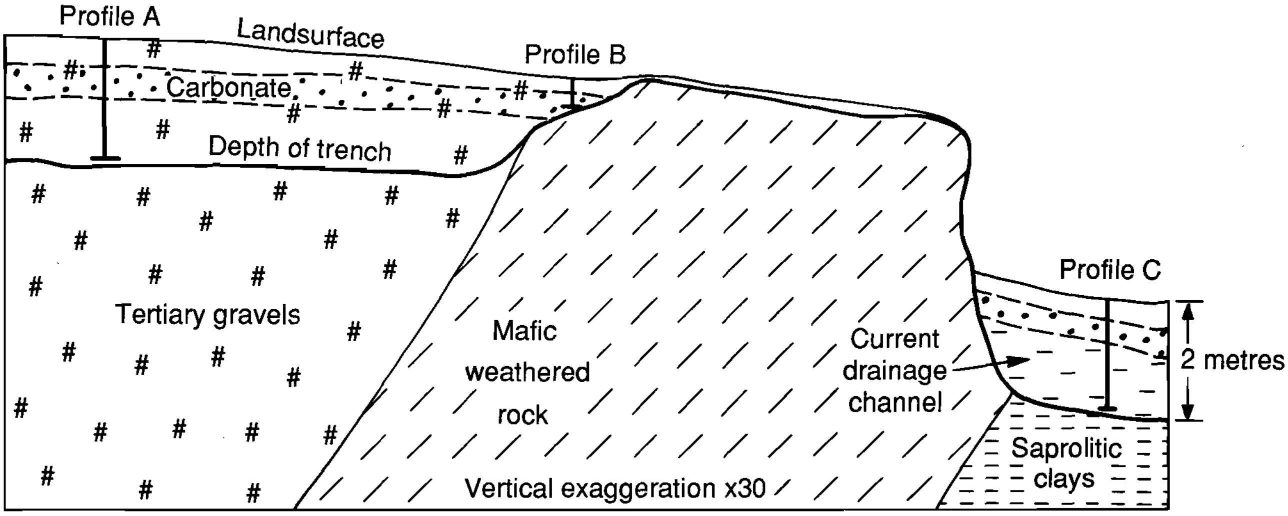

Figure 4: Section through part of the trench on 3700N showing position of profiles and depth of trench.

5. Results and Discussion.

All the profile, near-surface, auger, trench and vegetation geochemical results are plotted and tabulated in the Appendices. The most significant data are discussed below.

5.1. Profile samples.

Profiles were sampled in the three principal geomorphological sites of the trench on traverse 3700N. These were in soils developed on (i) the transported lateritic gravels in the Tertiary palaeochannel (profile A), (ii) the weathered mafic rock (B) and (iii) the current drainage channel (C) (Figure 4). Profiles A and B were taken directly over the southern limits of the known mineralization. An additional two shallow profiles (D and E) were sampled near the central section of supergene mineralization on traverses 4200N and 4300N.

5.1.1. Profile A (2278E, 3700N).

This profile is developed upon transported material associated with a Tertiary palaeochannel. The overburden consists primarily of a sediment of pisoliths and nodules which include fragments of amphibolite. Drilling indicates the overburden to be 10m thick and is comprised of gravels overlying mottled clays. The overburden is situated on clay-rich saprolite derived from mafic volcanics several tens of metres thick. There is some Au enrichment at the boundary between the clay-rich mottles in the palaeochannel and the clay-rich saprolite. Economic grades of Au occur as a supergene deposit within the saprolite at about 40m.

The principal horizons in the profile are as follows:

0-10cm. Red clay-rich sandy loam with ferruginous fragments (up to 20mm). Carbonate present as minor aggregates and coatings. Some organic material.

10-65cm. Sandy loam with gravels. Large amounts of carbonate present as coatings and aggregates progressively increasing then decreasing downwards.

65cm-2.2m. Sandy loam with gravels. Decreasing amounts of carbonate downwards with some present as pendants and lining old root channels. Little, if any, carbonate present in lower parts of the horizon.

The principal minerals present in the profile are hematite, goethite (in the gravels) and quartz. Calcite increases to a maximum at about 0.5m and then decreases. Little XRD-detectable calcite appears below about 1m. Kaolinite, although present, is not abundant. Some halite is present towards the base of the profile.

Near-surface material is rich in Ti, Fe, Mg and Ca, which are probably associated with the coarser material. Below this, Ca concentrations increase and are associated with the calcite. There appears to be an antipathetic relationship between Ca and Fe (Figure 5b) suggesting that calcite has been introduced at a later stage and has diluted the concentration of Fe minerals.

There is a very strong association between Au and the alkaline earth metals Ca, Mg and Sr (Figure 5a) throughout the profile. The lowest concentrations occur at the base of the soil profile (Figure 5b; Appendix 1). Peak concentrations of Au (0.26 ppm) and the alkaline earths (e.g. 16% CaO) occur at 45cm depth.

At the surface, As, Ce, Cr, Cu, Mn, Pb, Rb, Sb, Sr, V, W, Y, Zn and Zr amounts are high and are probably associated with the Mg, Ca, Fe and zircon minerals. Throughout the profile, Fe oxides appear to control the distributions of Ti, Al, As, Cr, Ga, Pb, Sb and V, and, to a lesser extent, with Y and Zr between 0.6m and 1.2m (Appendix 1). Concentrations of these elements are comparatively poor (especially Fe) when Ca contents are high and are consistent with the proposed dilution effect caused by the introduction of carbonate (Figure 5b).

Sulphur, Br and Na concentrations increase with depth (Appendix 1) particularly below about 1.6m. This may be due to continued evaporation of brackish drainage water that has flowed into the trench. Alternatively, the high salt content may be related to the very saline groundwater which occurs at about 10m depth.

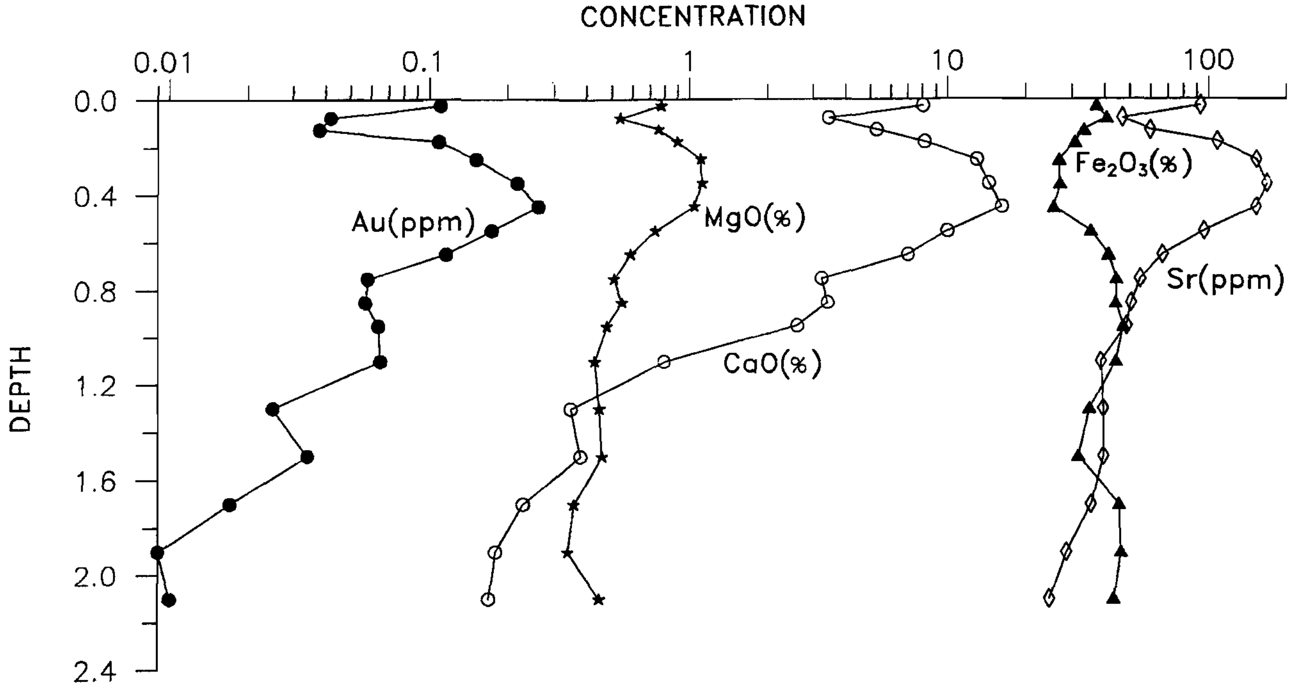

Figure 5a: Distribution of CaO, MgO, Sr and Au in Profile A.

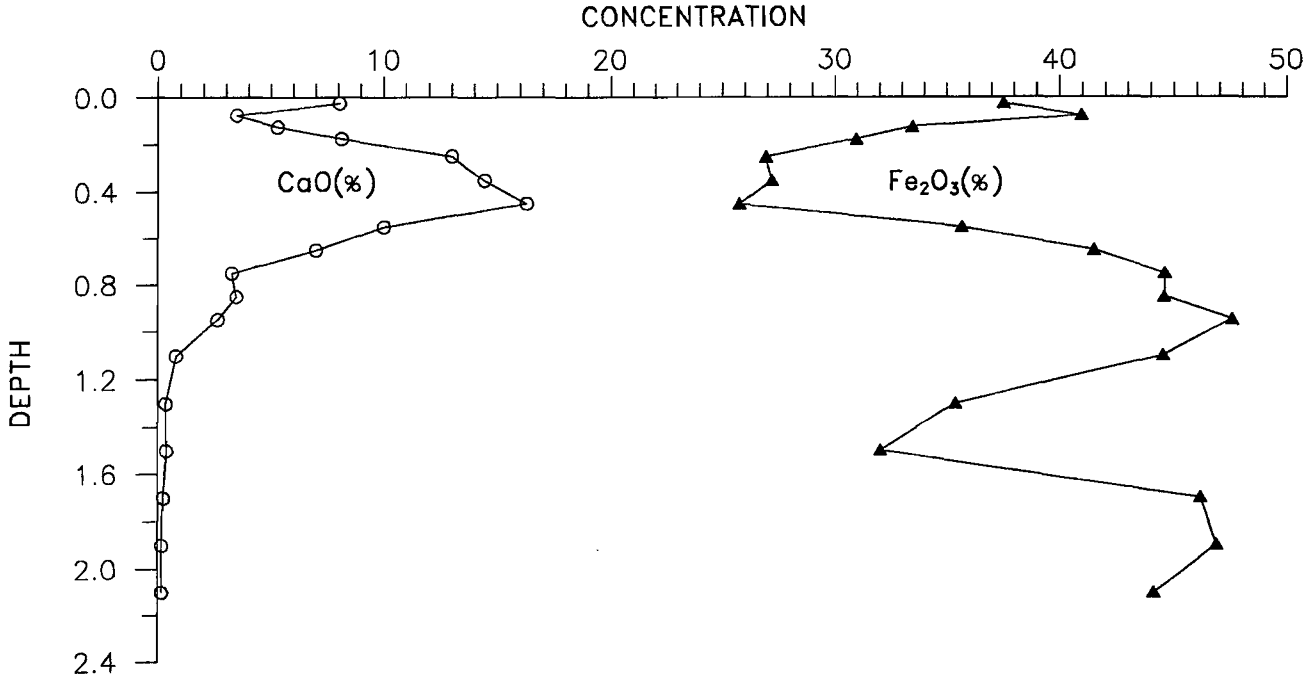

Figure 5b: Distribution of Fe_2O_3 and CaO in Profile A.

5.1.2. Profile B (2375E, 3700N).

This part of the trench is characterized by the presence of outcropping weathered mafic volcanics. The profile consists of a thin, poorly developed soil overlying ferruginous saprolitic fragments of Fe-rich nodules partially cemented by carbonate. Indurated, weathered mafic volcanics continue with depth. The zones of Au mineralization are as for Profile A.

The principal horizons in the profile are as follows:

0-5cm. Thin sandy soil with large quantities of ferruginous lithorelics. Carbonate present as coatings, aggregates and separated veneers. Some organic material is present.

5-80cm. Sub-rounded and angular cobbles of ferruginous lithorelics whose size and degree of induration increases with depth to become massive boulders (>10cm) of weathered rock at the bottom of the profile. Carbonate present as matrix, aggregates and coatings throughout the profile but becomes less abundant with depth.

The principal minerals present in the profile are hematite and goethite with some calcite and quartz. Hematite and goethite tend to increase in concentration down the profile while calcite decreases. The profile is kaolinite poor.

The relative influence of weathered mafic volcanic rocks and introduced carbonate are reflected in the subtle antipathetic relationship between Fe and Ca concentrations (Figure 6). Close examination of the ferruginous material indicates that any Ca present occurs as coatings or in cracks (see Section 5.6.3). The emplacement of calcite within the matrix and cracks is consistent with the late stage introduction noted in Profile A.

The distribution of Au shows a tendency to decrease down the profile and, on this evidence alone, is seen to be weakly related to the carbonate distribution (Figure 6). Maximum concentrations of Au (about 0.13 ppm) occur at about 0.5m and occur with CaO concentrations of about 9%. There is, however, a very strong association between Ca and Au. This is demonstrated by close examination of the special samples taken from this area: see section 5.6.3.

Interpretation of minor and trace element distributions in this profile is primarily determined by the distinction made between the Fe oxide and the calcite (Ca) phases and less so with Na and Si. Thus sympathetic associations are found with (i) As, Cu and V, and Fe, (ii) Mg, Pb and Sr, and Ca, (iii) Br and Na and (iv) Ti and Zr, and Si (Appendix 2). Many minor and trace elements, e.g. Ce, Nb and Rb show no distinct trends in distribution in the soil profile (Appendix 2).

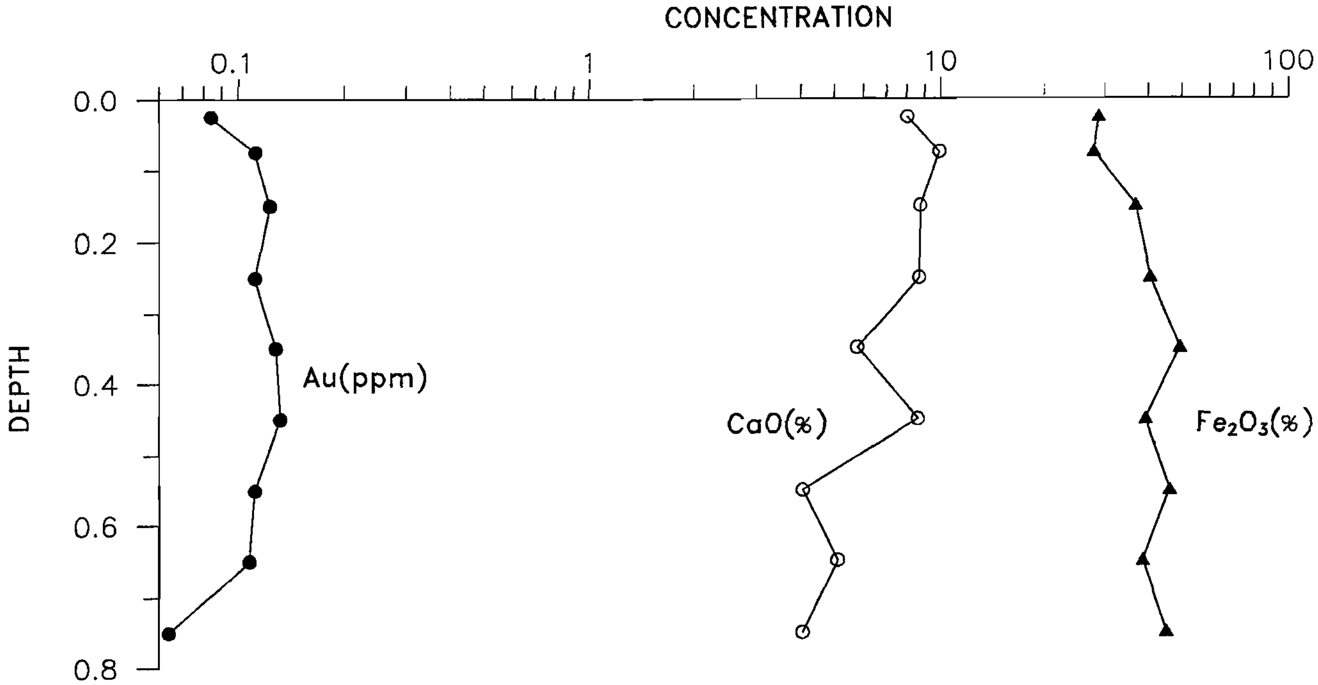

Figure 6: Geochemistry of Fe_2O_3, CaO and Au in Profile B.

5.1.3. Profile C (2505E, 3700N).

This profile is developed in the current drainage channel above unmineralized shales. It is dominated by considerable quantities of transported clay minerals and quartz. The boundary of the transported horizon which is near the base of the trench, is marked by the presence of clay-rich saprolite derived from underlying shales.

The principal horizons are as follows:

0-20cm. Clay-rich sand with appreciable quantities of ferruginous, siliceous and carbonate fragments and little organic material present.

20-60cm. Clay-rich sand with some carbonate and other coarse sized fragments present.

60-90cm. Mainly clay-rich sand with some present as friable aggregates. Minor quantities of coarse sized material present.

90-1.6m. Horizon dominated by coarse angular quartz with some finer sub-rounded quartz fragments. Some coarse lithorelics have similarities with the mafic volcanics found in Profile B.

1.6-1.8m. Yellow, grey and red clay-rich sand with some layered mica-rich nodules present. Little, if any, coarse quartz or ferruginous fragments present.

Calcite is restricted, in the upper part of the profile, to occasional small friable aggregates whose structure suggests they are derived from the calcite coating the adjacent mafic volcanics e.g. those found in Profile B. Goethite and hematite are associated with ferruginous fragments throughout the profile. The fragments present in the upper part of the profile also show similarities with the mafic volcanics of Profile B. Considerable quantities of quartz are present as angular detrital fragments (up to 5mm in length) that are especially in the lower parts of the profile immediately above the clay-rich saprolite. Clay minerals are present as kaolinite; muscovite increases in abundance at the base of the profile. Calcium and Mg decrease markedly down the profile and are associated with calcite and fragments of mafic volcanic rocks. Aluminium concentrations are closely related to the distribution of the clay minerals. Silicon contents are high throughout the profile but peak near the base where the volume of quartz fragments increases. Iron concentrations are low compared with Profiles A and B.

Gold distribution is predominantly associated with the fine (<0.2mm) fraction (Appendix 7). There may be a weak association between Au and Ca (Au = 0.035 ppm, CaO = 0.82 %) in the upper part of the profile (Figure 7) but the highest Au concentration (0.075 ppm) occurs in the fine fraction associated with kaolinite and muscovite.

Sodium, Br, Ga, Mo, Nb, Rb, Sb, Sr and Zr distributions are closely associated with Al. Their concentrations tend to be high at about 0.5m, low at 1.3m, before peaking in concentration at the bottom of the profile (1.7m). The elements are probably associated with cation-exchange or substitution sites on muscovite. Sulphur, Co, Mn, Ni and Zn abundances decrease down the profile and may be associated with more than one soil phase e.g. calcite, barite or organic matter.

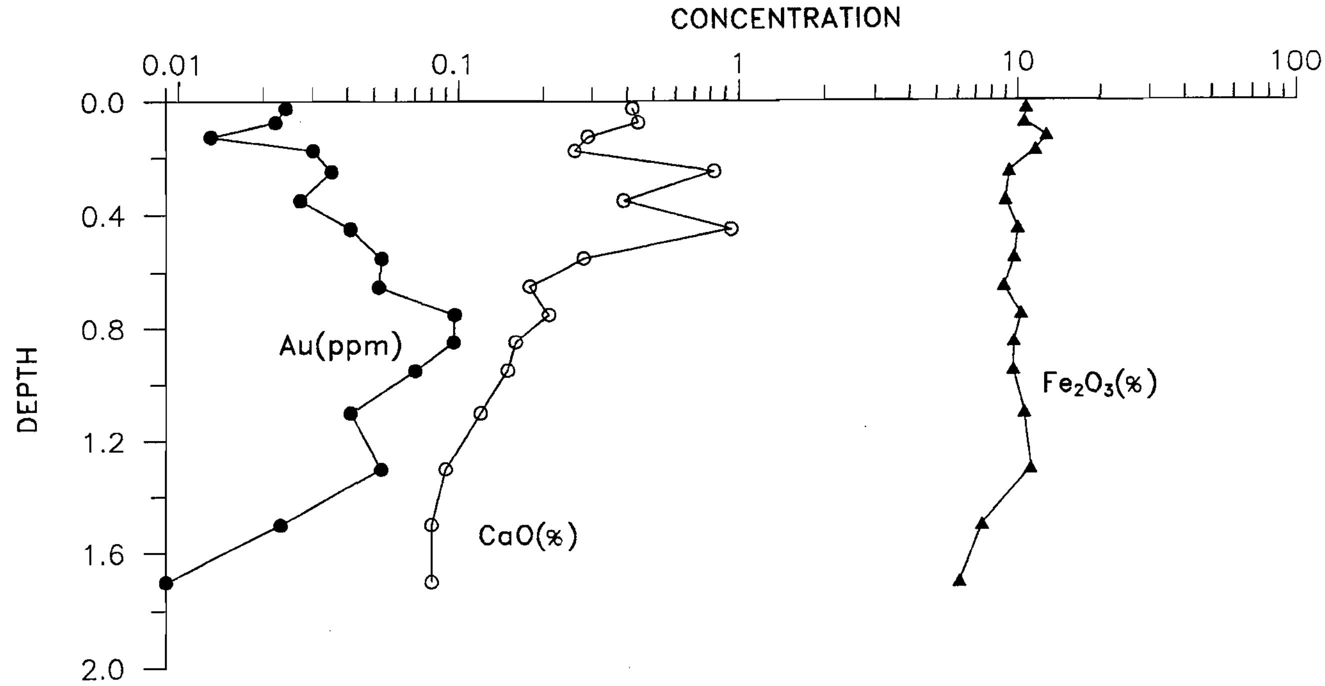

Figure 7: Distribution of Fe_2O_3, CaO and Au in Profile C.

5.1.4. Profile D (2420E, 4200N).

This soil profile, at the site of RC drill hole PSRC 231, has developed above ultramafic rocks (Scott, 1989b). The near-surface material is considered to have a strong transported component (Scott and Dickson, 1989). Beneath this horizon, mottled and clay-rich saprolite predominate for several tens of metres. Supergene mineralization occurs at about 40m. The principal horizons in the profile are as follows:

0-10cm. Clay-rich sand present with some organic litter.

10-50cm. Becoming increasingly rich in clay minerals and poor in quartz. Carbonate development increases with depth. Ferruginous fragments present throughout the profile. Large boulders of saprolite present in adjacent trench (c.f. Section 5.2.)

Quartz is the major mineral present (especially in the top 10cm) with kaolinite, hematite, goethite, calcite, talc and minor plagioclase(?). Quartz concentrations decrease, and carbonate and hematite concentrations increase with depth.

Silicon contents are closely related to the abundance of quartz. These are greatest near the surface and probably indicate transported material (Scott and Dickson, 1989). Iron is associated with the occurrence of hematite, Al with kaolinite, and Ca and Mg with calcite; the high Mg/Ca ratios (>1) suggest the calcite is present as a high-Mg variety, although some of the Mg will be present as talc. No dolomite was found.

The highest Au concentration (0.210 ppm) appears to be strongly related to the high Fe concentration (17.4 %) at the bottom of the profile (0.45m) but there may also be a weak association between Au and calcite (Figure 8).

Rubidium (especially), Mn, Ni, P, Zn and Zr concentrations appear to be related to Al concentrations (Appendix 1.4) although some of the Zn and Ni could occur with talc (c.f. Scott 1989b). Chromium and V distributions are associated with Fe (Appendix 3; cf also Scott (1989b)). Strontium, S, Na and Ba concentrations are closely related to those of Ca.

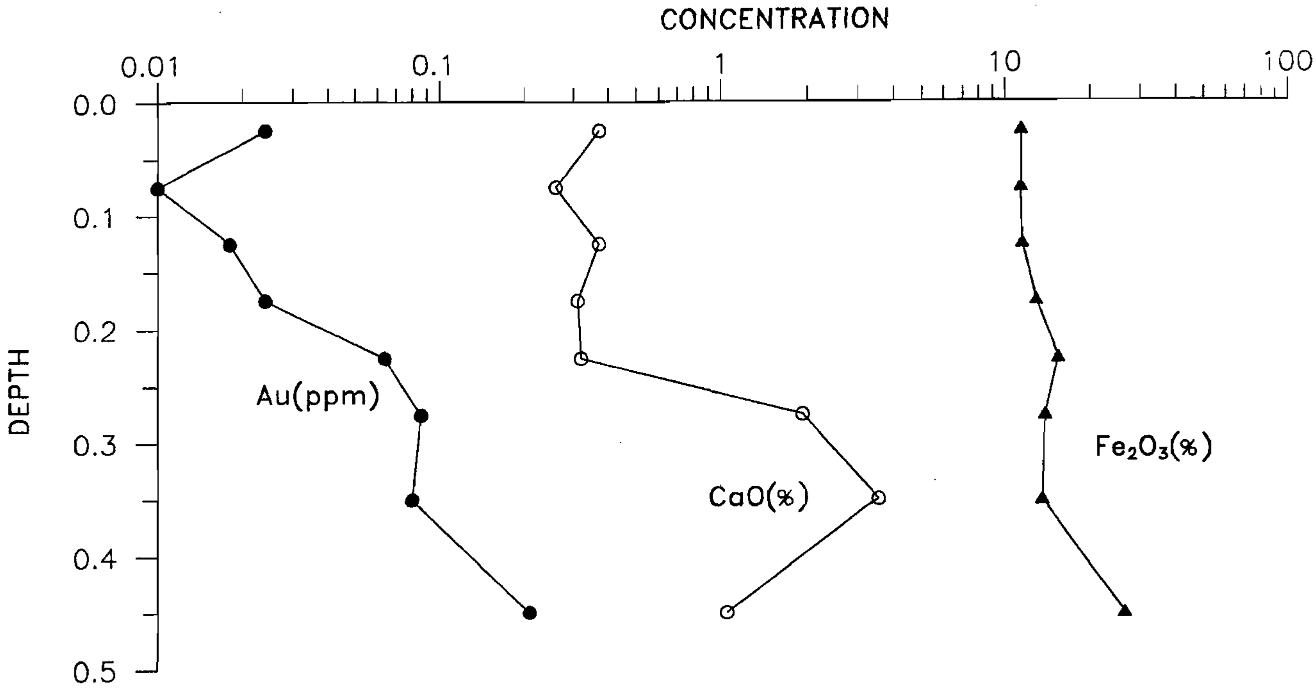

Figure 8: Distribution of Fe_2O_3, CaO and Au in Profile D.

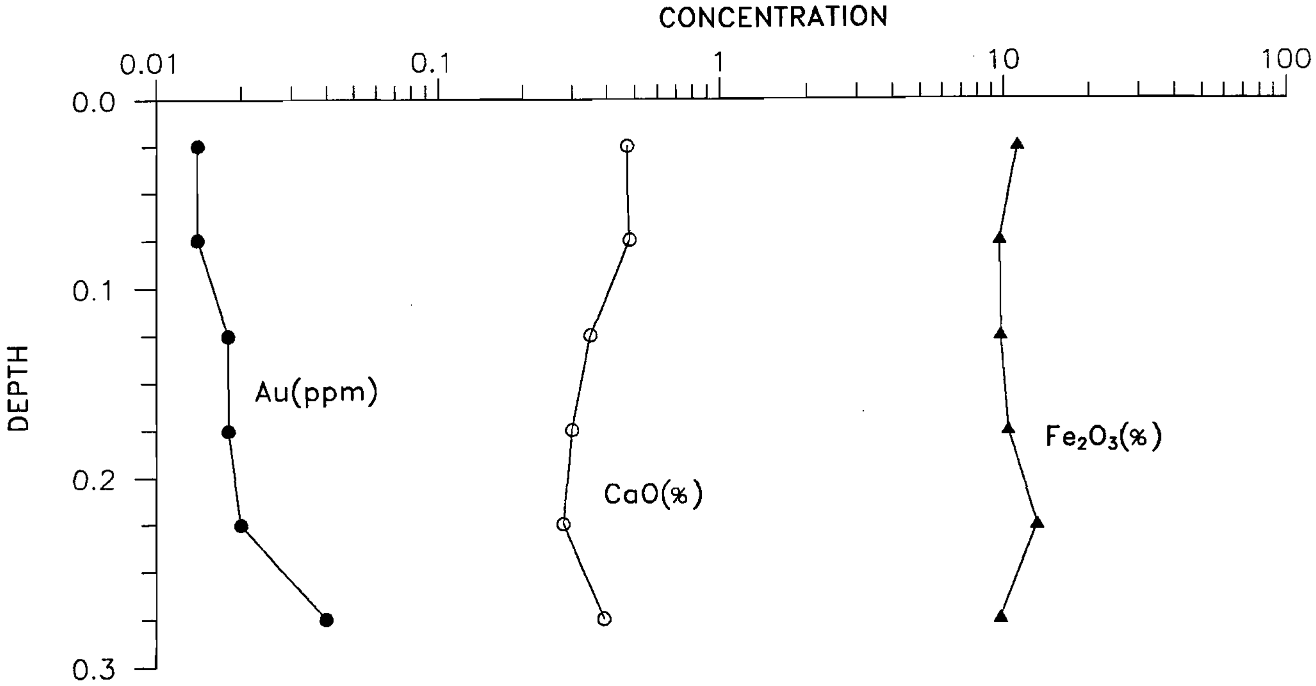

Figure 9: Distribution of Fe_2O_3, CaO and Au in Profile E.

5.1.5. Profile E (2340E, 4300N).

This shallow profile (30cm) is developed above ultramafic volcanic rocks 40m west of PSRC 227. It is similar in appearance to Profile D and consists of loamy sand overlying clay-rich sand.

The profile is rich in quartz, kaolinite and hematite with some talc and goethite, and trace amounts of anatase. No carbonates were detected by XRD in the top 30cm. However, calcite occurs in the 0-1m composite sample in PSRC 227 (Scott, 1990) and field observations in the adjacent trench suggest that carbonate is probably present below about 40cm i.e. beneath the depth of sampling.

Major element distributions are similar to those for Profile D. Silicon maxima concentrations are associated with quartz (although some Si will be in kaolinite and other silicates), Fe with hematite and most Al with kaolinite. Calcium concentrations are relatively poor.

The abundance of Au increases down the profile and does not appear to be associated with any particular mineral phase; the sharp increase in Au at the base of the profile, however, may be related to the top of the carbonate horizon.

Iron concentrations are strongly associated with As, Nb, Pb, V, Ba and Cr. Some cations (e.g. Ca, Ga, Mn, Pb, Rb), are strongly associated with the distribution of Al, where they may be present as interlayer ions in kaolinite, although most of the Mg, Cu, Ni, Zn will be associated with the occurrence of talc (Appendix 1.5; cf also Scott 1990).

5.2. Surface samples.

Surficial soil samples were collected over mineralization, adjacent to the trench at 4200N; rock samples from the trench were also collected. Analytical results are summarised in Appendix 2. The traverse crosses shales, ultramafic and mafic rocks. The soils are considered to have developed in shallow transported material (Scott and Dickson, 1989). Supergene mineralization occurs at about 40m.

There is a strong association between Au and Mg, Ca and Sr (Figure 10). The association is remarkable as it occurs, for Au and Ca, over almost seven orders of magnitude. Most of the Ca appears to be present as secondary low-Mg calcite (from probe studies) which occurs as friable aggregates (<2mm in diameter), coatings on ferruginous fragments and in the -63μm size fraction. Some of the Mg, however, is probably distributed between vermiculite-chlorite and talc which are present in considerable quantities in some samples. Strontium is commonly associated with calcite at Panglo (c.f. the profiles).

There is a strong association between Fe and As, Cr, Sb, V and, probably W, reflecting the incorporation of these elements into secondary Fe oxides (Appendix 2; see also Scott 1990). These associations are particularly well developed in the Fe-rich rocks.

The surface rock samples contain little calcite; any Ca is likely to be present as gypsum as implied by the association of Ca and S (Appendix 2). There is no association between Au and Ca in the rock samples along line 4200N.

The presence of large amounts of plagioclase in soils over various lithologies, although there is little or none in the rocks, is further evidence that these soils have developed on transported material (Appendix 2; see also Scott and Dickson, 1989).

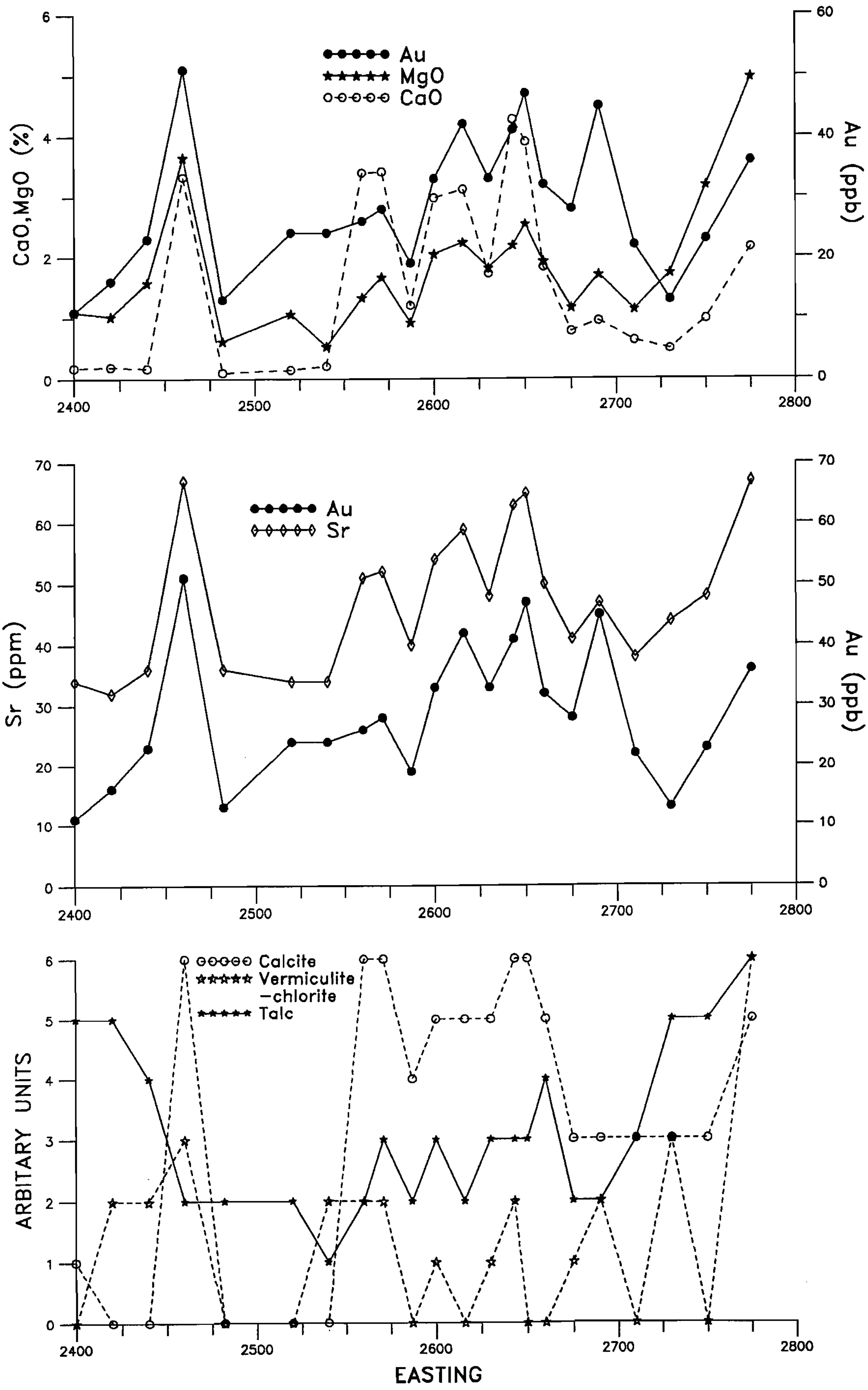

Figure 10: Distributions of a) Au, CaO, and MgO b) Au and Sr, and c) talc, calcite and vermiculite-chlorite in surficial soils at 4200N.

A more extensive suite of surficial soils from traverse 4200N and 3700N were specifically analysed for Au; the samples were not crushed or pulverized before digestion with cyanide solution. The procedure has similarities with the bulk leach extractable gold or BLEG technique but uses a smaller sample volume (500g compared with 1000g).

Results are compared with pulverized samples after fire assay fusion (Figure 11). Whereas it is clear that more Au was found by fire assay, the distributions are similar by the two methods. The ratio of background to anomaly is also similar being about 1:10 for 3700N and 1:5 for 4200N. This indicates that a significant quantity of Au (up to 100%) in these soils is freely available to chemical dissolution. It also implies that a large proportion of Au is associated with the fine fraction and not encapsulated within larger impervious soil aggregates or saprolitic fragments.

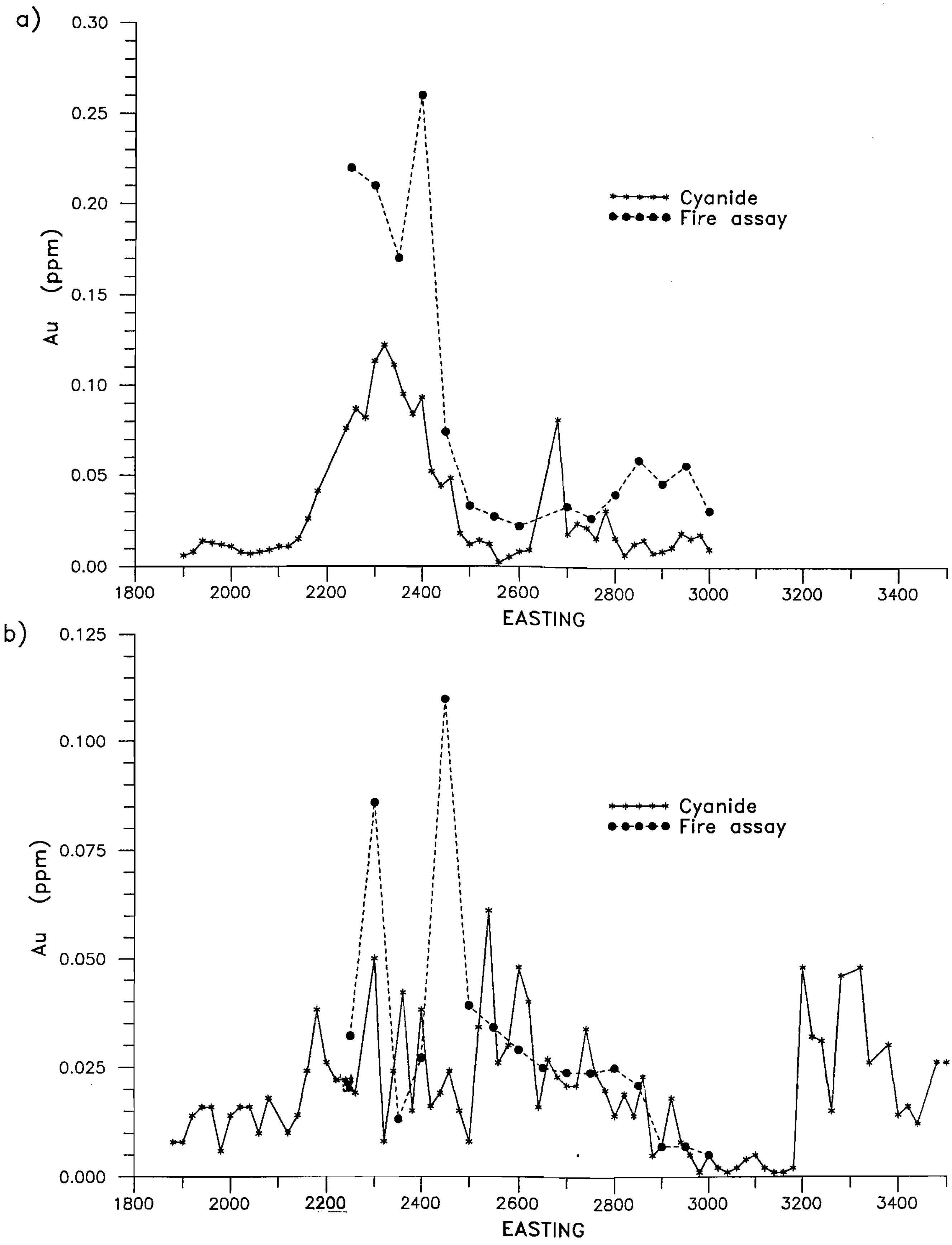

Figure 11: Comparison of fire assay-extractable Au from pulverized soil samples and cyanide-extractable Au in uncrushed soil samples from traverses a) 3700N and b) 4200N.

5.3. Auger samples.

The auger traverse on 3700N, drilled by Pancontinental Mining Ltd., sampled soils developed on the transported lateritic gravels, outcropping weathered mafic rock and the current saline drainage channel. The results show a strong association between sample type and composition (Appendix 3). The principal features of the distributions are discussed below:

(i) Au concentrations gradually increase, west to east, from the transported lateritic gravels (0.020 ppm) to the weathered mafic rock (0.170 ppm), and then decrease into the channel soils (0.020 ppm). One sample in the channel is particularly rich in Au (0.106 ppm). The Au here may be associated with transported fragments from the adjacent hill (Figure 12a; and also Profile C);

(ii) Silicon, Na and S, Rb, Zn and Zr contents are greatest in the saline clay-rich channel soils (Figure 12b; Appendix 3);

(iii) High Fe, Ca, Mg, Co, Ni, Cr, V, Mn, Cu and Sr contents generally occur in the lateritic gravels, in which they are associated with ferruginous saprolitic or carbonate fragments and weathered mafic rock (Figure 12 b; see Appendix 3);

(iv) Very high concentrations of Ca, S and Ba occur in the weathered mafic rock, probably associated with cements and thick coatings of carbonate and barite (see Section 5.6.3).

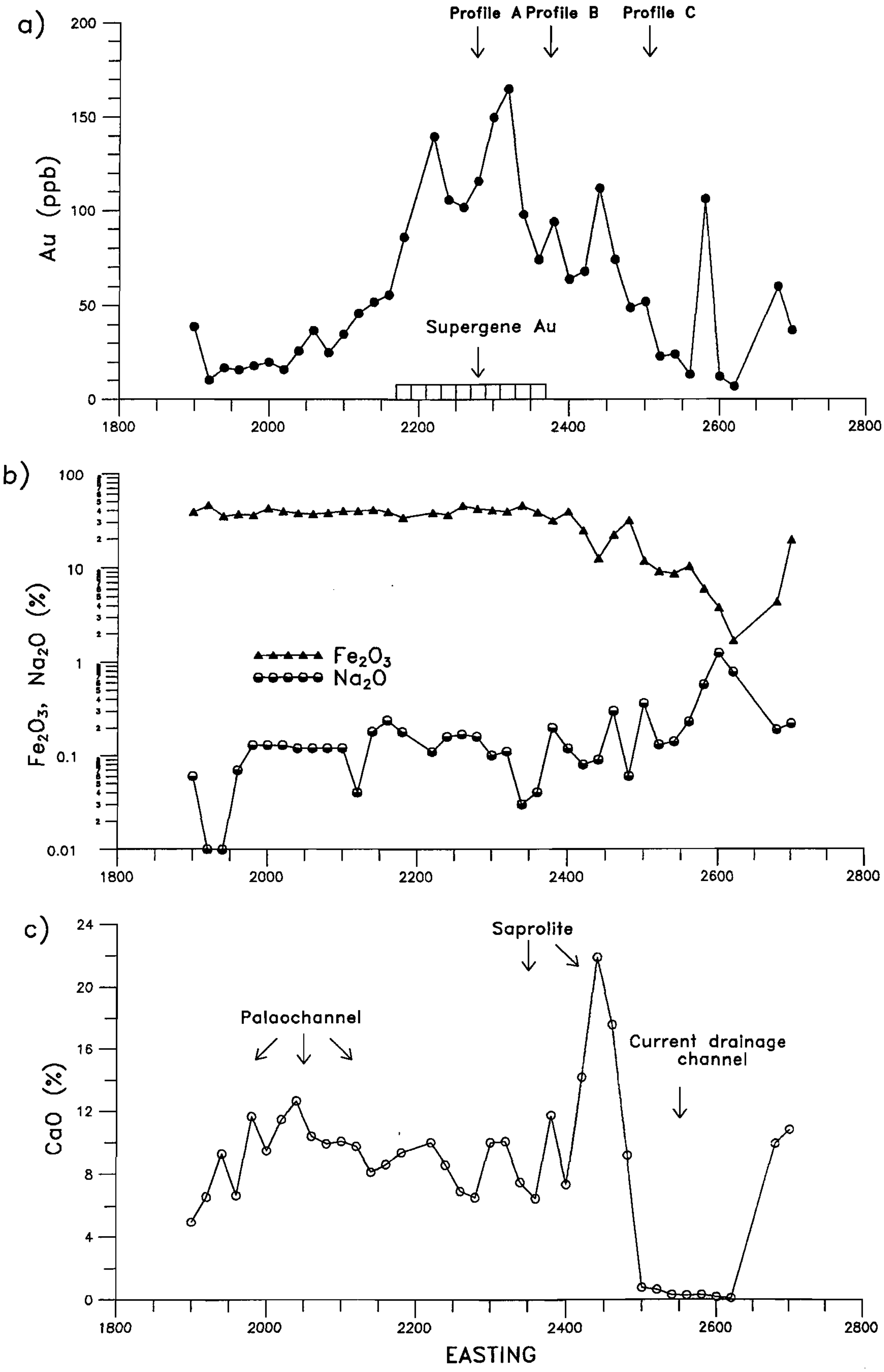

Figure 12: Distributions of a)Au, b)Fe_2O_3 and Na_2O, and c)CaO as shown by auger sampling 3700N.

5.4. Trench samples.

Trench samples from 3700N were collected and analysed for Au and As by Pancontinental Mining Ltd. Samples were taken at a constant level above the floor of the trench; the sampling depths were thus about 1.5m in the transported gravels and progressively shallower (to a few centimetres) as the trench crossed weathered rock.

Gold concentrations are highest in soils associated with the weathered rock whereas As concentrations are highest in the lateritic gravels (Figure 13). The Au anomaly in the trench samples is displaced with respect to those collected at the surface or by auger, and to the underlying supergene mineralization. This is because the carbonate horizon, in which the Au anomaly is located, was only sampled where the trench was shallow over the weathered rock (see Profile B) whereas in the transported gravels the barren horizon below the carbonate was sampled (see Profile A).

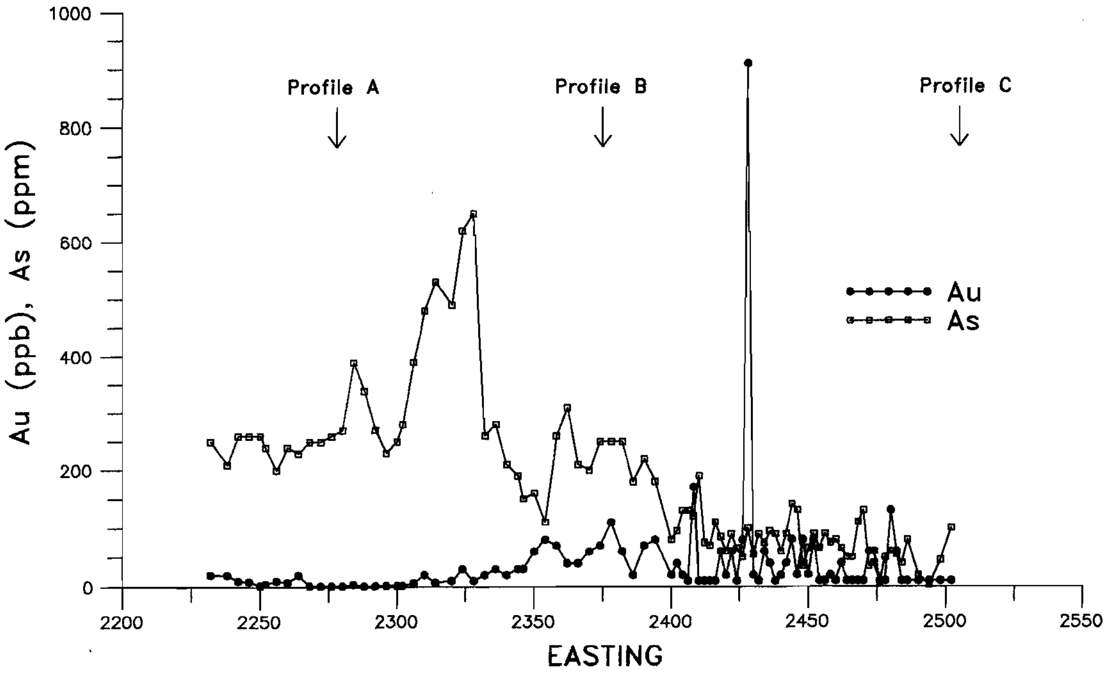

Figure 13: Distributions of Au and As in the trench on 3700N, as shown by sampling at a fixed height above the base.

5.5. Vegetation samples.

The occurrence of different plant species at Panglo is determined by soil type, geomorphology and lithology and herein lies the major problem with biogeochemical sampling in general. To make adequate comparisons between metal contents in plants along an entire traverse plants of the same species, age and condition should be sampled which is usually not possible in surveys of this type in Western Australia. However, this limitation was partly overcome by sampling where possible:

(i) several species and grouping them according to their genera;

(ii) *Eucalyptus* spp. and *Eremophila* spp. of similar trunk diameter and/or height.

Interpretation of the data are hindered because the soils were sampled by different procedures in different areas. Comparisons between the geochemistry of soils and vegetation should be made with caution since the horizon sampled may not reflect the zone used by the plants. This is particularly true for 4200N where samples were collected near the surface (5-20cm), which has considerable amounts of sand, and is unlikely to reflect the major zone of absorption of nutrients by the plants. Also, for 4200N, multi-element analyses of soils were restricted to a small part of the traverse (except for Au) limiting comparisons with plants.

Geochemical comparisons can be made more effectively between plant samples and soil samples on 3700N as augering of the top metre was performed. The root system of many shrub species e.g. *Eremophila* spp. occurs extensively within the top metre (rather than near the surface) and, consequently, they rely on penetration of surface rainfall for their water. However, *Eucalyptus* spp. can have, in addition to the near-surface root system, a long tap root (sometimes tens of metres in length) capable of absorbing nutrients and water from saprolitic clays and the water table, respectively i.e. they can be phreatophytic. Chemical contents of *Eucalyptus* spp., therefore, might represent a composite of that obtained by roots from two or more locations within the profile.

Neutron activation was initially used for the analysis of the plants, on a dry weight basis. However, the high Na contents of the plants caused a severe interference with Au, resulting in unacceptably high detection limits. The problem was circumvented by ashing the samples, digesting them in acid and analysing for Au by graphite furnace AAS.
Background Au concentration values for vegetation collected at about 4900N 2300E (see Figure 2), away from mineralization, averaged 0.036 ppm for *Eremophila* spp. and 0.012 ppm for *Eucalyptus* spp (see Appendix Section 5). Gold contents in vegetation at Panglo were generally lower than those found in other Western Australian studies (Smith and Keele, 1984; Lintern, 1989).

5.5.1. Traverse 4200N samples.

Eremophila spp. and *Atriplex* spp. occur most frequently on 4200N and, therefore, were sampled most frequently. Plant communities growing in soils developed over ultramafic/mafic rocks are open shrublands with *Eremophila* spp. and some *Atriplex* spp. whereas the communities growing over the sedimentary rocks which are mainly chenopods (saltbush). Geochemical differences are not great between individuals of the same genus growing on ultramafic rocks (generally located more to the western part of the traverse) and those growing on mafic rocks (Appendix 5).

Gold concentrations in vegetation are generally close to background and show at best a poor association with either cyanide-extractable Au from soils, lithology or economic mineralization (Figure 14a). Higher Au contents were found in *Eremophila* spp. (up to 0.024 ppm) and *Melaleuca* spp. (up to 0.132 ppm) as compared with *Atriplex* spp. (up to 0.018 ppm). The highest Au content (0.185 ppm) was recorded for *Dodonaea* sp. (a small halophytic shrub) but because its distribution was limited, only one specimen of this plant was sampled (Figure 14a) and so it is not known, therefore, whether this value is anomalous.

There are no significant differences in the compositions of *Eremophila* spp. and *Atriplex* spp., except for Ca, Na and Cu (Appendix 5), although *Eremophila* spp. are generally richer in all elements compared with *Atriplex* spp.

Calcium is an important macro-nutrient primarily required for mechanical strength. It is more richly concentrated in *Eremophila* spp. when compared with *Atriplex* spp. possibly because they require greater mechanical strength due to their height. Calcium concentrations are higher in the ash of *Eremophila* spp. than the soil. This may be of major importance when considering the origin of pedogenic carbonate.

Sodium is commonly present in large concentrations in plants adapted to growing in saline soils (e.g. the halophytes) and is involved in osmoregulation. Sodium concentrations are higher in *Atriplex* spp. than those in *Eremophila* spp.

Copper is a minor but essential plant nutrient contained in many enzymes and also in photosynthetic pathways. Copper is more richly concentrated in the ash of *Eremophila* spp. when compared with *Atriplex* spp. or the soil. The significance of this enrichment is not known.

5.5.2. Traverse 3700N samples.

Eremophila spp. and *Eucalyptus* spp. grow on the gravelly, well drained soils of the palaeochannel and those developed over mafic rocks. Halophytes grow in the clay-rich, poorly drained soils developed over the current drainage channel overlying sedimentary rocks (Figure 14b). *Eremophila* spp. and *Eucalyptus* spp. occur regularly along 3700N and were sampled most frequently (Appendix 5).

The distributions of Au shown by vegetation sampling are broadly similar to those found in soils; contrasts tend to be higher in gravelly soils. Gold contents are much higher in *Eremophila* spp. (up to 0.059 ppm) than *Eucalyptus* spp. (up to 0.042 ppm). *Eucalyptus* spp. east of the drainage channel contain more Au than *Eucalyptus* spp. found over mineralization to the west (Figure 14b) and may be of significance since they are also nearly double the background Au values for *Eucalyptus* spp. (0.012 ppm). Furthermore, the background data suggest that *Eucalyptus* spp. are not as effective as *Eremophila* spp. in accumulating Au. The Au content of *Eremophila* spp. on 3700N are generally richer than those on 4200N.

Apart from Au, there is little relationship between the composition of the vegetation and soils. This feature is most clearly seen with Fe, Mn, Ca, Ni and V: soil auger concentrations of these elements tend to decrease towards the drainage whereas in vegetation they tend to increase (Section 5.3; Appendix 3). Soils nearer the channel are thin because weathered rock occurs close to the surface. For *Eremophila* spp., the trend of slightly increasing concentrations of As, V and Ni, eastward and downslope towards the channel, may reflect the presence of these metals in forms more available for absorption by plants (e.g. from the breakdown of saprolite), in contrast to a less soluble form present in the gravelly soils. Sodium and ash concentrations are richest for plants in the channel vegetation samples and are comparable with halophytes found on 4200N.

The Cu contents of *Eremophila* spp. are higher than those in *Eucalyptus* spp. The values are comparable with those found for *Eremophila* spp. at 4200N and background areas, suggesting that appreciable quantities are required by this genus for normal plant function. Soil Cu contents are similar for the two traverses.

Sodium contents of *Eucalyptus* spp. are much greater than those found in *Eremophila* spp. but not as great as the salt-tolerant channel genera such as *Atriplex* spp. Sodium enrichment in *Eucalyptus* spp. may reflect the ability of its roots to reach, absorb and accumulate salts from the groundwater.

Calcium enrichment in *Eremophila* spp. is greater on 3700N than 4200N and may reflect higher abundance of pedogenic carbonate in the soil (Appendix 5).

Additional results for vegetation samples collected to the north of 3700N, but still in the gravelly soils, are recorded in Appendix 5. Metal concentrations are similar in magnitude to those found at locations on 3700N.

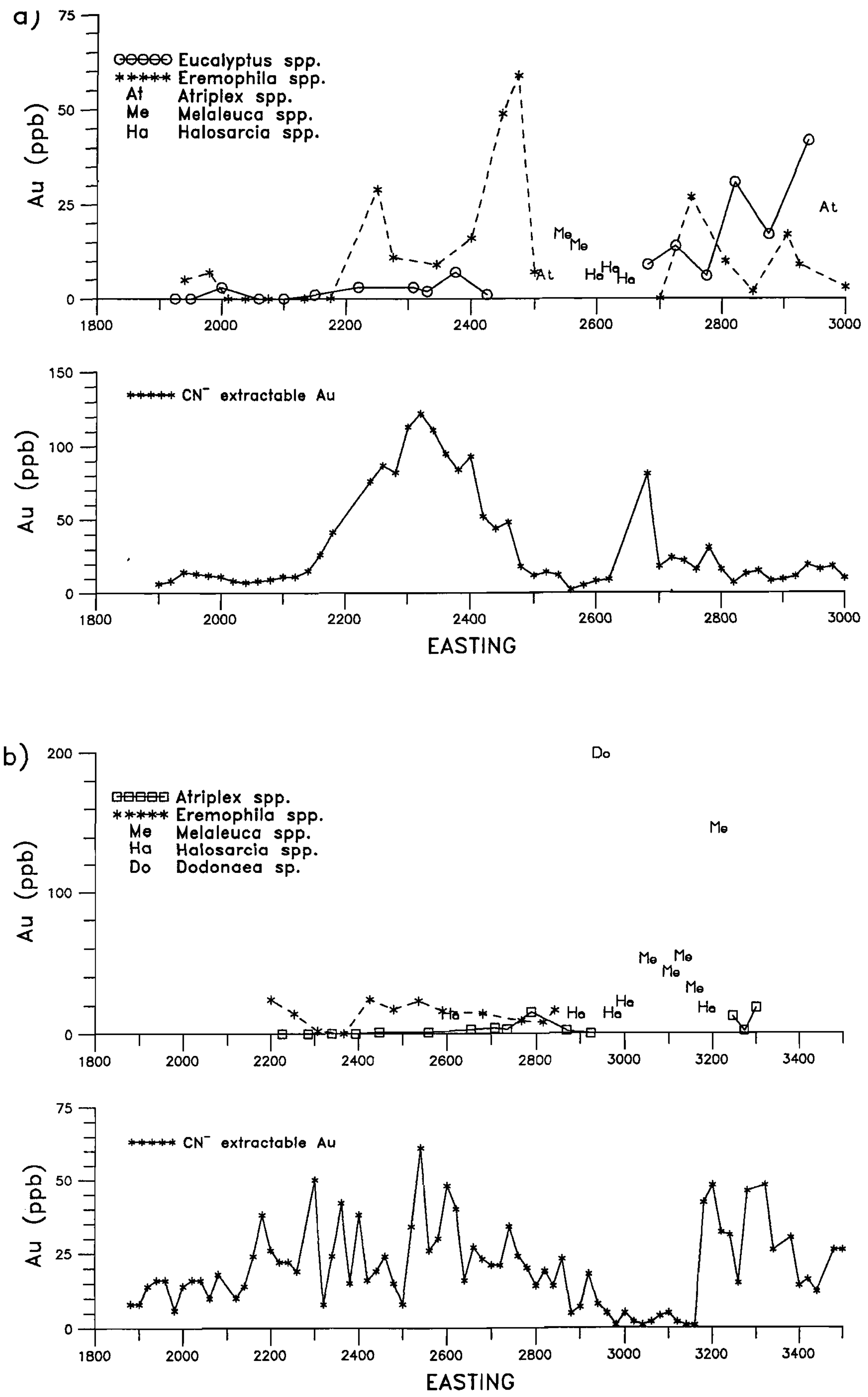

Figure 14: Au contents for vegetation and soils along traverse a) 3700N and b) 4200N

5.6. Special samples.

A more detailed examination of material similar to that found in Profile B was undertaken. It was important to establish the nature of the relationship between Au and carbonate in nodular material as the channel sampling procedure used in Profile B did not make the association clear. At the sample sites, the amount of carbonate coating the nodules varied in extent and thickness but tended to be greater closer to the soil surface. Lower in the profile the amount of soil and carbonate was poor or absent and the nodular material became more massive and indurated.

Special sample G1 (04-2112) was taken close to Profile B at 2377N 3700N from 30cm depth (Figure 2; Figure 3e). It comprises several sub-rounded and angular nodules up to 10 cm in diameter. Each nodule consists of a core of red ferruginized saprolite partially coated with pink coloured carbonate up to 3mm in thickness; some carbonate had penetrated into fine cracks in the nodules (Figure 15).

Special sample G2 (04-2129) was taken from 2455E 3700N at 30cm depth, 80m east and downslope of the first. The profile was similar in appearance to that described for the first special sample but contained boulder-sized material. It consists of sub-rounded, dark red cobbles and boulders of ferruginous saprolite up to 40cm in diameter (Figure 3e). The red core is partly surrounded by a very pale layer varying from a few millimetres to several centimetres thick. The core and pale layer are referred to herein as "red saprolite" and "white saprolite" respectively. Veneers of pink-coloured carbonate covered areas of the pale material (Figure 16) but the total amount of carbonate is less than in sample 04-2112.

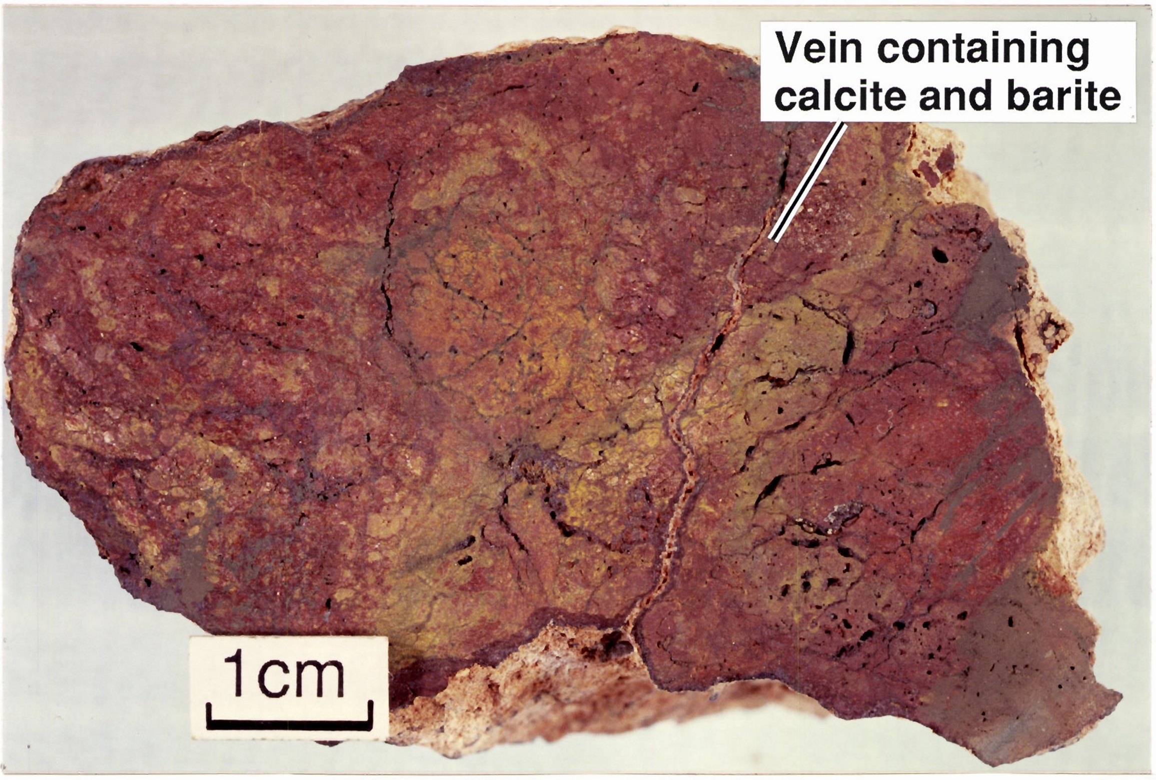

Figure 15: Sample G1 (04-2112). Photograph of a ferruginous carbonate-coated nodule. Note the prominent vein through the centre of the specimen which contains calcite and barite (see Figure 17).

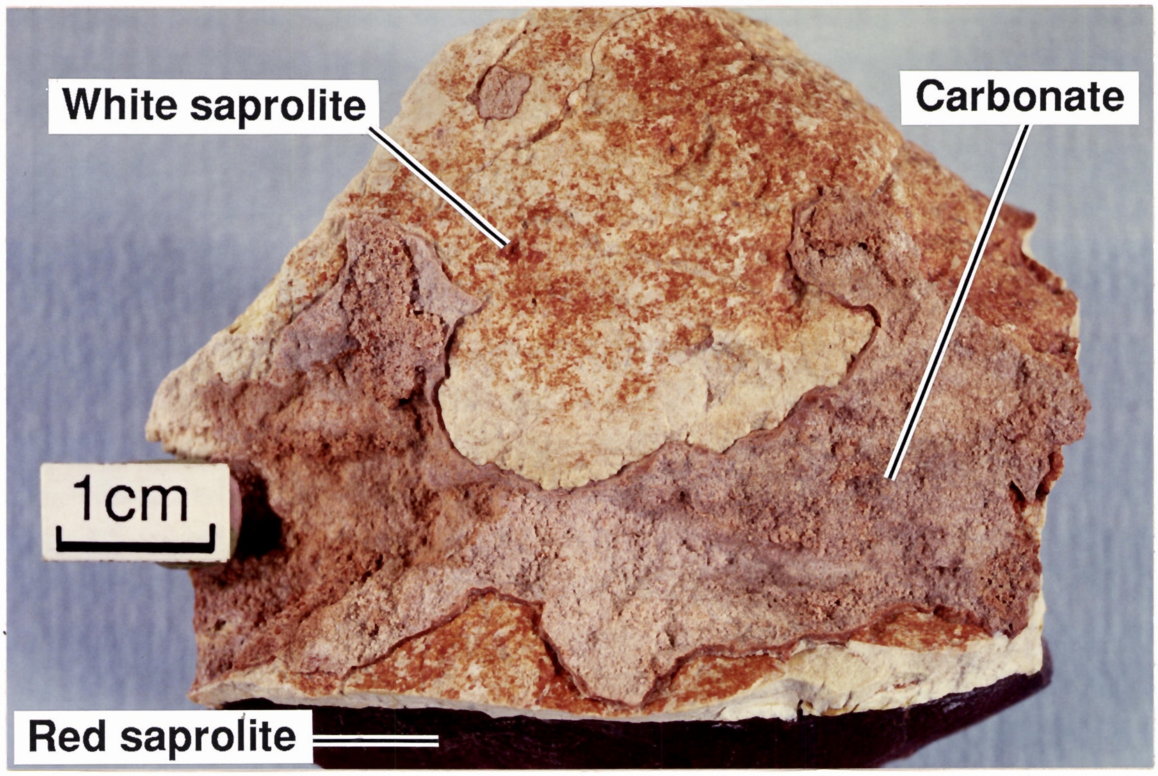

Figure 16: Sample G2 (04-2129). Photograph of a ferruginous nodule ("red saprolite") covered with pale saprolite ("white saprolite") and carbonate.

Representative photomicrographs, with interpretative diagrams, are shown in Figures 17 and 18. No visible Au was detected by the SEM which suggests that it is present as sub-micron particles.

Geochemical studies were undertaken on sample G2 only, as carbonate skins on sample G1 were tooo thin to be removed from the nodule surfaces without contamination from underlying material. Sample G2 was divided into carbonate (pink), white saprolite and red saprolite using a small hand drill. Detailed composition of each type can be found in Appendix 6. The results are summarized and contrasted in the table below by comparing elemental concentrations found in the carbonate with the saprolites (Table 2).

Amount	Carbonate	Red saprolite	White saprolite
High	Mg, Ca, Au, Ba, Cu, Mn	Si, Al, Fe, Ni, Ti, Cr, V, Zr	Si, Al, Ca, Na, Ti, Zr
Low	Si, Al, Fe, Na, Ti, Cr, V, Zr	Mg, Ca, Au, Ba, Cu, Mn	Fe, Mg, Au, Ba, Cr, Mn, V

Table 2: Comparison of element concentrations between the three types of material types.

Figure 17: Sample G1 (04-2122). Photomicrograph of a vein within a carbonate coated ferruginous saprolite nodule. The lower photomicrograph show details of the vein. Mineralogy estimated from SEM-EDAX analysis.

Figure 18: Sample G2 (04-2129). Photomicrograph of surface features of ferruginous saprolite nodules. The lower photomicrograph (c) show details of the surface for (b). Mineralogy estimated from SEM-EDAX analysis.

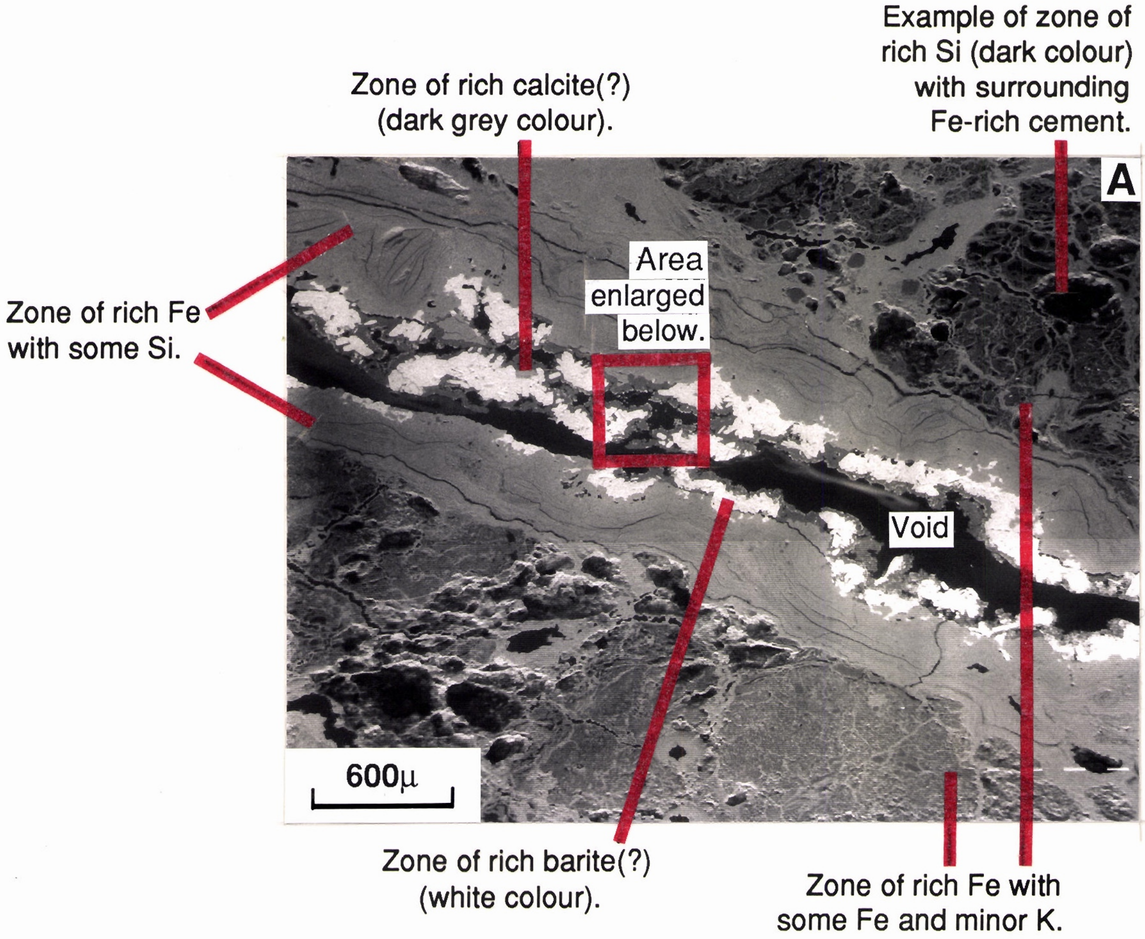
Example of zone of rich Si (dark colour) with surrounding Fe-rich cement.
Zone of rich calcite(?) (dark grey colour).
A
Area enlarged below.
Zone of rich Fe with some Si.
Void
600μ
Zone of rich barite(?) (white colour).
Zone of rich Fe with some Fe and minor K.

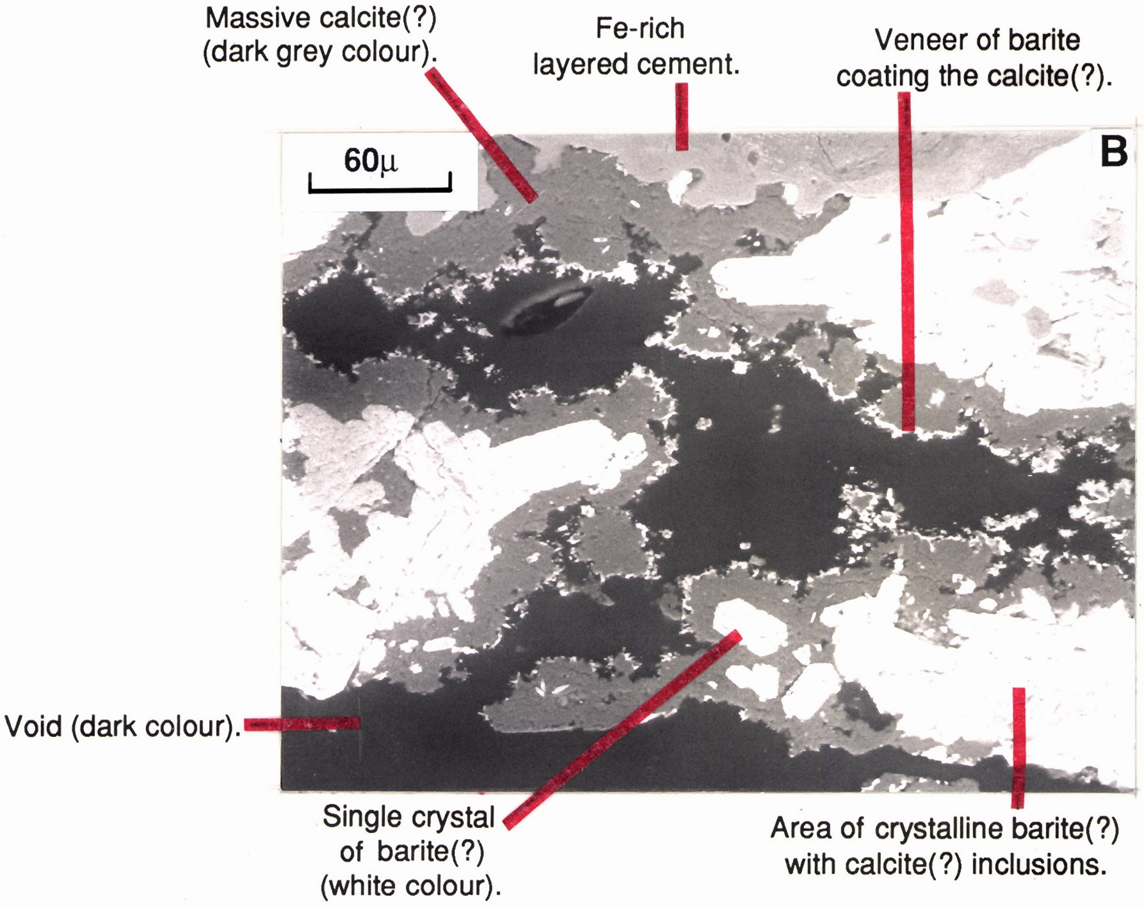
Massive calcite(?) (dark grey colour).
Fe-rich layered cement.
Veneer of barite coating the calcite(?).
60μ
B
Void (dark colour).
Single crystal of barite(?) (white colour).
Area of crystalline barite(?) with calcite(?) inclusions.

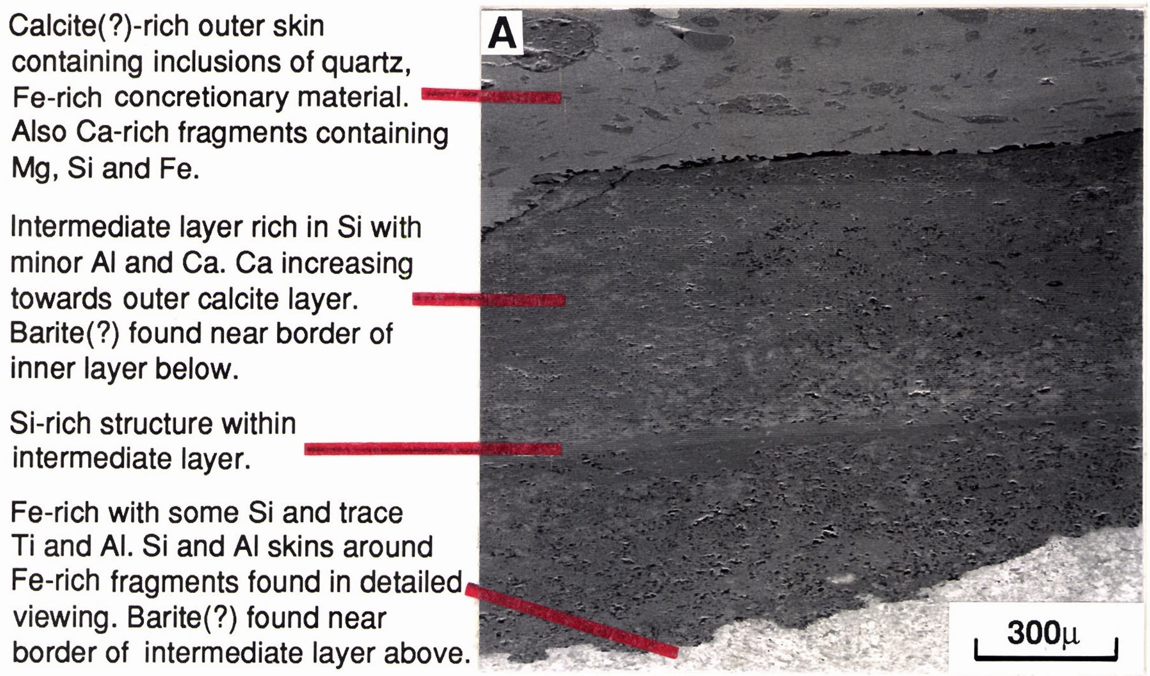
A
Calcite(?)-rich outer skin containing inclusions of quartz, Fe-rich concretionary material. Also Ca-rich fragments containing Mg, Si and Fe.
Intermediate layer rich in Si with minor Al and Ca. Ca increasing towards outer calcite layer. Barite(?) found near border of inner layer below.
Si-rich structure within intermediate layer.
Fe-rich with some Si and trace Ti and Al. Si and Al skins around Fe-rich fragments found in detailed viewing. Barite(?) found near border of intermediate layer above.
300μ

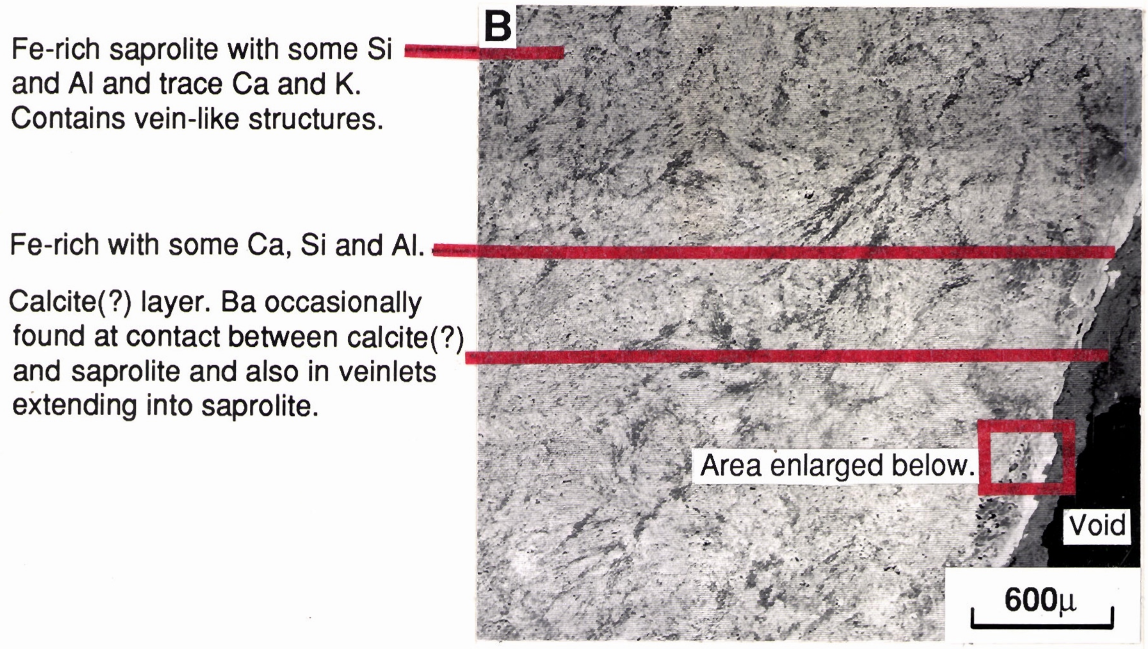
B
Fe-rich saprolite with some Si and Al and trace Ca and K. Contains vein-like structures.
Fe-rich with some Ca, Si and Al.
Calcite(?) layer. Ba occasionally found at contact between calcite(?) and saprolite and also in veinlets extending into saprolite.
Area enlarged below.
Void
600μ

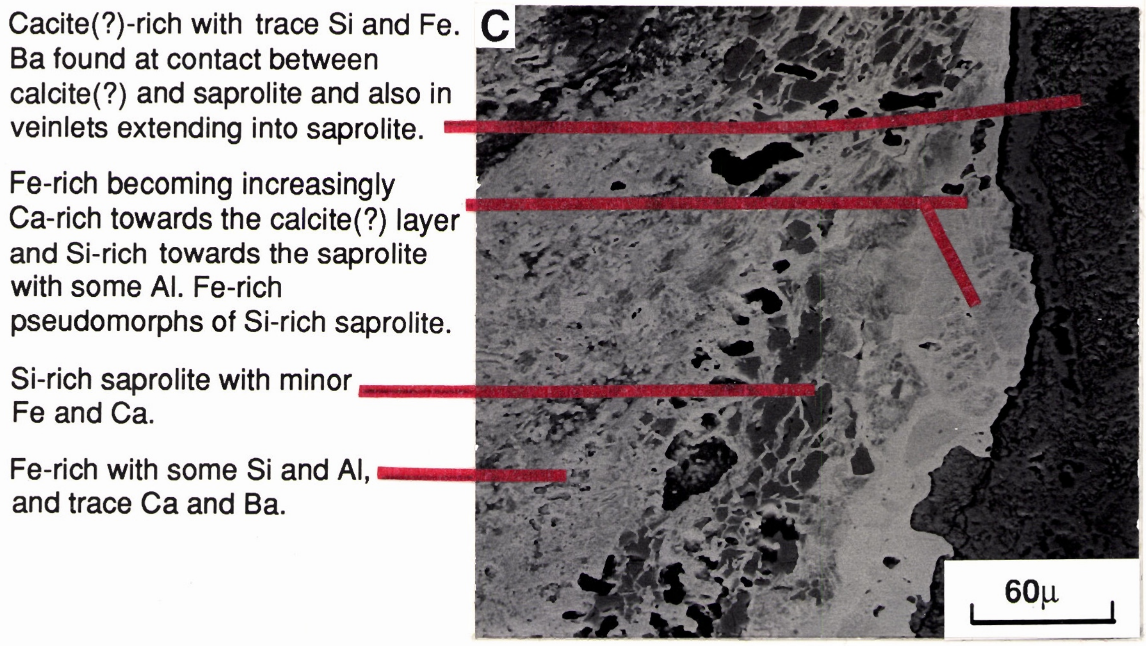
C
Cacite(?)-rich with trace Si and Fe. Ba found at contact between calcite(?) and saprolite and also in veinlets extending into saprolite.
Fe-rich becoming increasingly Ca-rich towards the calcite(?) layer and Si-rich towards the saprolite with some Al. Fe-rich pseudomorphs of Si-rich saprolite.
Si-rich saprolite with minor Fe and Ca.
Fe-rich with some Si and Al, and trace Ca and Ba.
60μ

There is a strong association between Au and the alkaline earth metals in these samples. The geochemical (Table 2) and photomicrograph (Figure 17) evidence suggests that Au has been transported in solutions containing Ca, Ba (and SO_4^{2-}) and Mn. Low concentrations of these elements in the saprolite suggest that they are derived from elsewhere in the regolith. Laboratory studies suggest that Au is highly mobile in carbonate-rich soils (Gray *et al*., 1990).

Petrological and SEM studies of the contents of veins within sample G1 reveal their depositional sequence to be Fe (as an oxide), Ba (as barite) and Ca (as a low Mg calcite) (Figure 17). Barite occurrences tend to be greater deeper into the veins suggesting that early solutions were rich in Ba and sulphate. Later, pore waters rich in Ca were prominent. Early in the third deposition stage, however, conditions once again favoured the formation of barite as it is found as a veneer on some of the calcite (Figure 17b). In general, however, calcite is much more abundant than barite. Barium tends to be richer in the shales rather than the mafic and ultramafic rocks (Scott, 1990; Scott and Dotter, 1990). Sections of sample G2 reveal a similar paragenetic sequence of Fe-and Ca-containing solutions invading the host saprolite (Figure 18a and b). Iron-rich solutions have penetrated pores and, seemingly, replaced (pseudomorphed) some of the Si minerals near the edge of, and within, the saprolite (Figure 18c). Subsequently, solutions rich in Ca have followed and formed often thick veneers, covering saprolite surfaces and, occasionally, have entered weakened areas to form calcite-rich veins.

The presence of carbonate-rich skins and veins suggests a weathering process having both physical and chemical components. It probably involves (i) invasion by carbonate and replacement of host minerals, (ii) slow, and possibly repeated, crystallization and dissolution of calcite and, finally, (iii) fracturing by crystal growth. The rate of fragmentation will depend locally on many factors including the micro water-regime, soil temperature and the concentration of Ca and bicarbonate ion in the pore water. Chemical replacement by calcite has been reported for quartz (Pettijohn, 1972; Millot *et al*, 1977) and Fe oxides (Nahon *et al*, 1977).

6. Discussions and Conclusions.

6.1. The Model.

The results demonstrate a strong association between Au and pedogenic carbonate. The association is particularly strong when the concentrations of Ca are greater than one or two percent. This result is consistent with that found in similar studies conducted at Mt. Hope (the Bounty mine), W.A. (Lintern, 1989; Lintern *et al*, 1990). The particular significance of the present study is the presence of Au-bearing, near-surface carbonate in 10m of transported overburden, which is, in turn, 30m above the main zone of supergene mineralization (Profile A; Figure 19). It is presumed that the Au is vertically derived from this mineralization either directly, or indirectly via the enrichment zone at the interface between the palaeochannel and the post-lateritic land surface at 10m depth (Figure 19). Similar Au anomalies developing in 4-6m of transported overburden have been reported by Lawrance (1988).

The precise mechanism by which the Au and calcite are associated has not been determined. However, the association between Au concentrations in vegetation and those in soils, and the high concentrations of Ca found in both vegetation and soil, suggests Au and Ca are absorbed by deep-rooted trees and plants, translocated to the leaves and deposited in soils by leaching or leaf fall. Subsequently, multiple recycling of the Au and Ca within the soil continues, by the same mechanisms, with less deeply rooted plants. The initial co-location of Au and Ca is thus due to their uptake and association within the vegetation. The model may also explain why higher Au contents are generally found in soils beneath woodland rather than soils beneath shrubland since the trees are deep rooted and have a greater opportunity to continue to supplement surface soils with Au derived from depth. Laboratory experiments at CSIRO support the model, as they suggest that Au is relatively soluble and mobile in soil environments (Gray *et al.*, 1990). The accumulation of carbonate in soils occurs in semi-arid climates where evaporation and evapo-transpiration exceed precipitation. Partially soluble elements such as Ca remain close to their source i.e. from Ca-containing rocks or groundwaters. At Panglo, the nearest present source of Ca are the groundwaters (Gray, 1990) which are at 5 to 10m depth.

The chemistry of the association between carbonate and gold may involve a complex series of steps (see Milnes and Hutton, 1983). One possible mechanism is as follows:

(i) Au and Ca, derived from vegetation and the former complexed as an organic ligand, are dissolved by meteoric water. The solubility of Ca^{2+} depends on the partial pressure of CO_2 and temperature.

(ii) High concentrations of CO_2 occurring in the soil (derived from soil micro-organism and root respiration) are dissolved in the water.

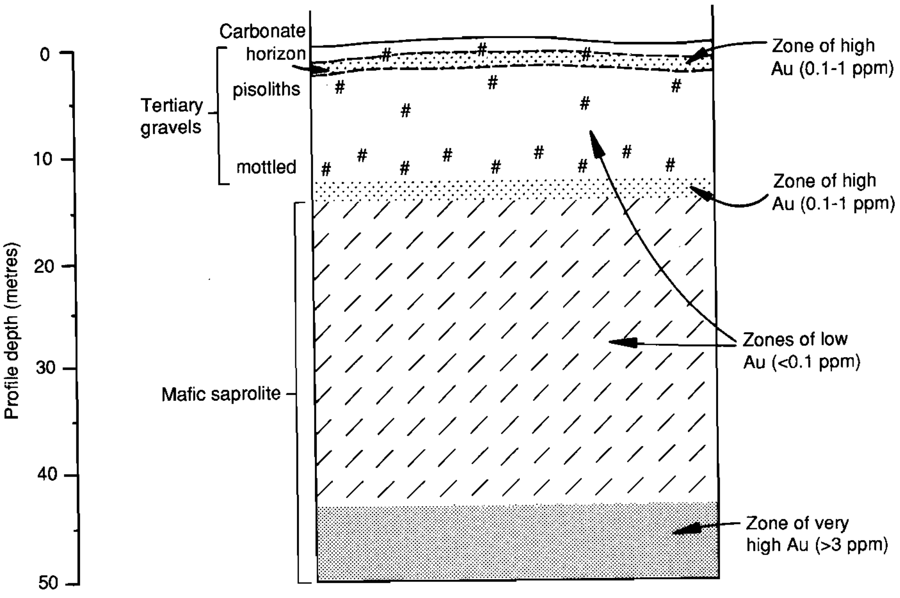

Figure 19: Stylized section through 3700N showing relative positions of Au mineralization in (i) the carbonate horizon, (ii) the post-lateritic land surface and (iii) the economic mineralization at 40m.

(iii) Water is removed from the soil by evaporation and roots, as it percolates downwards.

(iv) Ca^{2+} concentrations reach saturation and precipitate. Calcium precipitates as carbonate and Au becomes adsorbed onto it as an organic complex. The chemistry of precipitation of organic-Au complexes under these conditions are poorly understood.

(v) With the introduction of further water the dissolution process begins again. Laboratory experiments show that appreciable soil Ca and Au are soluble under normal atmospheric conditions (Gray *et al.*, 1990) and for Ca, at least, solubilities are increased with increased CO_2.

The downwards movement of Ca and Au in the profile to their present locations, therefore, is a result of an iterative process dependant on the percolation of water from a series of rainfall events and recycling via plant roots.

Carbonates are generally only retained in the landscape in regions in which rainfall is less than 600mm (Young, 1973). Pedogenic carbonates tend only to be abundant in areas of winter rainfall in which there is a long growing season and an extended period of high CO_2 (Butt *et al.*, 1978). In summer rainfall areas, carbonates tend to form valley calcretes. It is not clear why carbonates may occur as powdery nodules, massive boulders or only as thin coatings but probably involves a combination of soil processes and other factors. These include: porosity, mineralogy, vegetation, groundwater, temperature and rainfall. Carbonate-enriched soil horizons may be entirely absent, or separated from Au enrichment for a variety of reasons. These may include, for example, different (i) soil moisture, (ii) soil types, (iii) soil temperature, (iv) biological activity, (v) climatic regime and (vi) lithology. More data are obviously required on this topic. Although above background Au values are generally found in calcite, Au maxima concentrations in some soil profiles (e.g. Profile C) do not strictly correspond with Ca maxima concentrations. Carbonate-poor soils are also extremely common throughout Western Australia. In wet areas, for example those occurring at the Boddington gold mine in the Darling Range of Western Australia, Ca concentrations in laterite soils are poor whilst Au concentrations may still be rich. In desert areas, low CO_2 activity in the soil may lead to the formation of aluminosilicates or gypsum in place of carbonate. Clearly, further work is required to establish how calcrete forms and to investigate the mineralogical and geochemical associations of Au in soils in other environments.

6.2. Implications for exploration.

6.2.1. Soil sampling procedures.

The strong association of Au with pedogenic carbonate implies that carbonates are an extremely important exploration sample medium. Carbonates hold information on underlying Au mineralization even in areas of transported overburden and sampling provides, therefore, a low cost alternative to other techniques such as scout RAB drilling to bedrock. It is not certain that the association is present in all calcareous horizons. However, if present, it is important that the carbonate horizon is identified and correctly sampled. The study has shown that the depth of the main carbonate horizon can vary. Simple field test procedures using dilute hydrochloric acid can unequivocally identify the presence of soil carbonate. Dolomite is less reactive than calcite and takes slightly longer to effervesce. Field technicians should be encouraged to use the test and document the presence or absence of carbonate as part of routine soil sampling surveys, to assist in their interpretation.

Auger drilling and compositing the top metre will effectively sample the carbonate horizon in most areas, although some dilution from carbonate-poor horizons is to be expected. The size and signal response can be increased by coring the soil and selecting the richest carbonate zone, but this is probably operationally impractical.

In surface soil sampling particular attention should be paid to the presence of carbonate material at or near the surface as concretionary nodules or coatings. Commonly, carbonate is found directly on the surface and will be effectively sampled by this procedure (as in 4200N) but it also may be covered by shallow, recently transported material. Differences in sample depth of just a few centimetres may thus change the response for Au. If the carbonate is present as coatings on rocks or gravels, then the volume of the coated material should be considered. Large sized fractions (e.g. gravels) have a small surface area to volume ratio and will consequently give a low response.

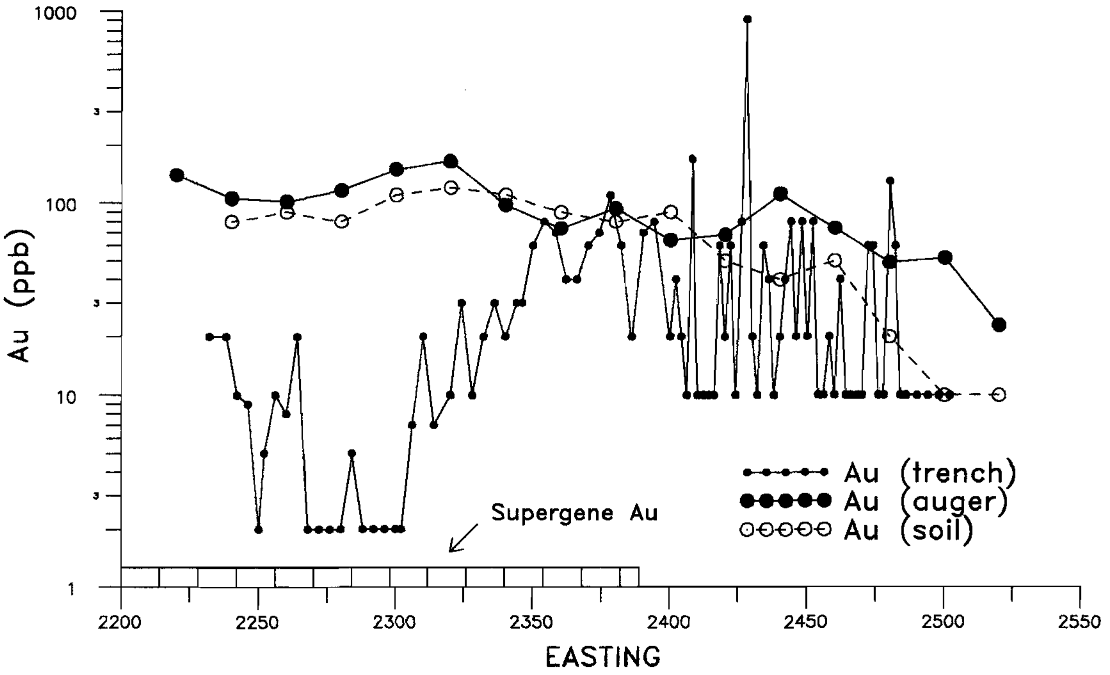

Figure 20: Comparison of Au results using different soil sampling procedures.

Of all the soil sampling procedures examined, trench sampling appears to be the most vulnerable to mis-interpretation yet potentially offers the greatest amount of information (Figure 20). The results have demonstrated how the depth of the trench is important for sampling. Trench sampling is performed by taking channel samples at a standard height (usually knee or waist) from the bottom of the trench. As carbonate is usually found within a metre of the surface, a 2m deep trench will be incorrectly sampled by the "standard" procedure and may miss the Au anomaly altogether. In a 1m (or less) deep trench samples are likely to contain carbonate and will be correctly sampled. The trench at 3700N becomes shallower from the gravels (e.g. at Profile A) to the partially weathered rock (e.g. at Profile B) as the earthmoving equipment cannot penetrate the harder material. Here, the "standard" procedures only samples the carbonates in the shallow part of the trench and so incorrectly locate the position of underlying mineralization (assuming vertical migration of Au). The error of location at 3700N is a few tens of metres but in certain circumstances a trench anomaly may be ignored as being false and underlying mineralization missed completely.

6.2.2. Vegetation sampling.

The importance of the role of vegetation sampling in gold exploration at Panglo appears less well defined and are attributable to biogeochemical sampling problems in general. The composition of vegetation reflects, to a great extent, a) the availability of the element in the vicinity of the root system and b) the ability of the plant to accumulate elements within its cell structures. Other more specific considerations for biogeochemical sampling include the particular plant organ sampled e.g. leaves, roots or branches, the age and health of the plant, genetically-determined individual variation and the time of year sampled. The major perceived advantage that biogeochemistry has over soil sampling is that it can, indirectly, potentially sample greater depths.

Despite the presence of Au in vegetation, it has been shown that biogeochemistry alone cannot be used as an exploration tool at Panglo as it does not correctly define the location of underlying mineralization on either traverse. There is some evidence that on 3700N, there is a relation between Au in vegetation and Au in soils, but on 4200N, there is no indication that the Au content of vegetation reflects either Au in soils or mineralization at depth. Vegetation Au contents are generally lower at Panglo relative to those reported at Mt. Hope (Lintern, 1989) and Norseman (Smith and Keele, 1984) particularly over mineralization. This probably reflects the depth to mineralization which at Panglo is about 40m and at Mt. Hope is within a few metres of the surface. If vegetation is to be sampled it was found at both Panglo and Mt. Hope that the shrub species (*Eremophila* and *Melaleuca* spp.) have higher Au concentrations than the trees (*Eucalyptus* spp.) over mineralization.

Carbonate-enriched soil horizons may be entirely absent, or separated from Au enrichment for a variety of reasons. These may include, for example, different (i) soil moisture, (ii) soil types, (iii) soil temperature, (iv) biological activity, (v) climatic regime and (vi) lithology. More data are obviously required on this topic. Although above background Au values are generally found in calcite, Au maxima concentrations in some soil profiles (e.g. Profile C) do not strictly correspond with Ca maxima concentrations.

6.2.3. Analytical methods.

The results of the cyanide extraction of unpulverized samples indicate that a large proportion of the Au found in soils is easily dissolved. This is not surprising as laboratory studies have shown that some soil Au will dissolve in water (Gray and Lintern, 1990). The cyanide extraction method has several advantages as a routine analytical procedure for exploration over other methods currently used such as fire assay fusion and *aqua regia* digestion (Fletcher and Horsky, 1988; Lintern, 1988). These advantages include opportunities to (i) reduce contamination risk from laboratory sample preparation procedures e.g. sample crushing and pulverization, (ii) take a larger more-representative sample size, (iii) to perform in-field preparation (and analysis, see Lintern, 1988) of soil digest solutions e.g. a few millilitres ready for analysis thus circumventing the need to transport several kilos of solid samples (iv) potentially lower analytical costs. The main disadvantage of cyanide digestion is the uncertainty of not knowing whether a large proportion of the Au has been solubilized effectively. This concern can be resolved, in part, by the inclusion of several check samples retained in solid form for total Au analysis.

7. REFERENCES.

Butt, C.R.M., Horwitz, R.C. and Mann, A.W., 1977. Uranium occurrences in calcrete and associated sediments in Western Australia. Division of Mineralogy Report FP16. CSIRO, Floreat Park, W.A. 6014, Australia.

Fletcher, K and Horsky, S., 1988. Determination of gold by cyanidation and graphite furnace atomic absorption spectroscopy. *Journal of Geochemical Exploration*, 30, 29-34.

Gray, D.J., 1990. Hydrogeochemistry of the Panglo deposit. (AMIRA P241: Weathering Processes). Division of Exploration Geoscience Restricted Report 125R. CSIRO, Floreat Park, W.A. 6014, Australia.

Gray, D.J., Lintern, M.J., and Longman G.D., 1990. Chemistry of Gold in Some Western Australian Soils. (AMIRA P241: Weathering Processes). Division of exploration Geoscience Restricted Report 126R. CSIRO, Floreat Park, W.A. 6014, Australia.

Lawrance, L.M., 1988. Geochemical dispersion anomalies in transported overburden around the quartz vein system at the Mount Pleasant Gold Mine, Western Australia. The Second International Conference on Prospecting in Arid Terrain, Perth, Western Australia. The Australian Institute of Mining and Metallurgy, Victoria, Australia.

Lintern, M.J., 1988. In-field analysis for gold. In Sample Preparation and Analyses for Gold and Platinum-Group Elements. Bulletin No. 8. Australian Institute of Geoscientists, N.S.W., Australia.

Lintern, M.J., 1989. Study of the distribution of gold in soils at Mt. Hope, Western Australia. (AMIRA P241: Weathering Processes). Division of Exploration Geoscience Restricted Report No. 24R. CSIRO, Floreat Park, W.A. 6014, Australia.

Lintern, M.J., Churchward, H.M. and Butt, C.R.M., 1990. Multi-element soil survey of the Mount Hope Area, Western Australia. (AMIRA P241: Weathering Processes). Division of Exploration Geoscience Restricted Report No. 109R. CSIRO, Floreat Park, W.A. 6014, Australia.

Millot G., Nahon D., Paquet H., Ruellan A. and Tardy Y., 1977. L'epigenie calcaire des roches silicatees dans les encroutements carbonates en pays subaride. Anti-Atlas, Maroc, Sci. Geol., Bull., 30, pp. 129-152. (Cited in Ruellan A., 1986. Calcrete Formation and its influences on rocks weathering and relief evolution: a review of the works of the French school. Proceedings of the XII Congress of the International Society of Soil Science).

Milnes, A.R. and Hutton, J.T., 1983. Calcretes in Australia. In "Soils: an Australian viewpoint". CSIRO/Academic Press. pp928.

Nahon D., Millot G., Paquet H., Ruellan A. and Tardy Y., 1977. Geochemie de la surface et formes du relief. VII. Digestion et effacement des cuirasses ferrugineuses par les encroutements calcaires en pays aride, Sahara de Mauritanie. Sci. Geol., Bull., 30, pp. 289-297

Norrish, K and Chappell, B.W., 1977. X-ray flourescence spectroscopy. In "Physical methods in Determinative Mineralogy." 2nd Edition (Ed. J. Zussman) ;; 201-272. (Academic Press).

Pettijohn, F.J., Potter, P.E. and Siever, R., 1972. Sand and Sandstone, Springer-Verlag, Berlin, Heidelberg.

Scott, K.M. and Dickson, B.L., 1989. Radioelements in weathered shales and mafic volcanics, Panglo gold deposit, Eastern Goldfields, W.A. (AMIRA P241: Weathering Processes). Division of Exploration Geoscience Restricted Report No. 41R. CSIRO, North Ryde, N.S.W. 2113, Australia.

Scott, K.M., 1989. Mineralogy and geochemistry of weathered mafic/ultramafic volcanics from Section 4200N at Panglo, Eastern Goldfields, W.A. (AMIRA P241: Weathering Processes). CSIRO Division of Exploration Geoscience Restricted Report No. 42R. CSIRO, North Ryde, N.S.W. 2113, Australia.

Scott, K.M., 1990. The mineralogy and geochemical effects of weathering on volcanics from the Panglo deposit, Eastern Goldfields, W.A. (AMIRA P241: Weathering Processes). CSIRO Division of Exploration Geoscience Restricted Report No. 143R. CSIRO, North Ryde, N.S.W. 2113, Australia.

Scott, K.M., and Dotter, 1990. The Mineralogy and geochemical effects of weathering on shales at the Panglo deposit, Eastern Goldfields, W.A. (AMIRA P241: Weathering Processes). CSIRO Division of Exploration Geoscience Restricted Report No. 171R. CSIRO, North Ryde, N.S.W. 2113, Australia.

Smith, B.H. and Keele, R.A., 1984. Some observations on the geochemistry of gold mineralization in the weathered zone at Norseman, Western Australia. *Journal of Geochemical Exploration*, 22, 21-42.

Young, A.Y., 1976. Tropical Soils and Soil Survey. Cambridge University Press, England. pp468

8. ACKNOWLEDGEMENTS.

The sponsors of AMIRA Project P241 are thanked for their support and in particular, R.W. Howard of Pancontinental Mining Ltd,, for allowing access to the site and for supplying maps, photographs and sections relating to the area. We are indebted to the staff at CSIRO. This includes J.F. Crabb and R.J. Bilz for sample preparation, J.W. Wildman and G.D. Longman for ICP analysis, M.K. Hart for XRF analysis and C.R. Steel and A. D. Vartesi for drafting. We also acknowledge C. Dornan for his valuable assistance with the SEM studies and XRD interpretation. Thanks also go to C.R.M. Butt for comments on earlier drafts of the manuscript.

9. APPENDICES.

1. Profile A-E samples: Tabulated and graphed data.

2. Near-surface samples: Tabulated and graphed data for 4200N.

3. Auger samples: Graphed data only.

4. Trench samples data: Tabulated data only

5. Vegetation sample data: Tabulated and graphed data.

6. Grab samples: Tabulated data.

7. Tabulated data for Profile C samples showing Au distribution analysis on two size fractions.

SAMPLE	EASTING	NORTHING	DEPTH(m)	SiO2	TiO2	Al203	Na2O	Fe2O3	S	MgO	CaO	P2O5
04-2085	2278	3700	0.025	31.80	0.82	8.59	0.27	37.53	0.052	0.78	8.06	0
04-2086	2278	3700	0.075	40.50	0.80	8.76	0.00	40.95	0.03	0.54	3.46	0
04-2087	2278	3700	0.125	42.20	0.70	8.82	0.04	33.47	0.03	0.76	5.30	0
04-2088	2278	3700	0.175	38.47	0.72	8.02	0.18	30.95	0.042	0.90	8.17	0
04-2089	2278	3700	0.250	32.91	0.54	7.57	0.08	26.93	0.065	1.11	13.02	0
04-2090	2278	3700	0.350	29.72	0.56	8.07	0.08	27.19	0.091	1.12	14.46	0
04-2091	2278	3700	0.450	29.41	0.55	11.16	0.47	25.73	0.085	1.05	16.29	0
04-2092	2278	3700	0.550	27.74	0.69	12.46	0.54	35.69	0.089	0.74	10.03	0
04-2093	2278	3700	0.650	23.76	0.73	12.45	0.77	41.52	0.075	0.59	7.03	0
04-2094	2278	3700	0.750	26.09	0.82	13.13	0.88	44.62	0.09	0.51	3.25	0
04-2095	2278	3700	0.850	29.05	0.88	11.95	0.88	44.57	0.085	0.55	3.44	0
04-2096	2278	3700	0.950	27.69	1.02	11.31	0.87	47.55	0.067	0.48	2.62	0
04-2097	2278	3700	1.100	27.95	0.83	12.13	1.01	44.54	0.061	0.43	0.80	0
04-2098	2278	3700	1.300	34.00	0.71	13.19	1.06	35.40	0.086	0.45	0.35	0
04-2099	2278	3700	1.500	35.93	0.65	13.80	1.21	32.04	0.089	0.46	0.38	0
04-2100	2278	3700	1.700	23.79	0.80	12.07	1.13	46.16	0.09	0.36	0.23	0
04-2101	2278	3700	1.900	22.25	0.74	12.29	1.52	46.89	0.144	0.34	0.18	0
04-2102	2278	3700	2.100	23.09	0.69	11.27	2.06	44.13	0.227	0.45	0.17	0

SAMPLE	As	Au	Ba	Be	Br	Ce	Co	Cr	Cu	Ga	Ge	Mn
04-2085	179	0.111	224	1	9	22	10	2501	63	22	0	368
04-2086	150	0.042	225	1	6	27	0	2742	54	23	1	423
04-2087	148	0.038	204	1	5	31	8	2337	56	24	1	412
04-2088	135	0.109	241	0	12	26	1	2021	54	19	2	358
04-2089	135	0.152	294	0	13	25	10	1931	60	17	0	320
04-2090	148	0.217	426	0	14	19	9	1793	62	18	0	278
04-2091	123	0.262	234	2	11	10	20	1537	61	19	0	182
04-2092	158	0.174	74	1	12	16	8	2218	69	24	0	202
04-2093	176	0.116	90	1	16	18	11	2568	68	28	3	191
04-2094	165	0.058	253	1	22	20	8	2708	54	29	1	209
04-2095	205	0.057	175	1	21	16	2	2969	48	28	2	155
04-2096	205	0.064	205	3	19	17	5	3249	55	28	2	186
04-2097	227	0.065	348	4	24	21	9	3119	54	33	2	174
04-2098	218	0.025	196	2	25	13	10	2210	51	24	0	154
04-2099	182	0.034	137	2	29	17	15	2098	57	27	0	158
04-2100	249	0.017	131	2	30	17	0	3362	52	35	0	166
04-2101	249	0.009	43	3	36	14	6	3106	52	33	1	180
04-2102	241	0.003	70	3	60	19	13	3306	60	33	0	168

SAMPLE	Mo	Nb	Ni	Pb	Rb	Sb	Sr	V	W	Y	Zn	Zr
04-2085	1	2	129	22	13	7	93	671	5	7	26	115
04-2086	2	5	138	20	16	7	47	762	1	7	28	136
04-2087	1	2	127	19	13	6	60	688	1	7	25	125
04-2088	1	8	121	12	14	5	108	636	2	8	22	119
04-2089	2	1	150	15	9	5	153	522	1	7	19	123
04-2090	2	1	127	13	8	5	168	610	1	8	16	94
04-2091	4	3	152	10	4	4	153	499	1	3	16	86
04-2092	2	4	152	14	3	5	96	680	1	4	13	94
04-2093	4	4	153	13	3	6	67	711	1	6	14	101
04-2094	0	1	162	16	5	7	55	606	1	6	15	107
04-2095	3	2	138	16	7	8	51	607	1	5	16	130
04-2096	7	4	152	16	7	8	49	794	1	6	11	133
04-2097	1	2	162	22	6	8	39	735	1	7	11	123
04-2098	2	4	155	17	9	6	40	577	1	4	21	125
04-2099	0	2	167	13	5	5	40	606	2	6	18	112
04-2100	1	2	165	17	6	9	36	843	1	5	14	121
04-2101	2	3	193	18	8	8	29	833	1	5	16	114
04-2102	0	2	194	17	7	8	25	901	1	3	15	113

Appendix 1: Tabulated and graphed data for Profile A.

SiO2 (%)

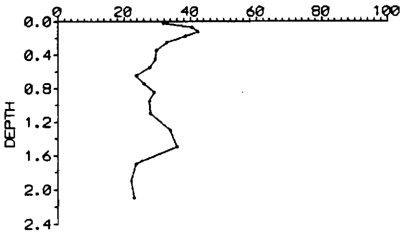

TiO2 (%)

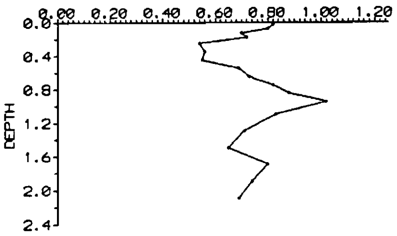

Al2O3 (%)

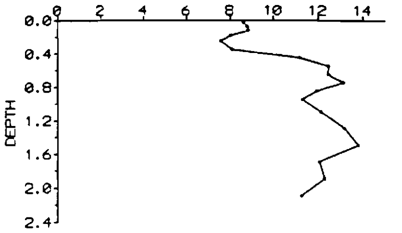

Na2O (%)

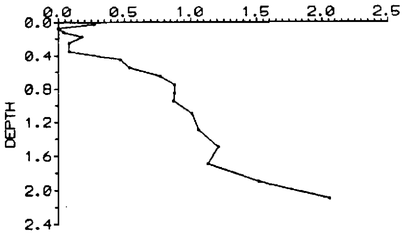

Fe2O3 (%)

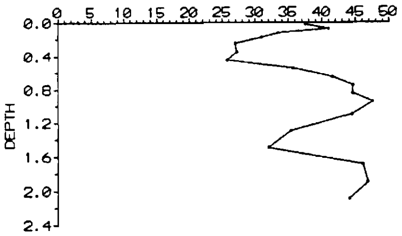

S (%)

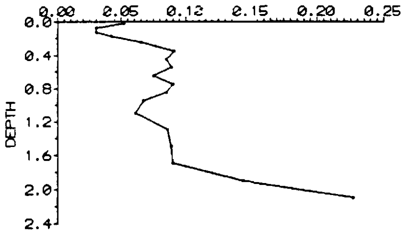

MgO (%)

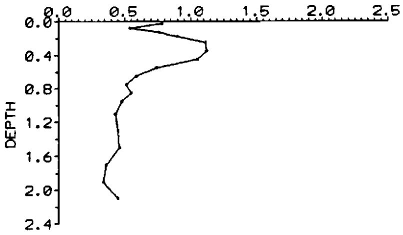

CaO (%)

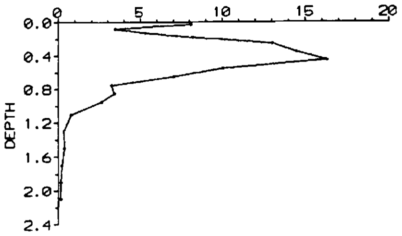

As (ppm)

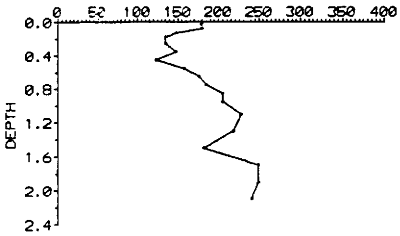

Au (ppm)

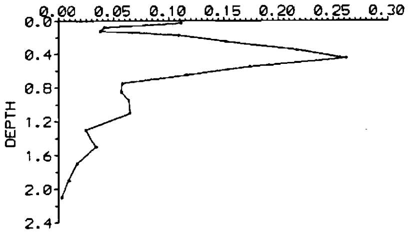

Ba (ppm)

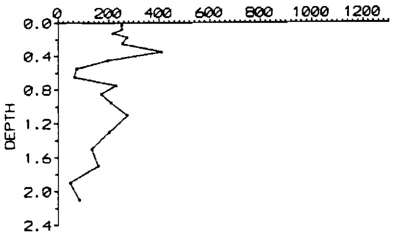

Br (ppm)

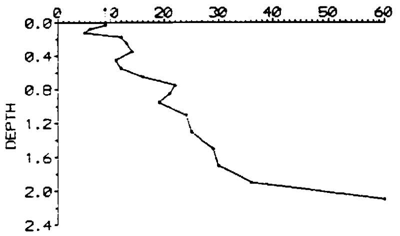

Ce (ppm)

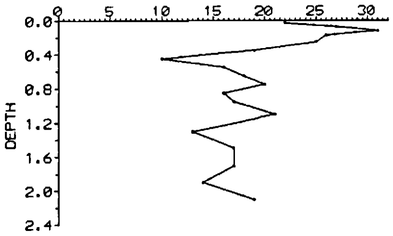

Co (ppm)

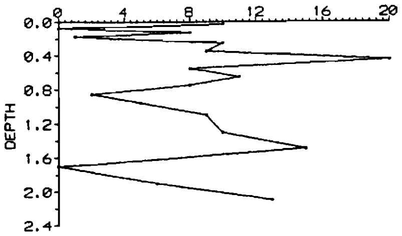

Cr (ppm)

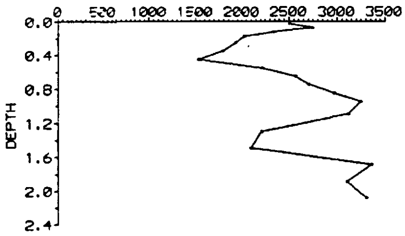

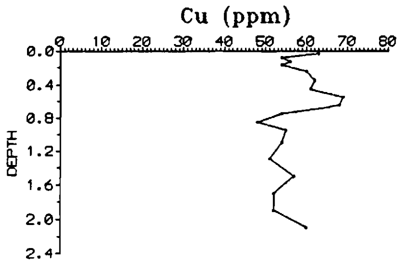
Cu (ppm)
0 10 20 30 40 50 60 70 80
DEPTH
0.0 0.4 0.8 1.2 1.6 2.0 2.4

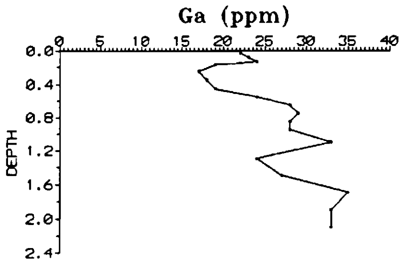
Ga (ppm)
0 5 10 15 20 25 30 35 40
DEPTH
0.0 0.4 0.8 1.2 1.6 2.0 2.4

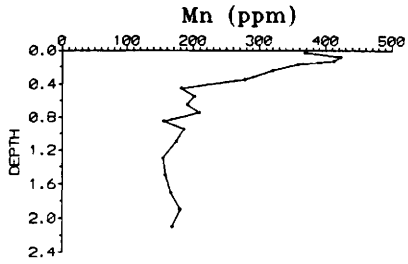
Mn (ppm)
0 100 200 300 400 500
DEPTH
0.0 0.4 0.8 1.2 1.6 2.0 2.4

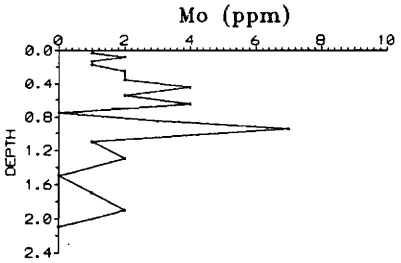
Mo (ppm)
0 2 4 6 8 10
DEPTH
0.0 0.4 0.8 1.2 1.6 2.0 2.4

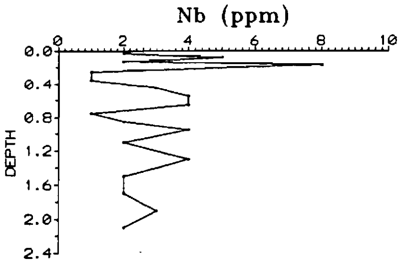
Nb (ppm)
0 2 4 6 8 10
DEPTH
0.0 0.4 0.8 1.2 1.6 2.0 2.4

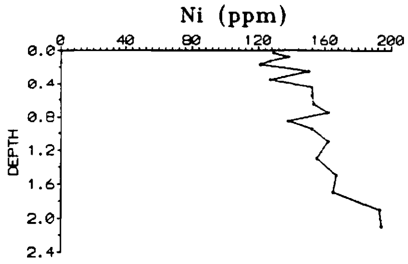
Ni (ppm)
0 40 80 120 160 200
DEPTH
0.0 0.4 0.8 1.2 1.6 2.0 2.4

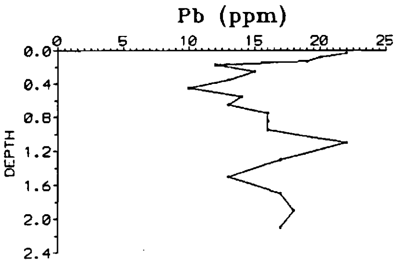
Pb (ppm)
0 5 10 15 20 25
DEPTH
0.0 0.4 0.8 1.2 1.6 2.0 2.4

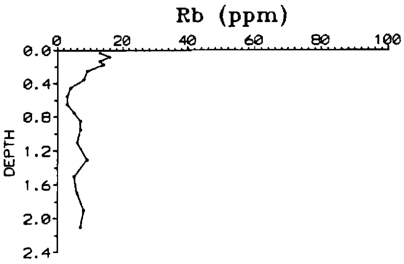
Rb (ppm)
0 20 40 60 80 100
DEPTH
0.0 0.4 0.8 1.2 1.6 2.0 2.4

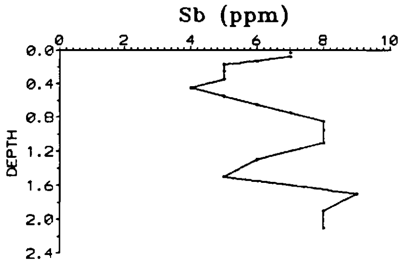
Sb (ppm)
0 2 4 6 8 10
DEPTH
0.0 0.4 0.8 1.2 1.6 2.0 2.4

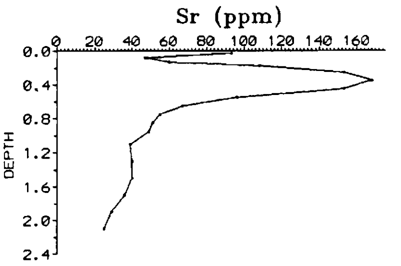
Sr (ppm)
0 20 40 60 80 100 120 140 160
DEPTH
0.0 0.4 0.8 1.2 1.6 2.0 2.4

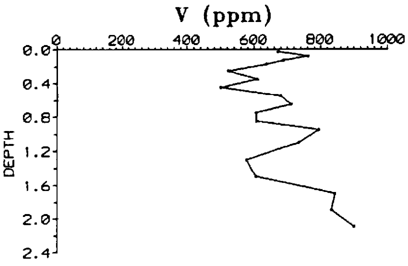
V (ppm)
0 200 400 600 800 1000
DEPTH
0.0 0.4 0.8 1.2 1.6 2.0 2.4

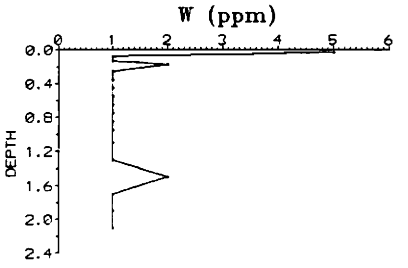
W (ppm)
0 1 2 3 4 5 6
DEPTH
0.0 0.4 0.8 1.2 1.6 2.0 2.4

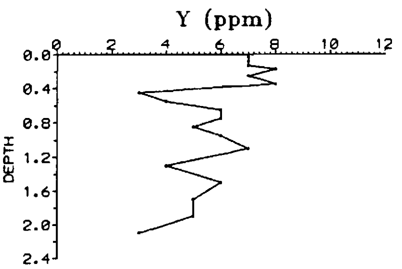
Y (ppm)
0 2 4 6 8 10 12
DEPTH
0.0 0.4 0.8 1.2 1.6 2.0 2.4

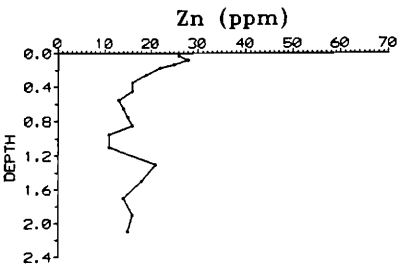
Zn (ppm)
0 10 20 30 40 50 60 70
DEPTH
0.0 0.4 0.8 1.2 1.6 2.0 2.4

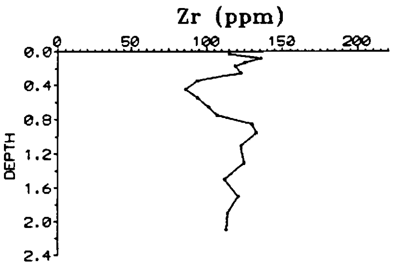
Zr (ppm)
0 50 100 150 200
DEPTH
0.0 0.4 0.8 1.2 1.6 2.0 2.4

SAMPLE	EASTING	NORTHING	DEPTH(m)	SiO2	TiO2	Al2O3	Na2O	Fe2O3	S	MgO	CaO	P2O5
04-2103	2375	3700	0.025	32.95	0.57	7.65	0.47	27.72	0.053	0.75	8.03	0
04-2104	2375	3700	0.075	33.32	0.50	8.20	0.32	30.72	0.064	0.87	9.94	0
04-2105	2375	3700	0.150	27.38	0.45	8.84	0.42	35.81	0.075	0.87	8.73	0
04-2106	2375	3700	0.250	23.49	0.47	8.43	0.38	43.16	0.063	0.78	8.69	0
04-2107	2375	3700	0.350	20.63	0.47	8.20	0.21	49.78	0.055	0.67	5.78	0
04-2108	2375	3700	0.450	24.93	0.50	8.26	0.13	41.04	0.058	0.94	8.59	0
04-2109	2375	3700	0.550	24.98	0.54	9.15	0.09	47.94	0.067	0.68	4.07	0
04-2110	2375	3700	0.650	29.52	0.60	10.49	0.13	39.91	0.058	0.83	5.09	0
04-2111	2375	3700	0.750	23.56	0.53	8.70	0.00	46.49	0.076	0.72	4.07	0

SAMPLE	As	Au	Ba	Be	Br	Ce	Co	Cr	Cu	Ga	Ge	Mn
04-2103	195	0.084	252	2	10	21	14	1435	61	16	1	420
04-2104	207	0.112	334	1	19	20	7	1115	70	16	0	289
04-2105	275	0.123	770	3	19	17	9	901	76	18	1	159
04-2106	335	0.112	658	2	14	21	3	1125	66	18	3	124
04-2107	373	0.128	702	2	12	17	0	1163	76	18	3	104
04-2108	305	0.132	825	0	11	16	0	1168	55	19	0	112
04-2109	316	0.112	1181	0	10	16	0	1018	57	17	1	72
04-2110	217	0.108	1192	0	9	10	0	1093	48	20	1	83
04-2111	278	0.064	1085	2	10	14	0	984	64	19	2	67

SAMPLE	Mo	Nb	Ni	Pb	Rb	Sb	Sr	V	W	Y	Zn	Zr
04-2103	3	3	111	9	17	5	85	553	1	7	30	115
04-2104	2	4	84	10	19	4	104	482	1	6	25	103
04-2105	2	2	61	12	15	4	105	612	1	5	18	96
04-2106	2	1	57	13	15	4	90	815	1	7	10	86
04-2107	4	0	47	8	13	4	74	993	1	7	8	85
04-2108	3	1	63	10	13	5	107	874	1	3	13	86
04-2109	8	3	41	8	15	4	88	941	1	8	13	92
04-2110	3	4	49	10	17	4	98	599	1	7	14	102
04-2111	3	0	39	6	16	4	96	857	1	7	9	83

Appendix 1: Tabulated and graphed data for Profile B.

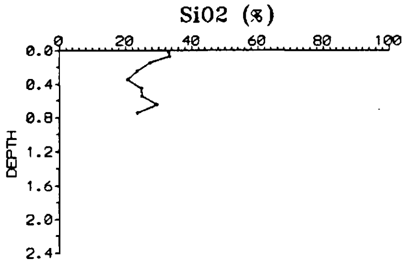
SiO2 (%)
0 20 40 60 80 100
0.0 0.4 0.8 1.2 1.6 2.0 2.4
DEPTH

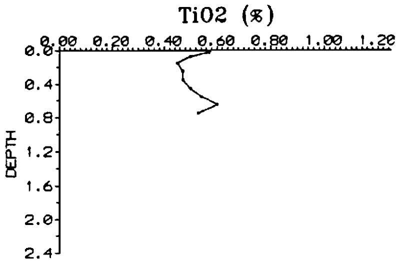
TiO2 (%)
0.00 0.20 0.40 0.60 0.80 1.00 1.20
0.0 0.4 0.8 1.2 1.6 2.0 2.4
DEPTH

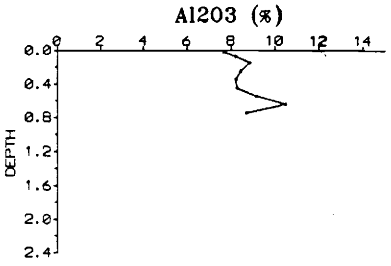
Al2O3 (%)
0 2 4 6 8 10 12 14
0.0 0.4 0.8 1.2 1.6 2.0 2.4
DEPTH

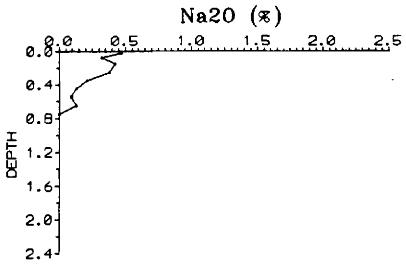
Na2O (%)
0.0 0.5 1.0 1.5 2.0 2.5
0.0 0.4 0.8 1.2 1.6 2.0 2.4
DEPTH

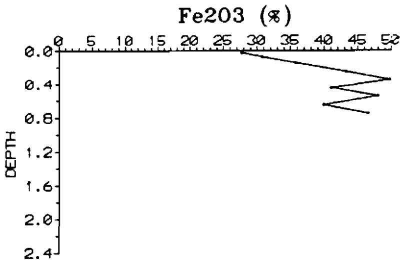
Fe2O3 (%)
0 5 10 15 20 25 30 35 40 45 50
0.0 0.4 0.8 1.2 1.6 2.0 2.4
DEPTH

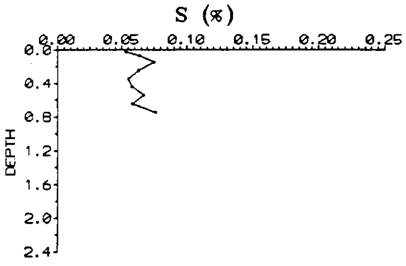
S (%)
0.00 0.05 0.10 0.15 0.20 0.25
0.0 0.4 0.8 1.2 1.6 2.0 2.4
DEPTH

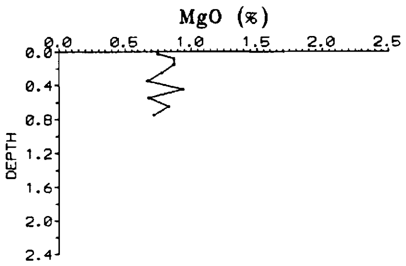
MgO (%)
0.0 0.5 1.0 1.5 2.0 2.5
0.0 0.4 0.8 1.2 1.6 2.0 2.4
DEPTH

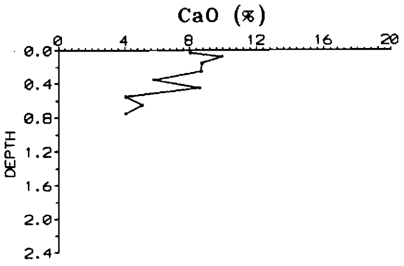
CaO (%)
0 4 8 12 16 20
0.0 0.4 0.8 1.2 1.6 2.0 2.4
DEPTH

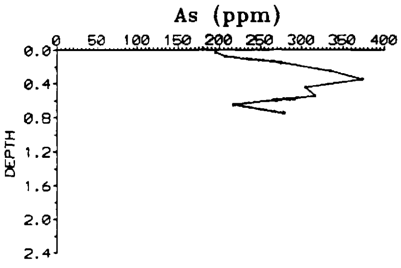
As (ppm)
0 50 100 150 200 250 300 350 400
0.0 0.4 0.8 1.2 1.6 2.0 2.4
DEPTH

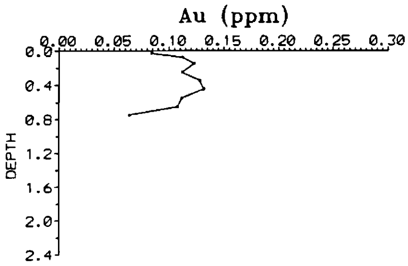
Au (ppm)
0.00 0.05 0.10 0.15 0.20 0.25 0.30
0.0 0.4 0.8 1.2 1.6 2.0 2.4
DEPTH

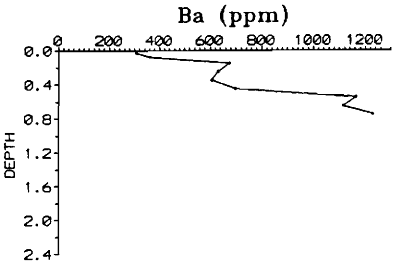
Ba (ppm)
0 200 400 600 800 1000 1200
0.0 0.4 0.8 1.2 1.6 2.0 2.4
DEPTH

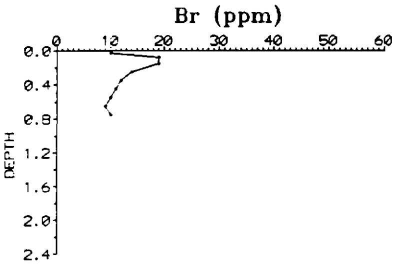
Br (ppm)
0 10 20 30 40 50 60
0.0 0.4 0.8 1.2 1.6 2.0 2.4
DEPTH

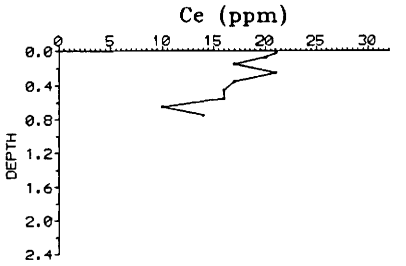
Ce (ppm)
0 5 10 15 20 25 30
0.0 0.4 0.8 1.2 1.6 2.0 2.4
DEPTH

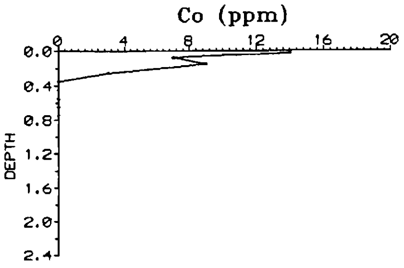
Co (ppm)
0 4 8 12 16 20
0.0 0.4 0.8 1.2 1.6 2.0 2.4
DEPTH

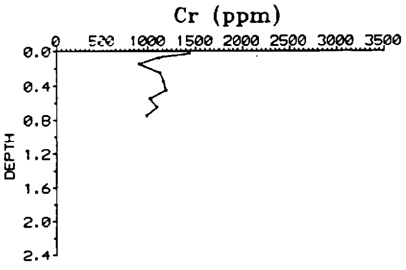
Cr (ppm)
0 500 1000 1500 2000 2500 3000 3500
0.0 0.4 0.8 1.2 1.6 2.0 2.4
DEPTH

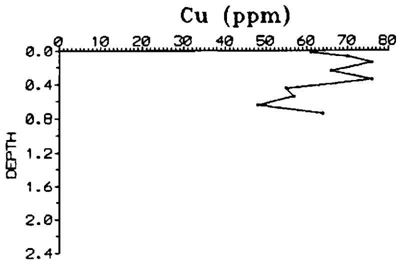
Cu (ppm)

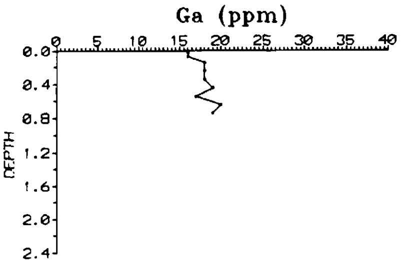
Ga (ppm)

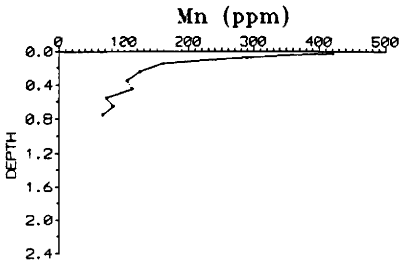
Mn (ppm)

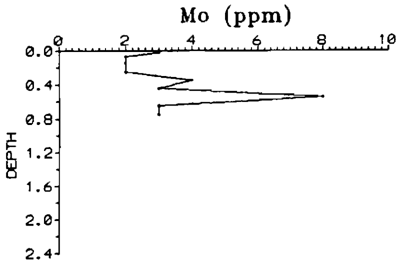
Mo (ppm)

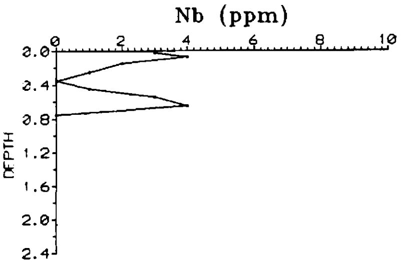
Nb (ppm)

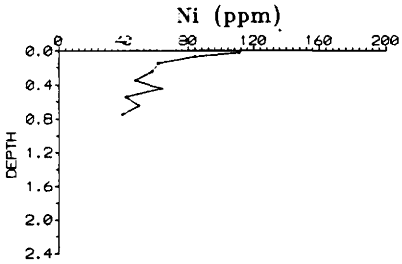
Ni (ppm)

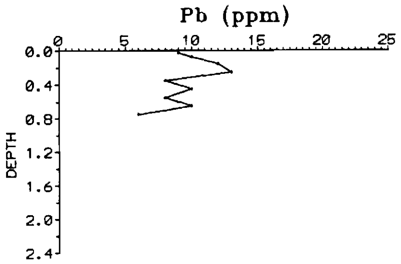
Pb (ppm)

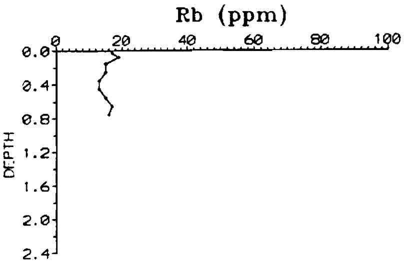
Rb (ppm)

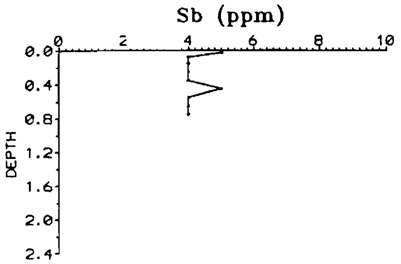
Sb (ppm)

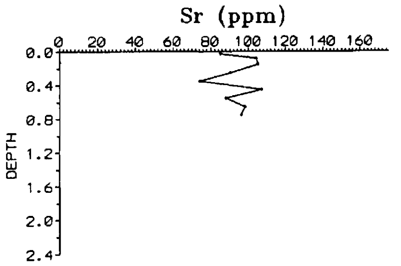
Sr (ppm)

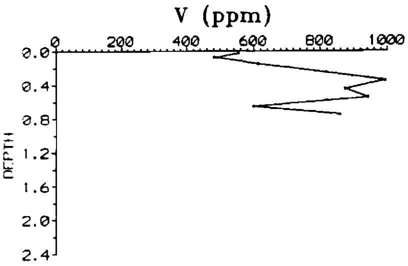
V (ppm)

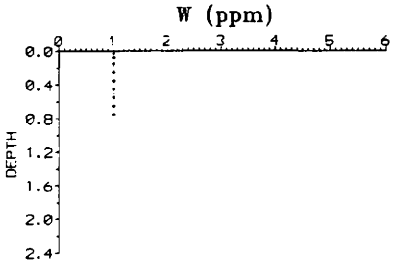
W (ppm)

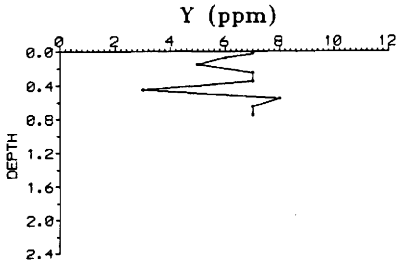
Y (ppm)

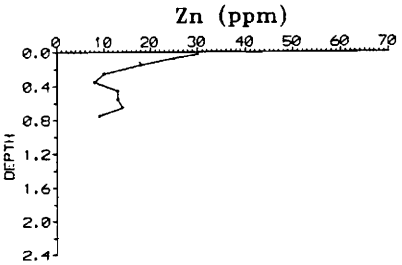
Zn (ppm)

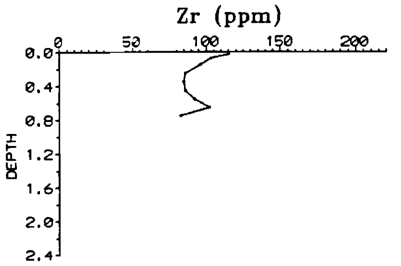
Zr (ppm)

SAMPLE	EASTING	NORTHING	DEPTH(m)	SiO2	TiO2	Al2O3	Na2O	Fe2O3	S	MgO	CaO	P2O5
04-2113	2505	3700	0.025	64.05	0.63	10.64	0.42	10.19	0.142	1.81	0.42	0
04-2114	2505	3700	0.075	73.28	0.58	8.70	0.29	11.13	0.117	1.69	0.44	0
04-2115	2505	3700	0.125	70.63	0.63	8.41	0.29	12.61	0.084	1.48	0.29	0
04-2116	2505	3700	0.175	67.11	0.62	9.72	0.29	11.31	0.118	1.46	0.26	0
04-2117	2505	3700	0.250	66.20	0.65	10.48	0.43	8.67	0.161	1.63	0.82	0
04-2118	2505	3700	0.350	70.06	0.74	9.31	0.44	8.37	0.189	1.43	0.39	0
04-2119	2505	3700	0.450	63.02	0.58	11.31	0.43	9.57	0.213	1.77	0.94	0
04-2120	2505	3700	0.550	62.83	0.57	12.79	0.42	9.36	0.177	2.33	0.28	0
04-2121	2505	3700	0.650	69.46	0.56	8.52	0.31	8.38	0.131	1.58	0.18	0
04-2122	2505	3700	0.750	65.92	0.63	8.82	0.43	9.87	0.086	1.69	0.21	0
04-2123	2505	3700	0.850	71.27	0.78	7.08	0.31	9.21	0.096	1.17	0.16	0
04-2124	2505	3700	0.950	71.69	0.85	7.14	0.44	9.16	0.122	0.89	0.15	0
04-2125	2505	3700	1.100	75.09	0.42	5.26	0.18	10.04	0.111	0.46	0.12	0
04-2126	2505	3700	1.300	75.19	0.30	4.90	0.18	11.26	0.11	0.31	0.09	0
04-2127	2505	3700	1.500	74.75	0.37	8.59	0.31	7.72	0.045	0.34	0.08	0
04-2128	2505	3700	1.700	69.27	0.43	12.65	0.45	5.30	0.004	0.35	0.08	0

SAMPLE	As	Au	Ba	Be	Br	Ce	Co	Cr	Cu	Ga	Ge	Mn
04-2113	150	0.024	395	1	7	14	19	385	58	18	1	318
04-2114	144	0.022	401	1	6	15	19	429	54	14	1	314
04-2115	180	0.013	446	0	6	19	16	424	59	16	2	309
04-2116	173	0.030	419	0	6	16	18	413	62	16	2	324
04-2117	150	0.035	352	0	5	14	11	322	60	16	2	239
04-2118	142	0.027	344	0	4	20	19	299	51	16	1	184
04-2119	162	0.041	495	0	6	17	6	349	53	21	1	211
04-2120	174	0.053	537	0	6	23	7	350	57	21	2	230
04-2121	160	0.052	430	0	4	17	8	310	47	17	2	162
04-2122	182	0.097	376	0	5	22	15	357	49	16	2	188
04-2123	190	0.096	287	0	4	19	7	322	45	14	1	128
04-2124	184	0.070	307	1	4	16	13	321	43	14	2	123
04-2125	215	0.041	393	0	4	11	12	308	54	13	1	122
04-2126	230	0.053	413	0	4	12	0	408	48	14	1	61
04-2127	153	0.023	426	0	3	16	5	275	42	16	2	59
04-2128	206	0.009	361	0	4	11	0	105	55	25	3	10

SAMPLE	Mo	Nb	Ni	Pb	Rb	Sb	Sr	V	W	Y	Zn	Zr
04-2113	1	3	98	11	39	4	72	236	5	11	57	129
04-2114	5	0	93	10	27	4	59	229	4	10	56	112
04-2115	6	5	84	9	25	4	56	276	1	8	65	112
04-2116	3	5	95	12	34	4	63	258	1	10	63	126
04-2117	4	4	82	9	41	3	76	195	4	11	56	145
04-2118	1	7	64	11	38	3	72	181	1	11	48	155
04-2119	2	4	68	11	47	3	102	239	1	9	50	149
04-2120	2	5	76	13	53	3	100	231	1	10	55	151
04-2121	4	7	53	11	37	3	75	200	3	11	41	147
04-2122	4	5	65	13	38	3	62	236	1	10	50	157
04-2123	4	7	46	17	32	3	55	188	6	12	42	171
04-2124	4	9	42	18	34	3	63	192	5	11	41	185
04-2125	6	3	29	11	22	4	63	199	2	7	38	114
04-2126	4	0	24	9	21	4	66	219	3	4	34	94
04-2127	3	4	17	14	58	5	107	166	2	6	18	148
04-2128	8	9	7	18	95	10	166	120	1	7	6	205

Appendix 1: Tabulated and graphed data for Profile C.

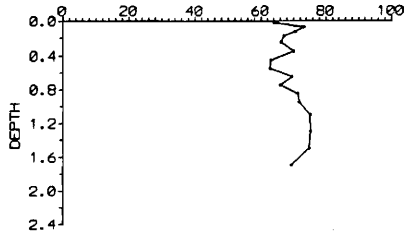
SiO2 (%)

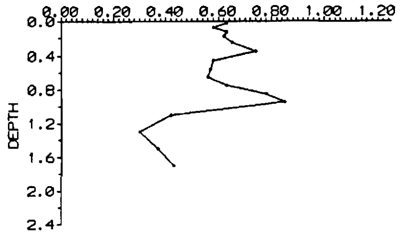
TiO2 (%)

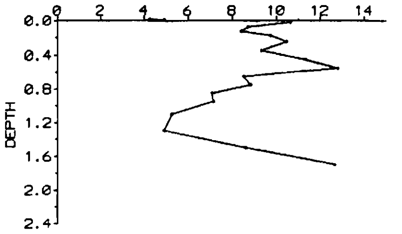
Al2O3 (%)

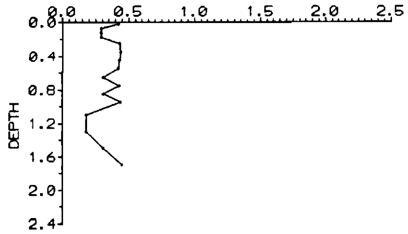
Na2O (%)

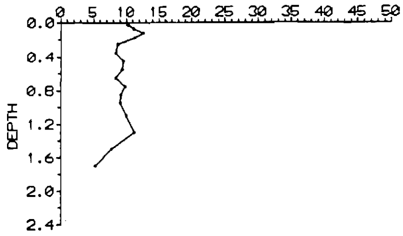
Fe2O3 (%)

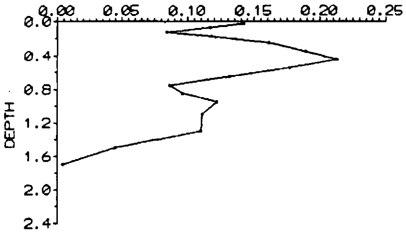
S (%)

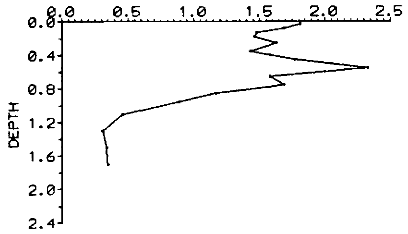
MgO (%)

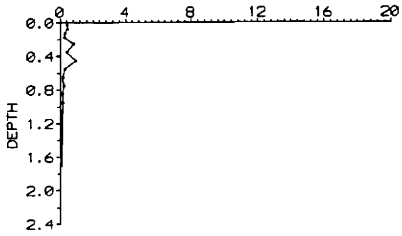
CaO (%)

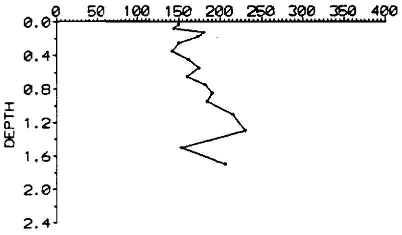
As (ppm)

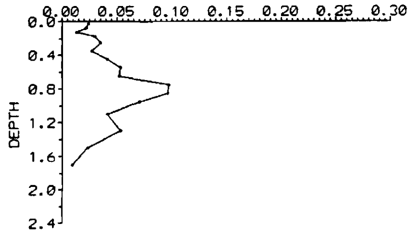
Au (ppm)

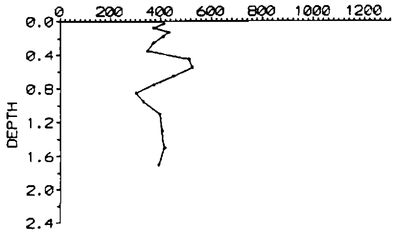
Ba (ppm)

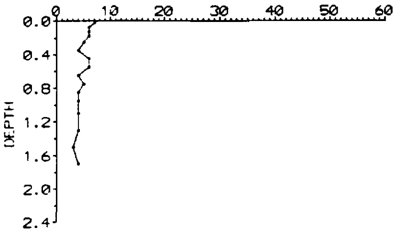
Br (ppm)

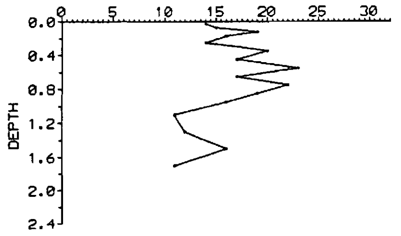
Ce (ppm)

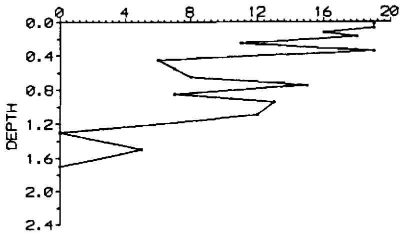
Co (ppm)

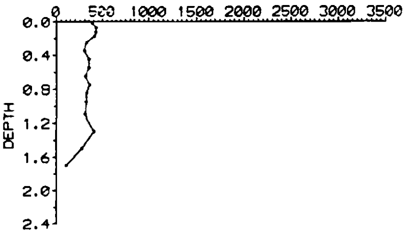
Cr (ppm)

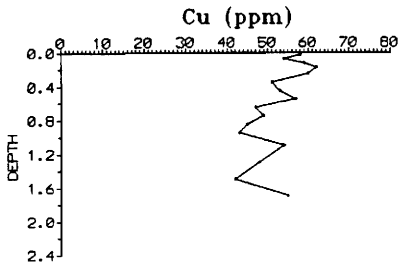
Cu (ppm)

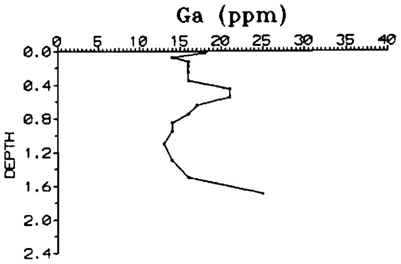
Ga (ppm)

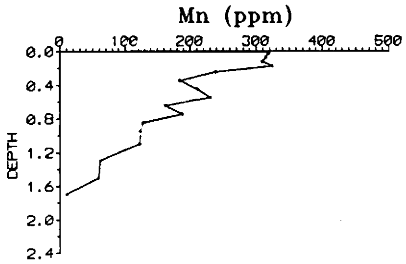
Mn (ppm)

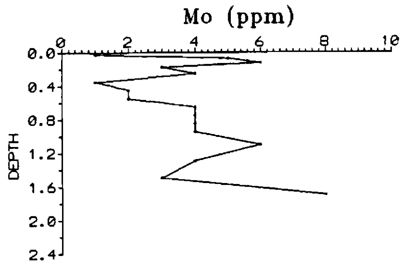
Mo (ppm)

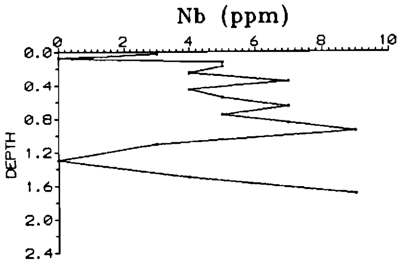
Nb (ppm)

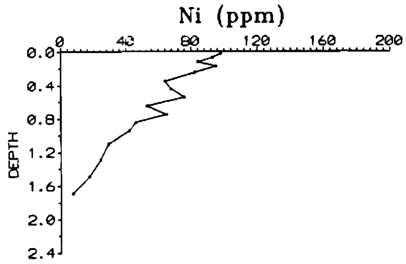
Ni (ppm)

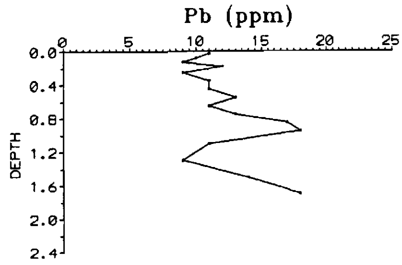
Pb (ppm)

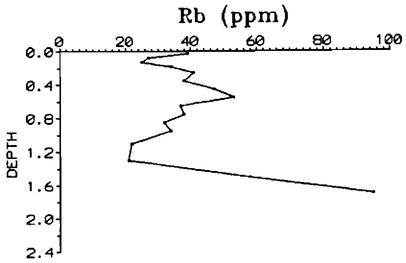
Rb (ppm)

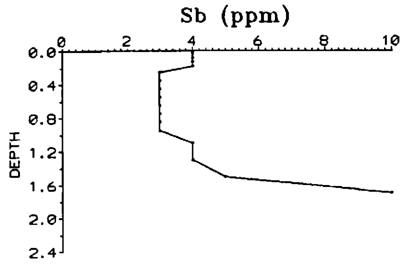
Sb (ppm)

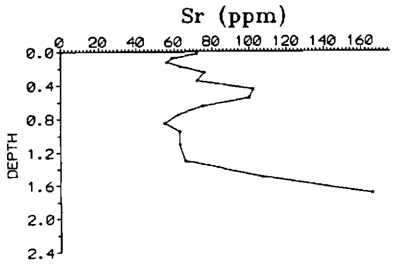
Sr (ppm)

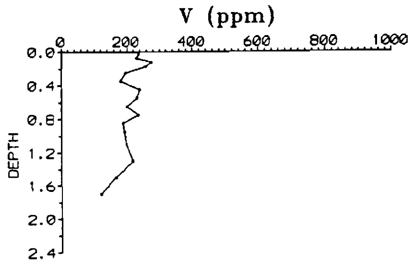
V (ppm)

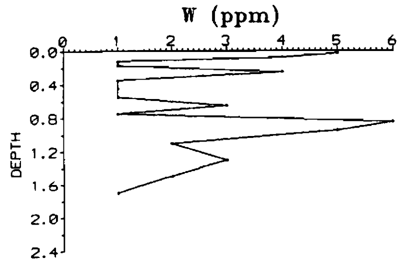
W (ppm)

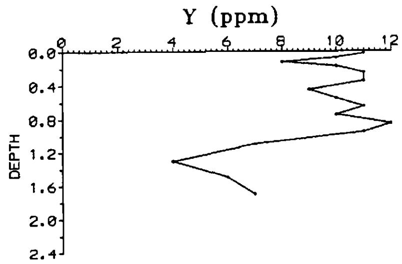
Y (ppm)

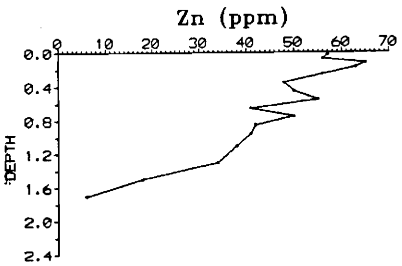
Zn (ppm)

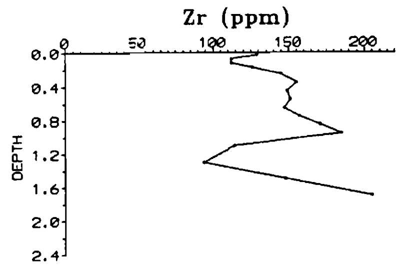
Zr (ppm)

SAMPLE	EASTING	NORTHING	DEPTH(m)	SiO2	TiO2	Al2O3	Na2O	Fe2O3	S	MgO	CaO	P2O5
04-2200	2420	4200	0.025	67.0	0.63	10.6	0.22	11.4	0.054	1.99	0.37	0.08
04-2201	2420	4200	0.075	73.6	0.55	8.2	0.22	11.4	0.038	1.50	0.26	0.05
04-2202	2420	4200	0.125	61.1	0.73	14.8	0.28	11.5	0.042	2.73	0.37	0.09
04-2203	2420	4200	0.175	62.2	0.62	12.7	0.27	12.9	0.036	2.50	0.31	0.05
04-2204	2420	4200	0.225	57.9	0.59	12.6	0.35	15.5	0.039	3.94	0.32	0.04
04-2205	2420	4200	0.275	56.0	0.55	11.5	0.36	13.9	0.046	4.83	1.93	0.05
04-2206	2420	4200	0.350	55.9	0.56	10.5	0.37	13.6	0.062	4.36	3.54	0.04
04-2207	2420	4200	0.450	54.6	0.60	7.6	0.16	26.7	0.046	2.03	1.05	0.00

SAMPLE	As	Au	Ba	Be	Br	Ce	Co	Cr	Cu	Ga	Ge	Mn
04-2200	-	0.024	268	0.0	-	25	20	683	63	1	0	679
04-2201	-	0.010	256	0.0	-	27	17	677	59	1	0	634
04-2202	-	0.018	304	0.4	-	31	30	687	84	2	2	829
04-2203	-	0.024	354	0.0	-	32	22	776	79	1	0	785
04-2204	-	0.064	453	0.0	-	29	18	884	96	2	2	643
04-2205	-	0.086	554	0.0	-	31	18	848	95	1	1	515
04-2206	-	0.080	916	0.0	-	26	20	802	91	1	0	465
04-2207	-	0.210	882	0.0	-	33	19	1650	108	1	0	426

SAMPLE	Mo	Nb	Ni	Pb	Rb	Sb	Sr	V	W	Y	Zn	Zr
04-2200	-	5	166	12	33	-	42	210	-	13	61	116
04-2201	-	3	151	10	25	-	36	201	-	11	47	98
04-2202	-	6	243	17	48	-	49	209	-	17	79	120
04-2203	-	6	213	13	39	-	44	228	-	14	73	101
04-2204	-	4	206	16	38	-	44	285	-	15	71	95
04-2205	-	2	183	13	34	-	60	274	-	12	65	92
04-2206	-	4	173	11	32	-	84	285	-	13	58	94
04-2207	-	6	159	17	18	-	53	547	-	11	44	71

Appendix 1: Tabulated and graphed data for Profile D.

SiO2 (%)

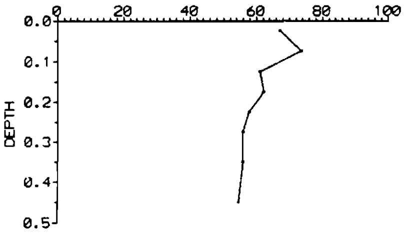

TiO2 (%)

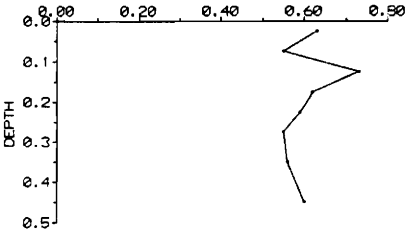

Al2O3 (%)

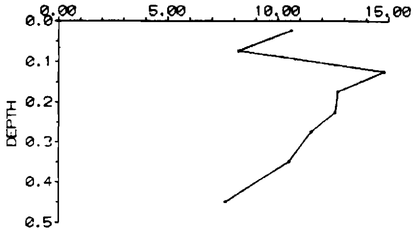

Na2O (%)

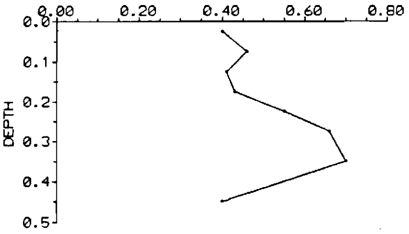

Fe2O3 (%)

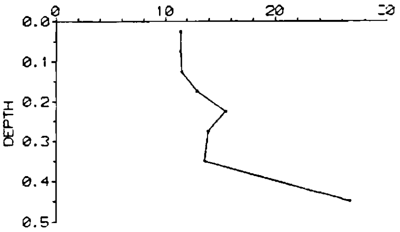

S (%)

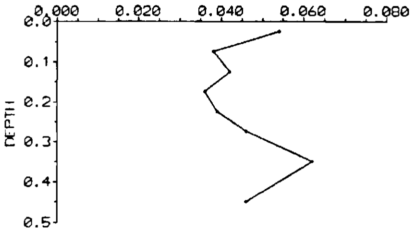

MgO (%)

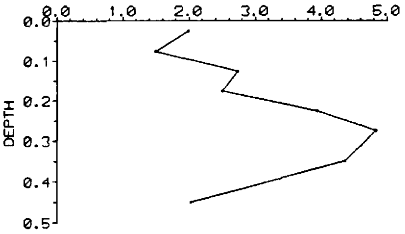

CaO (%)

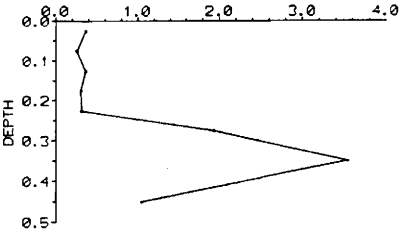

No As Data

Au (ppm)

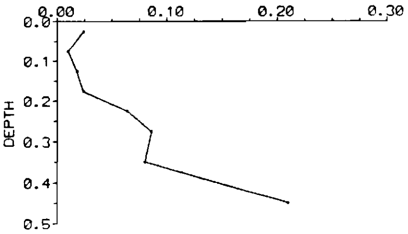

Ba (ppm)

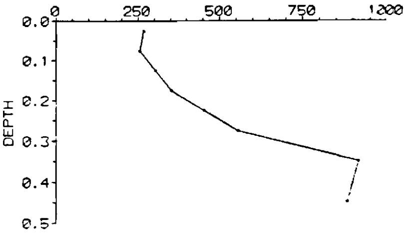

No Br Data

Ce (ppm)

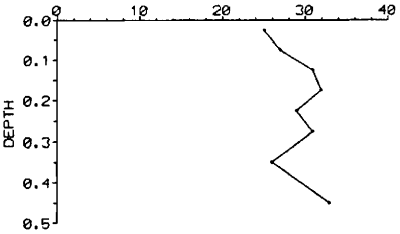

Co (ppm)

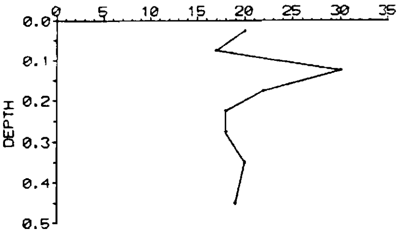

Cr (ppm)

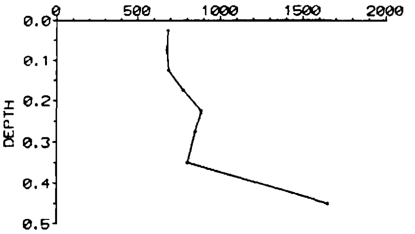

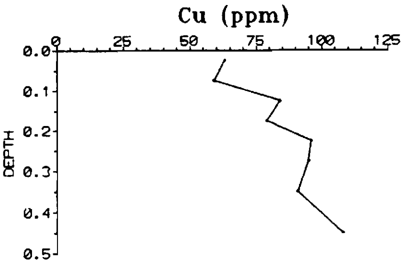

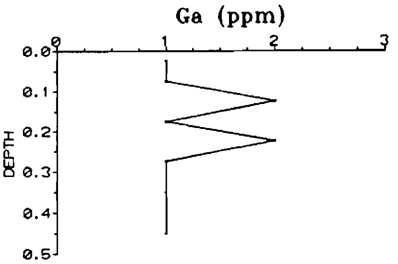

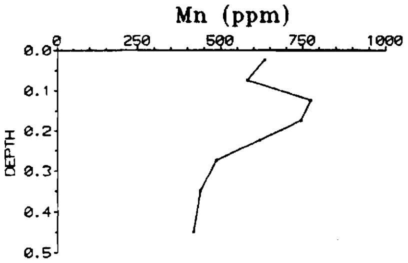

No Mo Data

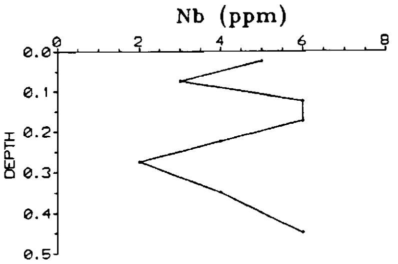

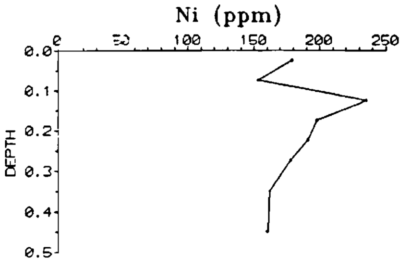

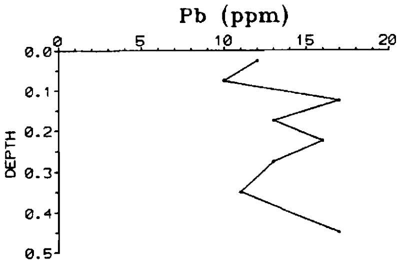

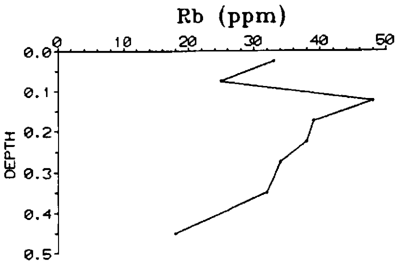

No Sb Data

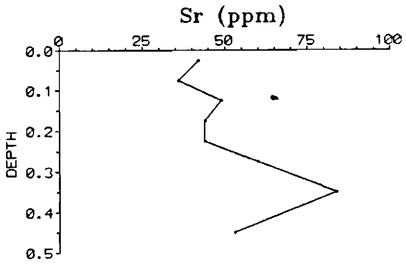

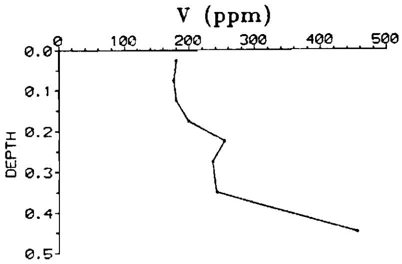

No W Data

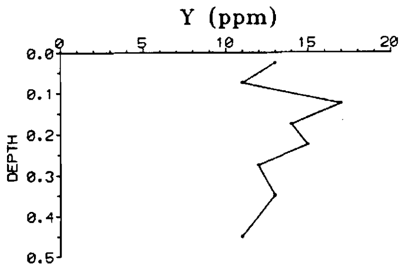

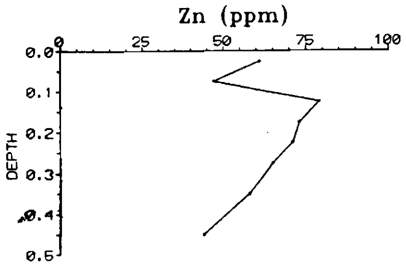

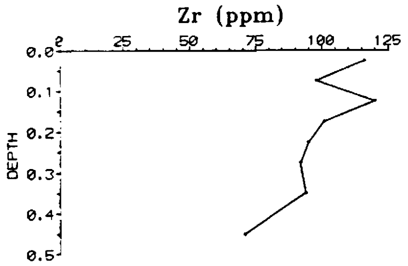

SAMPLE	EASTING	NORTHING	DEPTH(m)	SiO2	TiO2	Al2O3	Na2O	Fe2O3	S	MgO	CaO	P2O5
04-2217	2340	4300	0.025	59.8	0.71	12.59	0.29	16.78	0.064	2.14	0.47	0.06
04-2218	2340	4300	0.075	64.57	0.68	12.27	0.4	14.55	0.086	2.08	0.48	0.04
04-2219	2340	4300	0.125	68.28	0.68	9.88	0.4	14.67	0.184	1.51	0.35	0.05
04-2220	2340	4300	0.175	68.28	0.62	9.04	0.3	15.82	0.188	1.32	0.3	0.01
04-2221	2340	4300	0.225	64.34	0.67	9.41	0.4	20.29	0.145	1.29	0.28	0.03
04-2222	2340	4300	0.275	64.57	0.66	12.65	0.63	14.84	0.181	1.95	0.39	0.04

SAMPLE	Ag	As	Au	Ba	Be	Bi	Ce	Co	Cr	Cs	Cu	Ga	Ge	La
04-2217	2	93	0.014	251	0.559	2	15	23	1085	2	81	20	0	16
04-2218	0	75	0.014	242	0.86	2	12	29	944	1	76	17	1	17
04-2219	1	84	0.018	208	0.009	0	11	17	993	1	68	14	0	12
04-2220	1	89	0.018	217	0.005	0	10	18	1067	1	61	14	0	14
04-2221	4	117	0.02	257	0.259	3	8	13	1337	0	69	16	0	19
04-2222	1	79	0.04	220	0.301	1	14	16	972	2	77	17	0	15

SAMPLE	Mn	Mo	Nb	Ni	Pb	Rb	Sb	Sc	Sr	V	W	Y	Zn	Zr
04-2217	834	1	5	224	17	37	1	23	46	293	0	15	70	123
04-2218	801	2	5	212	15	35	1	21	49	246	3	13	66	124
04-2219	653	2	4	173	11	28	0	18	44	254	1	14	51	140
04-2220	608	2	5	163	11	24	6	18	41	269	0	14	46	118
04-2221	629	0	8	171	17	24	3	20	40	353	2	12	46	120
04-2222	729	0	5	203	13	34	3	22	41	250	0	14	61	123

Appendix 1: Tabulated and graphed data for Profile E.

SiO2 (%)

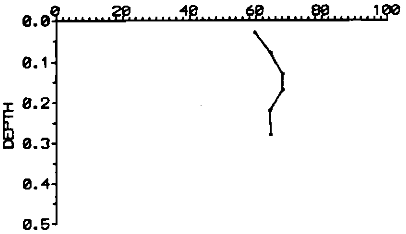

TiO2 (%)

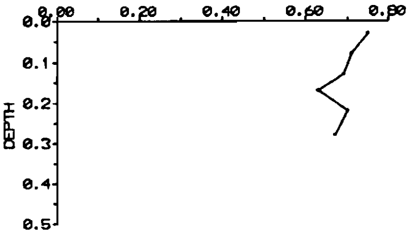

Al2O3 (%)

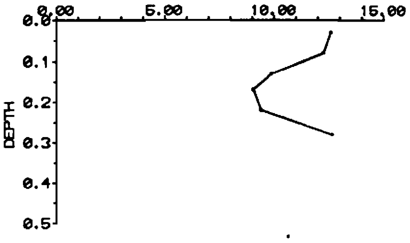

Na2O (%)

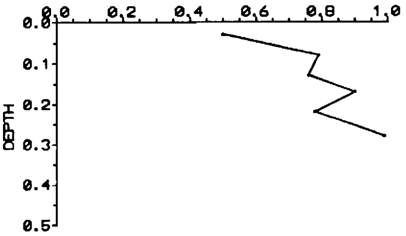

Fe2O3 (%)

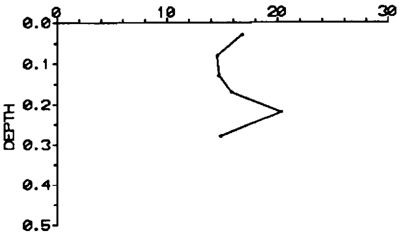

S (%)

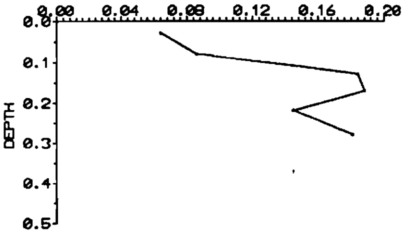

MgO (%)

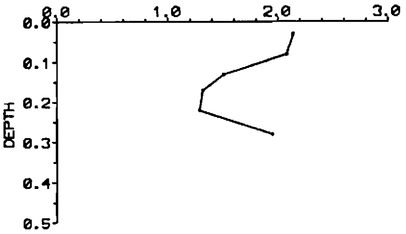

CaO (%)

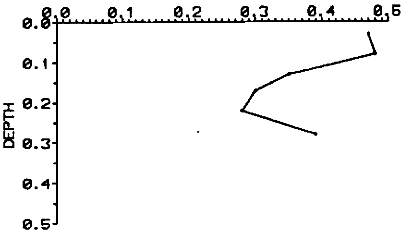

As (ppm)

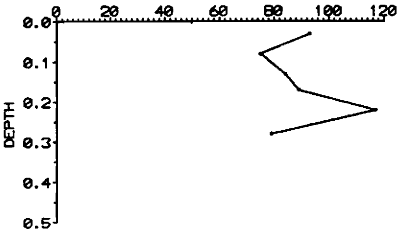

Au (ppm)

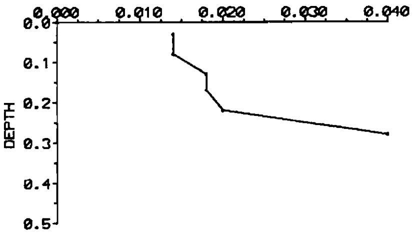

Ba (ppm)

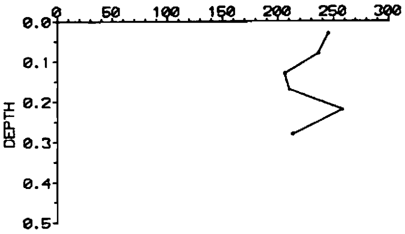

No Br Data

Ce (ppm)

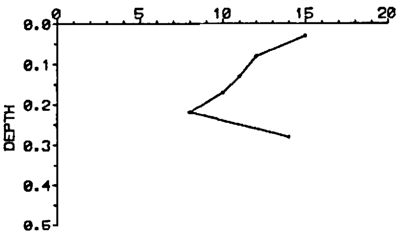

Co (ppm)

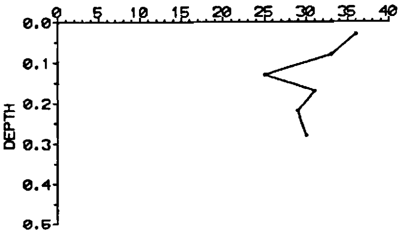

Cr (ppm)

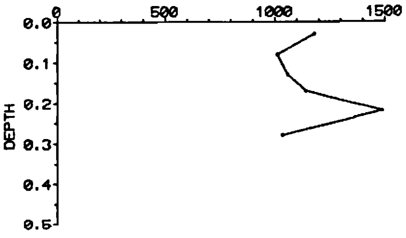

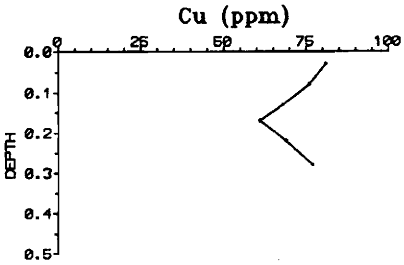
Cu (ppm)
0 25 50 75 100
DEPTH
0.0 0.1 0.2 0.3 0.4 0.5

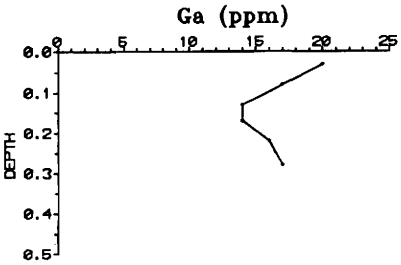
Ga (ppm)
0 5 10 15 20 25
DEPTH
0.0 0.1 0.2 0.3 0.4 0.5

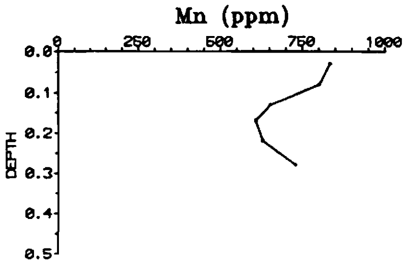
Mn (ppm)
0 250 500 750 1000
DEPTH
0.0 0.1 0.2 0.3 0.4 0.5

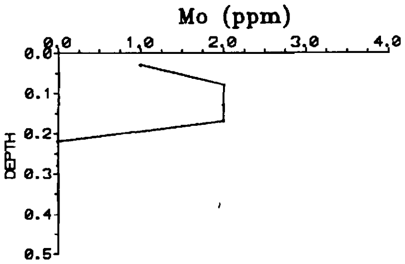
Mo (ppm)
0.0 1.0 2.0 3.0 4.0
DEPTH
0.0 0.1 0.2 0.3 0.4 0.5

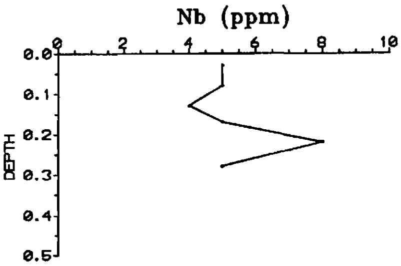
Nb (ppm)
0 2 4 6 8 10
DEPTH
0.0 0.1 0.2 0.3 0.4 0.5

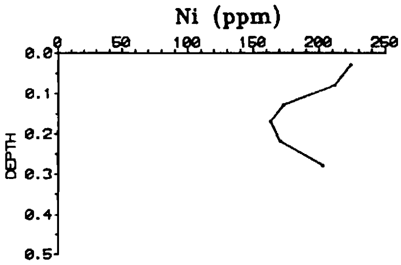
Ni (ppm)
0 50 100 150 200 250
DEPTH
0.0 0.1 0.2 0.3 0.4 0.5

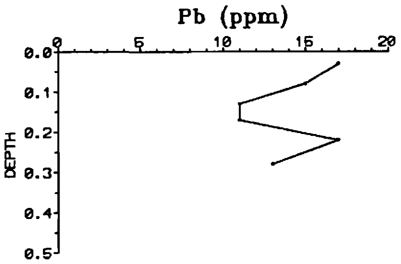
Pb (ppm)
0 5 10 15 20
DEPTH
0.0 0.1 0.2 0.3 0.4 0.5

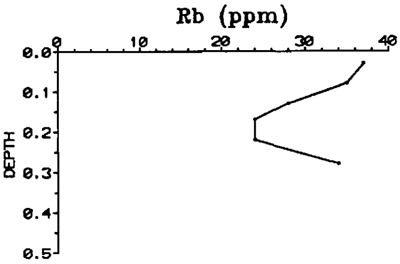
Rb (ppm)
0 10 20 30 40
DEPTH
0.0 0.1 0.2 0.3 0.4 0.5

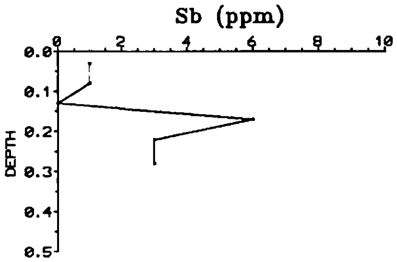
Sb (ppm)
0 2 4 6 8 10
DEPTH
0.0 0.1 0.2 0.3 0.4 0.5

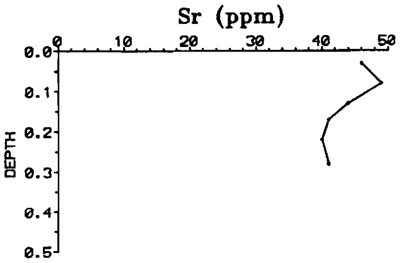
Sr (ppm)
0 10 20 30 40 50
DEPTH
0.0 0.1 0.2 0.3 0.4 0.5

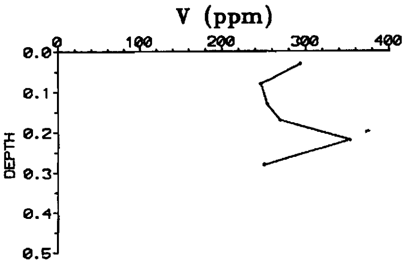
V (ppm)
0 100 200 300 400
DEPTH
0.0 0.1 0.2 0.3 0.4 0.5

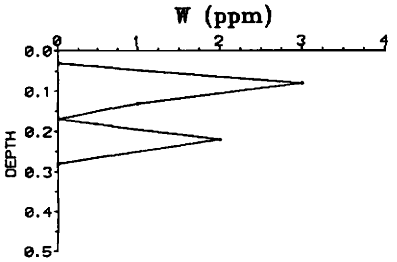
W (ppm)
0 1 2 3 4
DEPTH
0.0 0.1 0.2 0.3 0.4 0.5

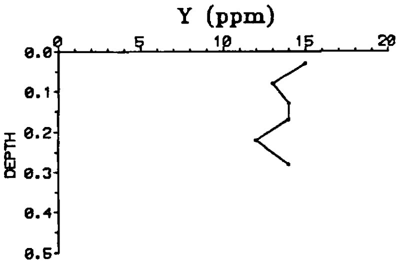
Y (ppm)
0 5 10 15 20
DEPTH
0.0 0.1 0.2 0.3 0.4 0.5

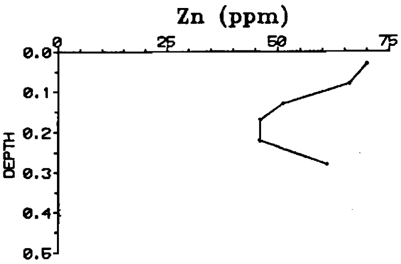
Zn (ppm)
0 25 50 75
DEPTH
0.0 0.1 0.2 0.3 0.4 0.5

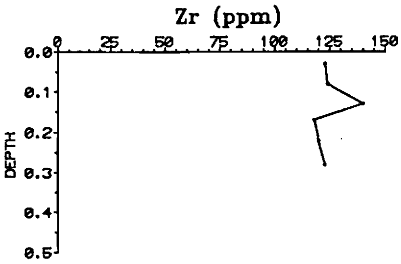
Zr (ppm)
0 25 50 75 100 125 150
DEPTH
0.0 0.1 0.2 0.3 0.4 0.5

SAMPLE	EASTING	NORTHING	SiO2	TiO2	Al2O3	Na2O	Fe2O3	S	MgO	CaO	P2O5	K2O	Ag	As	Au(ppb)	B	Ba
108083	2690	4200	75.6	0.11	5.1	0.38	14.5	0.008	0.05	0.02	<0.1	0.30	0.10	190	3	100	71
108085	2675	4200	78.6	0.73	11.6	0.61	0.5	0.2112	0.47	0.04	<0.1	2.89	0.40	35	69	500	520
108087	2660	4200	93.4	0.14	3.5	0.49	0.3	0.0272	0.11	0.06	<0.1	1.00	0.10	16	42	40	230
108090A	2645	4200	27.3	0.68	9.1	0.42	52.1	0.008	0.23	0.07	<0.1	0.54	0.10	2920	54	150	110
108090B	2645	4200	51.9	1.61	25.7	2.21	2.9	0.0448	0.47	0.10	<0.1	1.72	0.10	74	28	80	460
108092A	2630	4200	32.0	0.77	8.7	0.84	45.6	0.016	0.25	0.02	<0.1	0.08	0.10	220	26	150	9
108092B	2630	4200	64.3	1.25	16.3	2.74	1.2	0.0528	0.80	0.11	<0.1	0.33	0.20	26	110	100	44
108094	2616	4200	63.6	0.43	20.8	0.11	0.6	0.0832	0.88	0.02	<0.1	5.02	0.10	41	10	100	610
108096A	2600	4200	48.5	0.30	10.7	0.80	25.7	0.0912	0.82	0.13	<0.1	3.08	0.20	1910	3	150	300
108096B	2600	4200	57.1	0.60	20.9	1.60	2.5	0.3648	1.31	0.06	<0.1	6.40	0.20	120	14	100	640
108098A	2587	4200	28.9	0.49	6.9	0.70	51.8	0.008	0.32	0.02	<0.1	0.82	0.10	1540	340	150	150
108098B	2587	4200	59.3	1.48	17.9	3.59	1.6	0.0608	0.74	0.18	<0.1	2.30	0.10	38	79	150	440
108101A	2560	4200	19.0	1.18	11.8	0.59	54.7	0.008	0.40	0.10	<0.1	2.03	0.20	4980	3	200	340
108101B	2560	4200	45.2	2.39	28.8	2.84	2.3	0.032	0.76	0.05	<0.1	4.34	0.20	43	65	120	840
108103	2555	4200	9.3	0.69	7.0	0.24	69.3	0.0192	0.33	0.08	0.44	1.27	0.10	1430	160	120	210
108105A	2540	4200	23.2	0.86	9.6	0.39	54.5	0.008	0.38	0.14	<0.1	1.83	0.30	830	950	1000	50
108105B	2540	4200	55.8	1.76	11.3	1.19	9.9	0.008	5.98	0.09	<0.1	1.16	0.10	140	350	400	230
108107A	2520	4200	9.5	0.92	3.9	0.23	73.1	0.008	0.53	0.08	0.26	0.12	0.20	2540	3	200	300
108107B	2520	4200	30.4	1.08	9.9	0.24	2.1	3.424	1.85	16.30	<0.1	1.84	0.20	33	59	100	440
108110	2460	4200	39.9	2.36	30.0	3.59	3.1	0.1024	1.19	0.39	<0.1	3.82	0.20	140	84	150	570

SAMPLE	Co	Cr	Cu	Ga	Ge	Mn	Mo	Ni	Pb	Sb	Sc	Sn	Sr	V	W	Y	Zn	Zr
108083	49	130	150	30	5	155	10	67	<5	7	8	1	21	87	8	2	74	55
108085	3	85	20	40	5	155	2	<20	17	3	32	20	130	110	6	14	11	230
108087	3	21	3	10	4	155	1	23	<5	1	3	2	20	20	5	4	5	57
108090A	13	380	97	40	6	310	8	82	<5	1	28	2	23	560	12	8	160	62
108090B	3	150	14	40	2	155	2	90	<5	2	49	3	28	220	19	20	95	130
108092A	6	630	81	50	3	155	3	45	<5	2	22	2	12	730	1	7	52	52
108092B	5	65	18	30	1	155	3	23	<5	3	19	3	13	49	13	6	8	82
108094	3	250	17	40	3	155	1	50	56	2	18	15	50	81	9	8	12	150
108096A	36	450	180	60	3	155	60	76	14	24	21	3	56	140	10	8	60	130
108096B	11	93	29	60	3	155	3	27	16	1	23	5	130	92	14	7	27	170
108098A	9	480	83	50	3	465	8	51	<5	3	20	1	33	740	22	4	46	34
108098B	12	120	13	30	2	155	2	37	<5	2	53	2	64	290	49	8	10	86
108101A	46	540	130	40	6	387	10	190	9	2	48	2	36	840	40	14	560	100
108101B	13	210	26	50	2	155	1	300	<5	2	73	2	50	430	40	15	360	140
108103	10	370	110	30	4	155	3	83	39	7	37	5	22	360	28	8	240	46
108105A	21	1940	240	40	4	387	8	86	<5	4	43	3	25	650	11	14	260	61
108105B	38	470	57	40	3	465	8	120	<5	2	34	8	32	240	17	18	150	150
108107A	17	860	99	80	5	1394	10	36	8	7	41	3	36	1350	8	5	690	55
108107B	9	160	18	25	2	155	2	50	5	2	39	2	75	180	13	6	280	70
108110	27	320	11	40	4	155	2	150	8	2	73	3	43	460	1	14	360	140

SAMPLE	Quartz	Hematite	Goethite	Maghemite	Muscovite	Vermiculite/ Chlorite	Kaolinite	Smectite	Talc	Halite	Sulfates	Others
108083	6	4	5		3	3	4	1	4	3	?Gypsum	
108085	6				5	4				4	6Alunite	
108087	6				5	3				4		
108090A	6	6	4	1	3	5		1	4			
108090B	6		4		5	6	6		6	6		
108092A	6	5	4	1		2	4		1	3	?Gypsum	
108092B	6	1			3	5	6	3	6	6		Paragonite
108094	6	1			6	5			6	6	?Gypsum	
108096A	6	4	5		4	6		1		3		Paragonite
108096B	6				6	2				6	6Alunite	
108098A	6	5	4	1	3	2	3	1	4			
108098B	6				6		6	3	6	6	?Gypsum	Paragonite, 5Plagioclase
108101A	6	6	4	1	5	3	4		2	3	3Gypsum	
108101B	6				6	5	6		5	6		
108103	6	5	6	1	4	5			6			
108105A	6	5	5	2	3	3		1	3			
108105B	6	3	3	1	5	6	5	6	6			4Plagioclase
108107A	6	6	3	1	5	5	4	2	6			
108107B	6				6		4	6	3		6Gypsum	
108110	6		3		6	3	6	1	4	6	4Gypsum	

Appendix 2: Tabulated and Graphed data for surficial rock samples along 4200N.
The mineralogical key is as follows: 6=major, 5=abundant, 4=moderate, 3=significant, 2=minor and 1=trace.
Bi, Tl <3 ppm.

SAMPLE	EASTING	NORTHING	SiO_2	TiO_2	Al_2O_3	Na_2O	Fe_2O_3	S	MgO	CaO	P_2O_5	K_2O	Ag	As	Au(ppb)	B	Ba
108078	2775	4200	52.2	0.73	14.8	0.28	8.8	0.02	4.97	2.16	<0.1	1.13	0.05	46	36	50	300
108079	2750	4200	64.0	0.61	11.2	0.23	9.8	0.02	3.19	0.98	<0.1	0.79	0.05	53	23	40	310
108080	2730	4200	69.1	0.60	10.1	0.31	8.7	0.02	1.73	0.49	<0.1	0.91	0.05	63	13	40	290
108081	2710	4200	72.0	0.51	8.4	0.27	10.3	0.02	1.14	0.63	<0.1	0.72	0.05	95	22	40	290
108082	2690	4200	66.6	0.63	10.9	0.41	9.2	0.02	1.70	0.95	<0.1	0.82	0.05	91	45	40	310
108084	2675	4200	68.4	0.54	8.0	0.25	13.6	0.02	1.17	0.78	<0.1	0.57	0.05	180	28	40	390
108086	2660	4200	66.7	0.60	10.2	0.26	8.8	0.02	1.92	1.83	<0.1	0.77	0.05	91	32	50	320
108088	2650	4200	59.7	0.52	11.9	0.25	6.8	0.02	2.54	3.90	<0.1	0.97	0.05	66	47	60	330
108089	2643	4200	63.6	0.44	9.8	0.29	6.9	0.02	2.19	4.27	<0.1	0.77	0.05	80	41	50	310
108091	2630	4200	65.7	0.58	10.0	0.28	9.3	0.02	1.81	1.72	<0.1	0.82	0.05	87	33	50	330
108093	2616	4200	63.5	0.59	10.3	0.63	7.6	0.02	2.24	3.12	<0.1	0.94	0.05	62	42	60	320
108095	2600	4200	67.4	0.57	9.3	0.50	7.8	0.02	2.05	2.98	<0.1	0.83	0.05	72	33	40	280
108097	2587	4200	75.1	0.57	5.9	0.35	11.3	0.02	0.93	1.21	<0.1	0.53	0.05	120	19	50	300
108099	2571	4200	67.5	0.50	7.8	0.39	9.9	0.02	1.67	3.42	<0.1	0.63	0.05	84	28	40	290
108100	2560	4200	64.5	0.53	7.0	0.17	15.3	0.02	1.34	3.40	<0.1	0.50	0.05	100	26	40	440
108104	2540	4200	60.9	0.68	5.5	0.31	27.8	0.02	0.54	0.21	<0.1	0.30	0.05	160	24	50	420
108106	2520	4200	63.8	0.61	9.8	0.62	15.7	0.02	1.07	0.15	<0.1	0.88	0.05	160	24	80	380
108108	2482	4200	66.8	0.79	9.1	0.58	16.0	0.02	0.62	0.10	<0.1	0.66	0.05	65	13	60	300
108109	2460	4200	56.1	0.45	8.4	2.25	11.7	0.056	3.66	3.33	<0.1	0.47	0.05	85	51	70	600
108111	2440	4200	61.7	0.62	10.4	0.82	15.0	0.02	1.58	0.17	<0.1	0.71	0.05	97	23	60	360
108112	2420	4200	68.6	0.62	7.4	0.27	16.7	0.02	1.03	0.20	<0.1	0.50	0.05	110	16	35	280
108113	2400	4200	68.2	0.56	8.0	0.37	15.8	0.02	1.10	0.18	<0.1	0.57	0.05	100	11	40	330

SAMPLE	Co	Cr	Cu	Ga	Ge	Mn	Mo	Ni	Pb	Sb	Sc	Sn	Sr	V	W	Y	Zn	Zr
108078	43	780	77	20	1	852	6	380	<50	1	10	3	67	150	5	13	83	120
108079	32	750	62	10	0.3	620	5	270	<50	1	7	1	48	160	5	11	68	100
108080	22	570	50	10	1	465	3	170	<50	1	9	3	44	150	3	11	60	120
108081	18	600	51	10	0.3	465	5	130	<50	2	7	5	38	170	3	10	57	99
108082	22	520	54	10	0.5	620	4	150	<50	2	9	3	47	160	5	11	64	120
108084	19	800	66	15	0.5	387	8	140	<50	2	15	4	41	240	5	10	56	95
108086	22	500	57	10	0.5	465	3	150	<50	1	20	3	50	150	5	10	57	110
108088	23	400	61	15	0.8	465	3	160	<50	1	17	3	65	130	3	11	55	99
108089	20	380	58	10	0.3	310	3	140	<50	1	9	2	63	120	4	10	49	87
108091	20	560	54	10	0.3	465	2	150	<50	1	8	3	48	160	1	10	54	110
108093	22	440	57	10	0.3	620	2	150	<50	1	17	1	59	130	4	10	51	120
108095	19	430	51	10	1	620	3	140	<50	1	10	2	54	130	2	10	46	110
108097	14	640	43	10	0.4	465	3	96	<50	2	13	2	40	190	7	8	43	97
108099	20	580	52	8	0.2	465	3	130	<50	1	8	1	52	180	5	10	45	93
108100	20	970	58	10	0.3	465	3	130	<50	2	7	4	51	230	9	10	52	79
108104	21	1760	56	15	0.4	697	4	130	<50	4	8	5	34	450	12	9	55	86
108106	19	830	56	15	0.4	620	3	130	<50	3	25	3	34	260	10	10	84	100
108108	18	970	47	10	0.3	620	3	120	<50	2	26	3	36	260	6	9	47	160
108109	18	760	60	15	0.3	387	5	140	<50	2	21	5	67	220	9	9	43	72
108111	23	960	60	15	0.3	775	3	180	<50	2	17	3	36	260	4	10	57	94
108112	19	1130	49	12	2	697	3	160	<50	2	7	5	32	230	8	9	46	90
108113	20	1070	50	12	0.3	620	3	160	<50	3	22	4	34	260	6	9	49	83

SAMPLE	Quartz	Plagioclase	Hematite	Goethite	Maghemite	Calcite	Muscovite	Vermiculite/ Chlorite	Kaolinite	Smectites	Talc	Rutile	Others
108078	6	4	3	4	1	5	5	6	6	1	6		
108079	6		3	3	1	3	3		5	3	5	3	
108080	6	6	3		3	3	5	3	5		5		
108081	6	3	3	3	4	3	2		4		3	1	
108082	6	2	3	2	2	3	3	2	4	3	2	2	
108084	6	4	4	3	2	3	1	1	4		2	2	Paragonite
108086	6	3	3	4	4	5	4		5	4	4	3	Paragonite
108088	6	2	3	3	1	6	3		4		3		
108089	6	2	3	3	1	6	2	2	4	2	3		Paragonite
108091	6	6	3	4	3	5	3	1	5		3		
108093	6	2	3	2	1	5	3		4	3	2	2	
108095	6	5	3	3	1	5	3	1	4	1	3	?5	?6Amphibole
108097	6	3	3	3	1	4	2		3	1	2		
108099	6		4		3	6	3	2	4		3	2	
108100	6	3	3	3	1	6	2	2	4		2	2	
108104	6	6	4		2		2	2	3	1	1		Paragonite
108106	6		4	4	2		2		4		2	2	?1Amphibole Paragonite
108108	6	4	4		2		1		5		2	2	
108109	6	6	4		4	6	1	3	4		2		6Halite
108111	6	3	4	4	3		3	2	5	2	4	1	6Amphibole
108112	6	3	4	3	2		2	2	4	1	5	4	
108113	6	3	4		3	1	3		5	1	5	2	

Appendix 2: Tabulated and Graphed data for surficial soil samples along 4200N.
The mineralogical key is as follows: 6=major, 5=abundant, 4=moderate, 3=significant, 2=minor and 1=trace.
Bi, Tl <3 ppm.

2. Near-surface samples: Graphed data for 4200N

***** Soil
●●●●● Fe-rich weathered rock
○○○○○ Fe-poor weathered rock

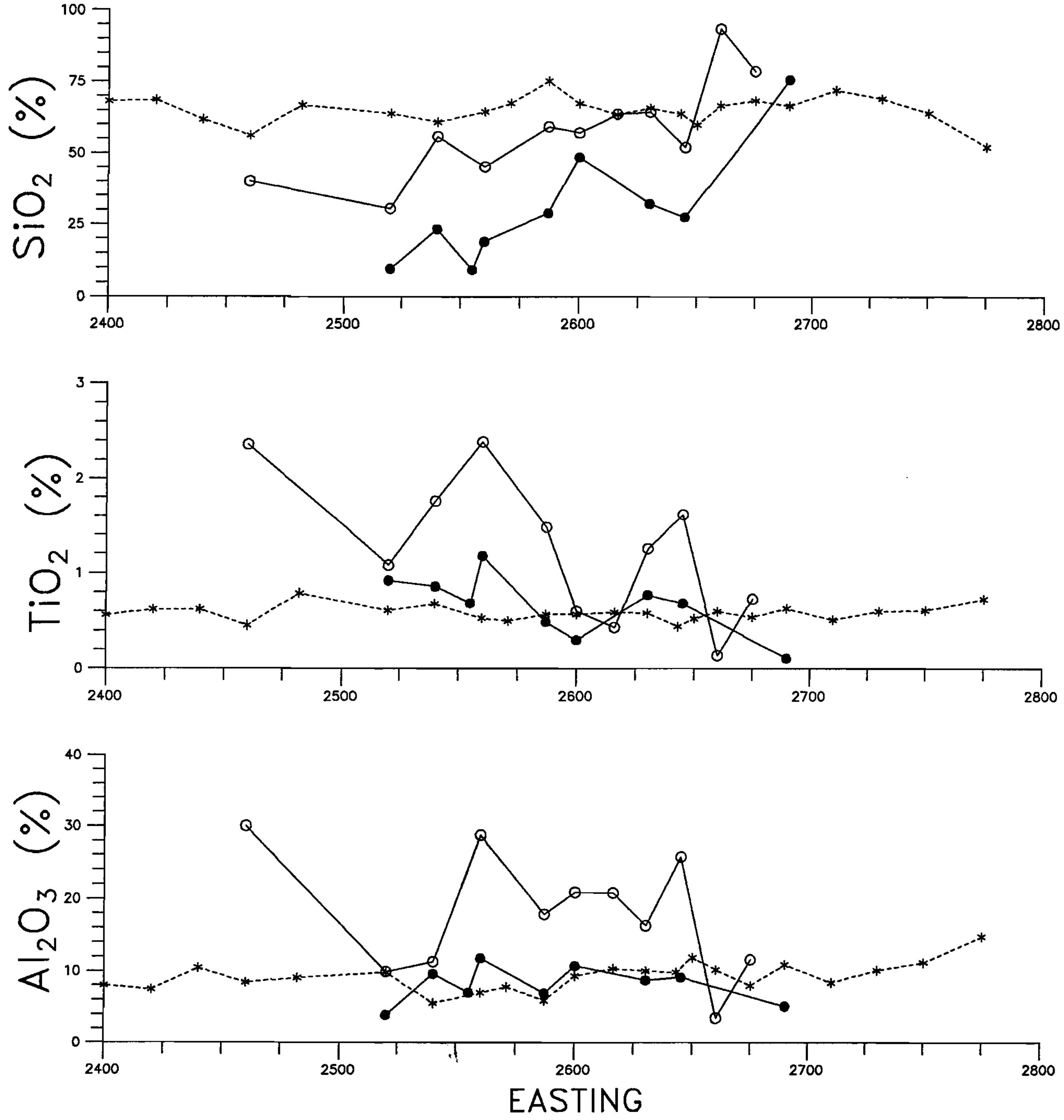

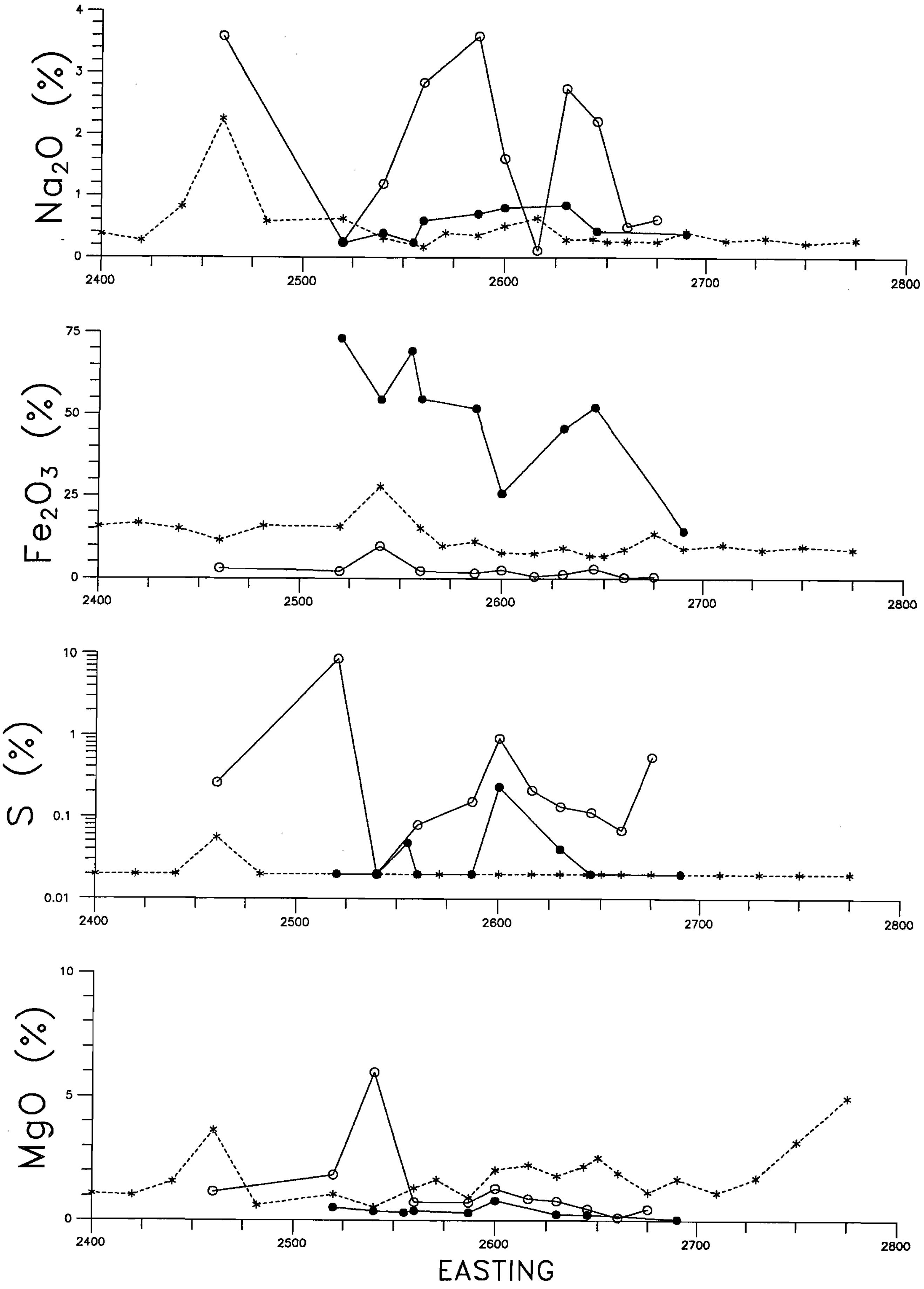
Na$_2$O (%)
4
3
2
1
0
Fe$_2$O$_3$ (%)
75
50
25
0
S (%)
10
1
0.1
0.01
MgO (%)
10
5
0
2400
2500
2600
2700
2800
EASTING

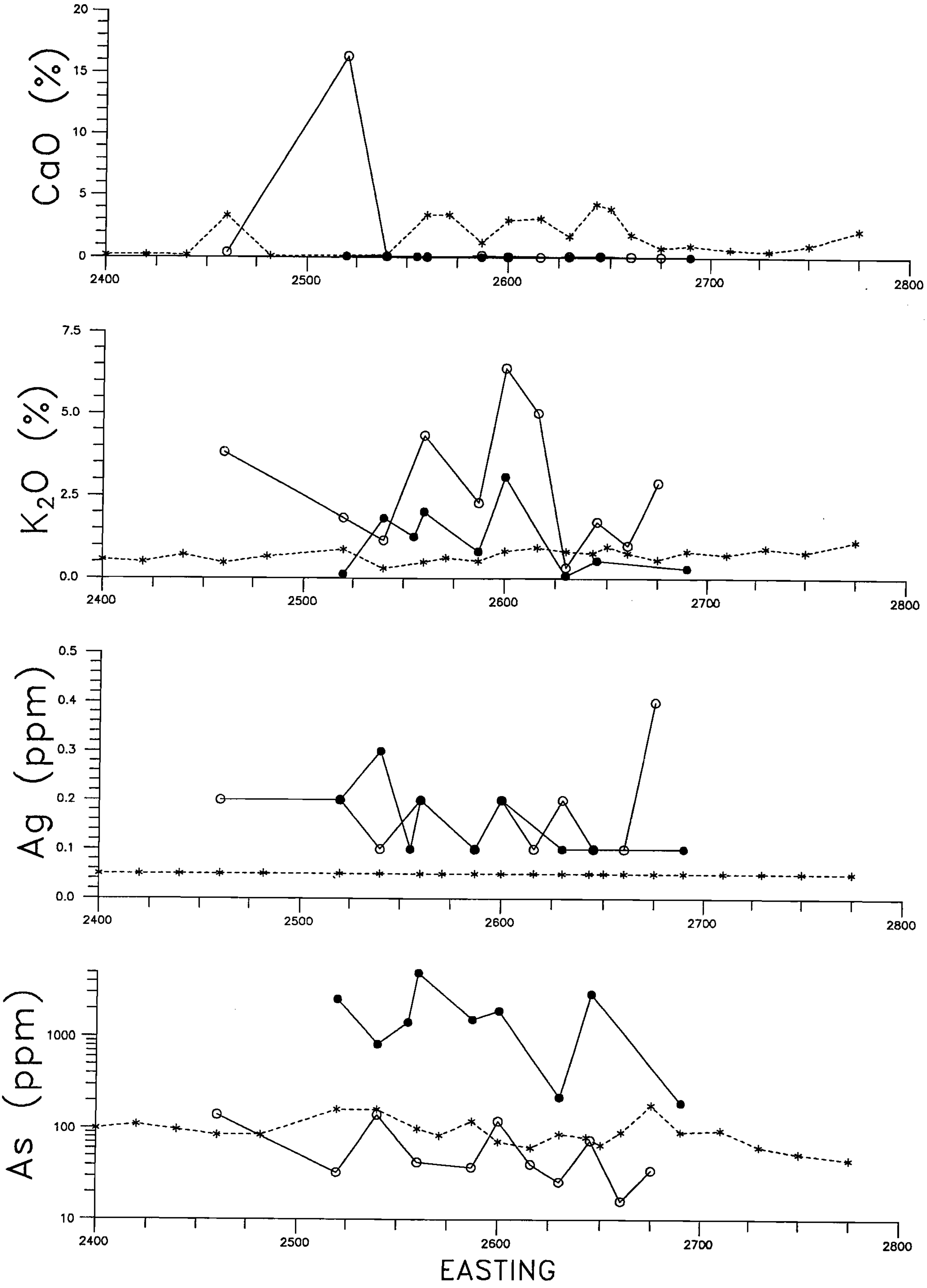
CaO (%)
20
15
10
5
0
K$_2$O (%)
7.5
5.0
2.5
0.0
Ag (ppm)
0.5
0.4
0.3
0.2
0.1
0.0
As (ppm)
1000
100
10
2400
2500
2600
2700
2800
EASTING

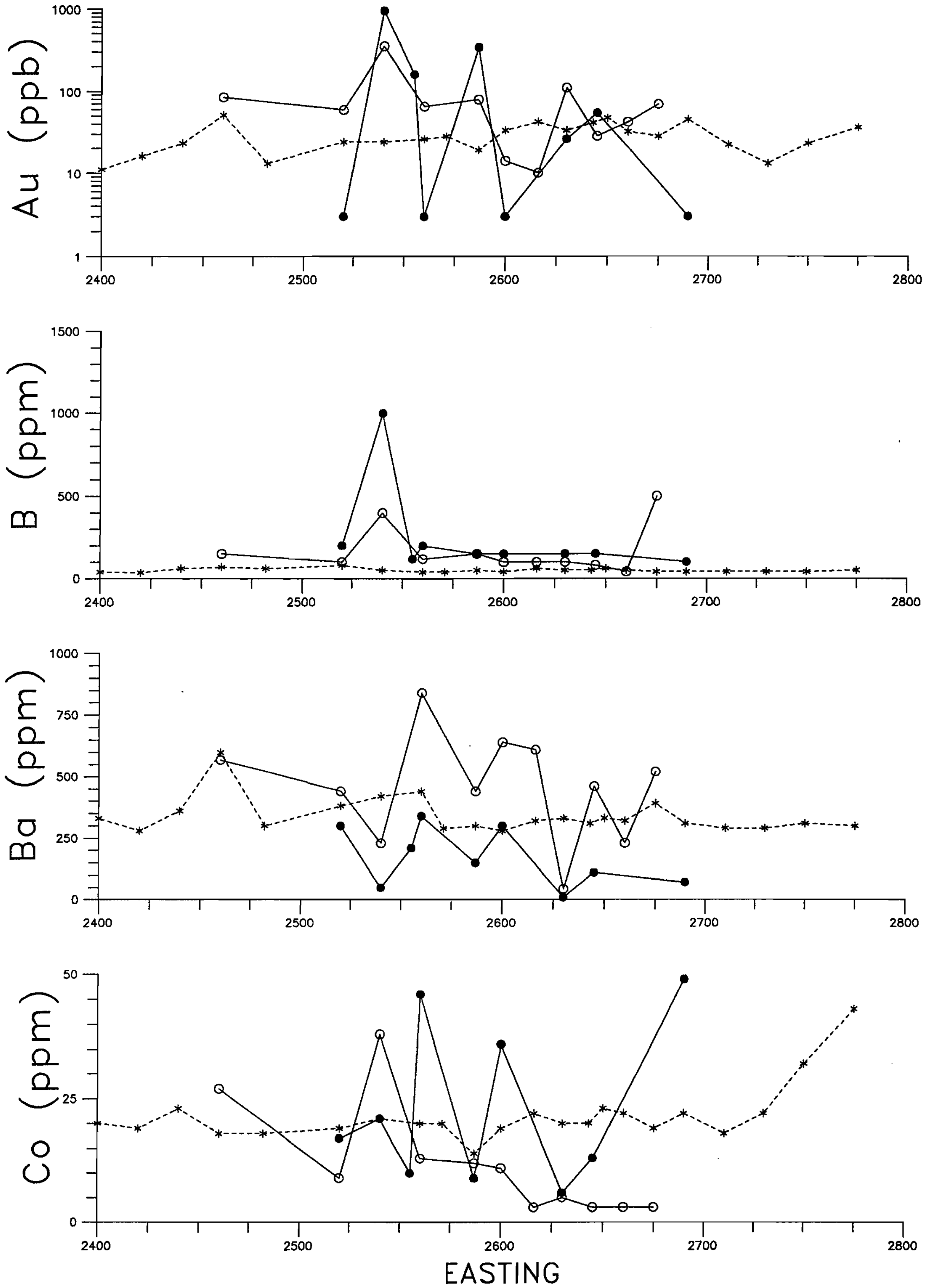
Au (ppb)
1000
100
10
1
B (ppm)
1500
1000
500
0
Ba (ppm)
1000
750
500
250
0
Co (ppm)
50
25
0
2400
2500
2600
2700
2800
EASTING

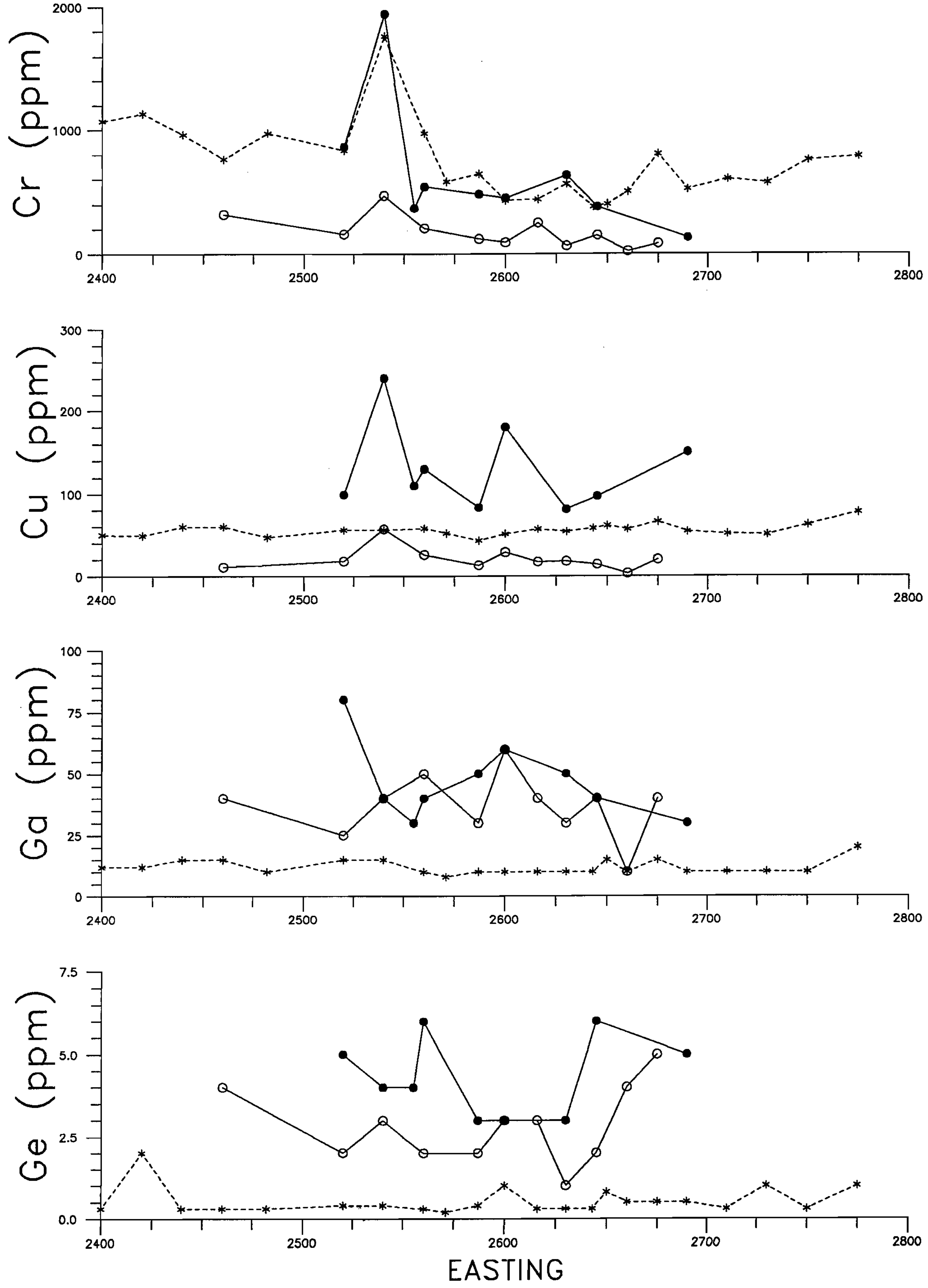
Cr (ppm)
2000
1000
0
Cu (ppm)
300
200
100
0
Ga (ppm)
100
75
50
25
0
Ge (ppm)
7.5
5.0
2.5
0.0
2400
2500
2600
2700
2800
EASTING

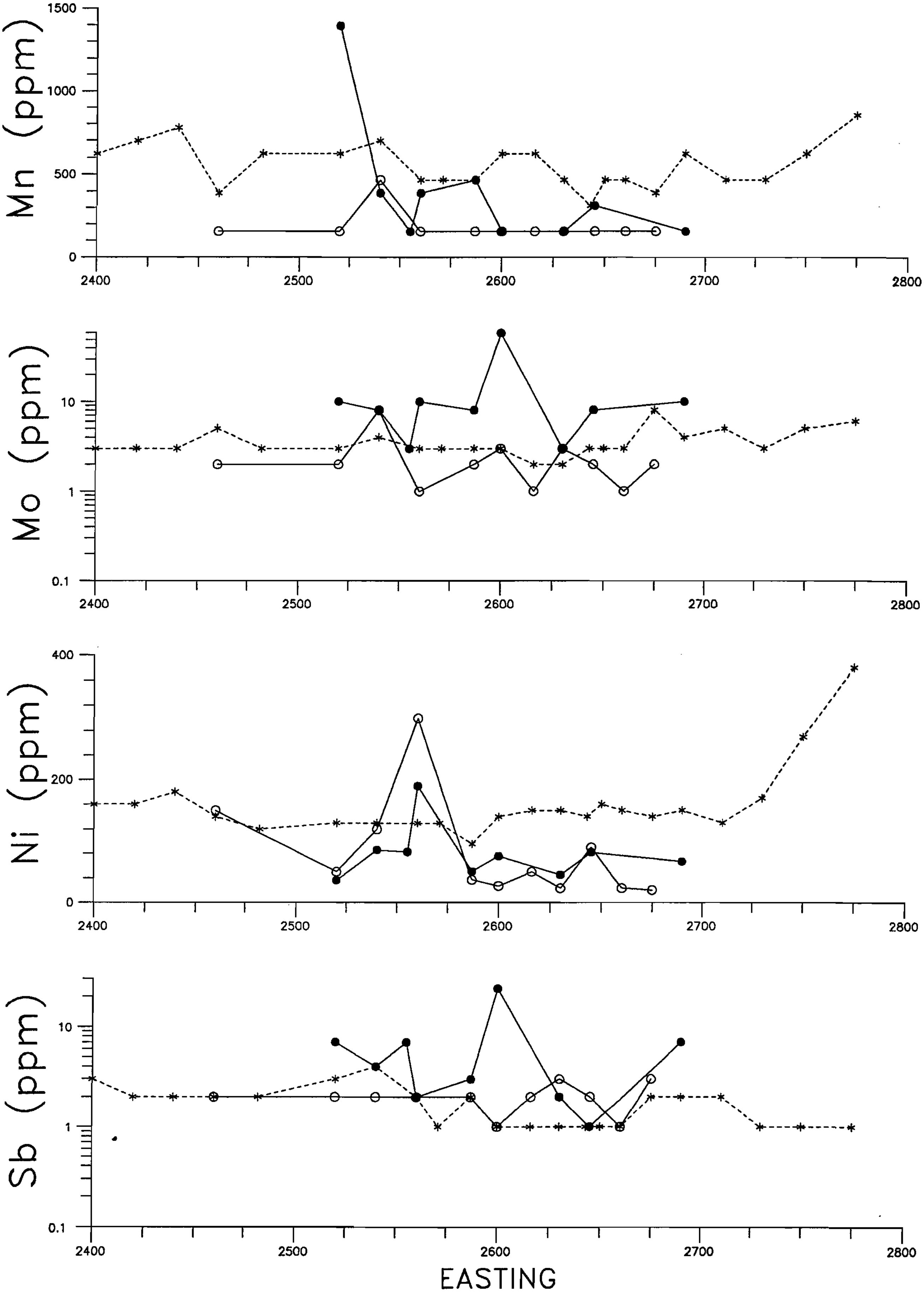
Mn (ppm)
1500
1000
500
0
Mo (ppm)
10
1
0.1
Ni (ppm)
400
200
0
Sb (ppm)
10
1
0.1
2400
2500
2600
2700
2800
EASTING

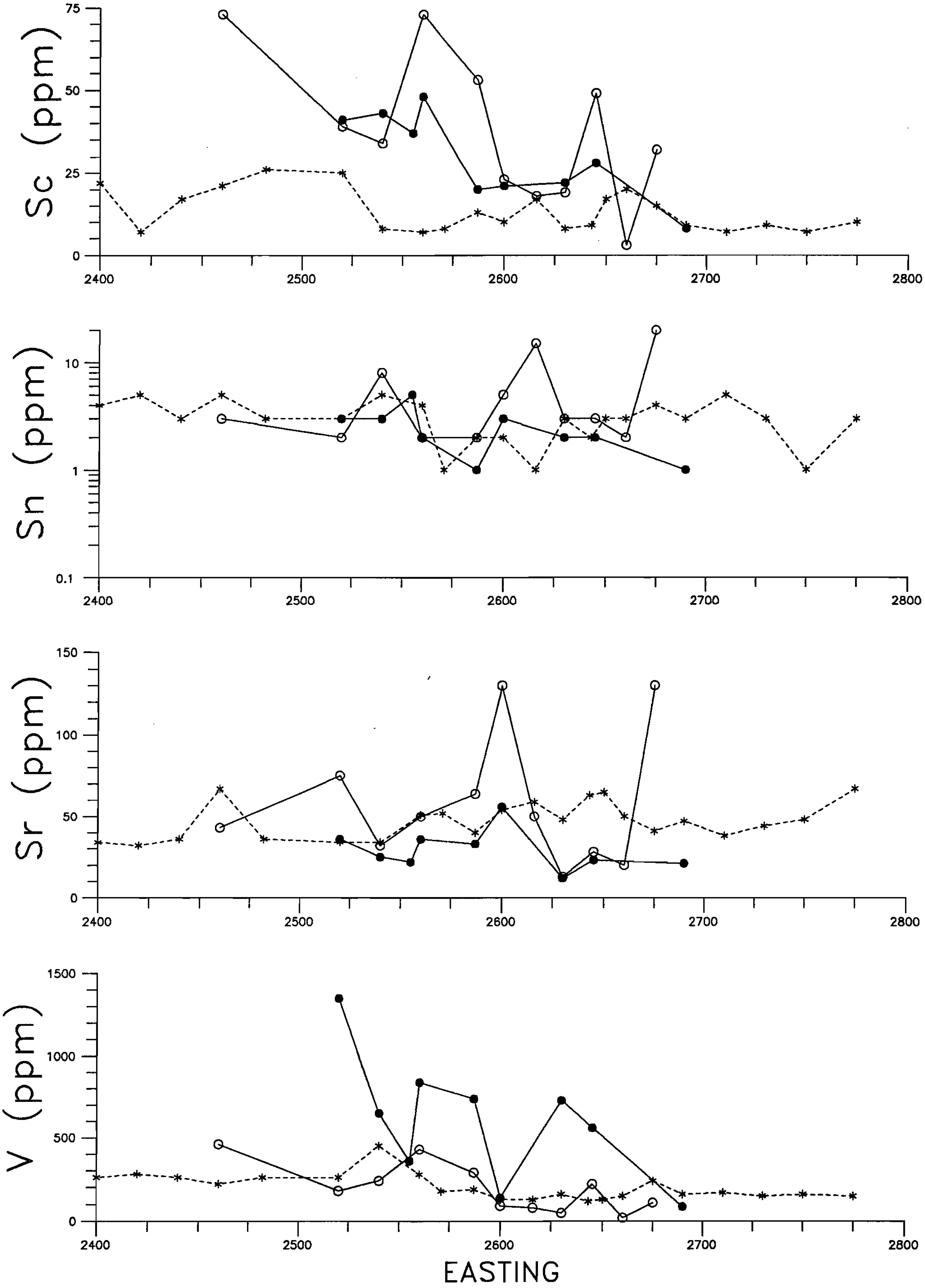
Sc (ppm)
0
25
50
75
Sn (ppm)
0.1
1
10
Sr (ppm)
0
50
100
150
V (ppm)
0
500
1000
1500
2400
2500
2600
2700
2800
EASTING

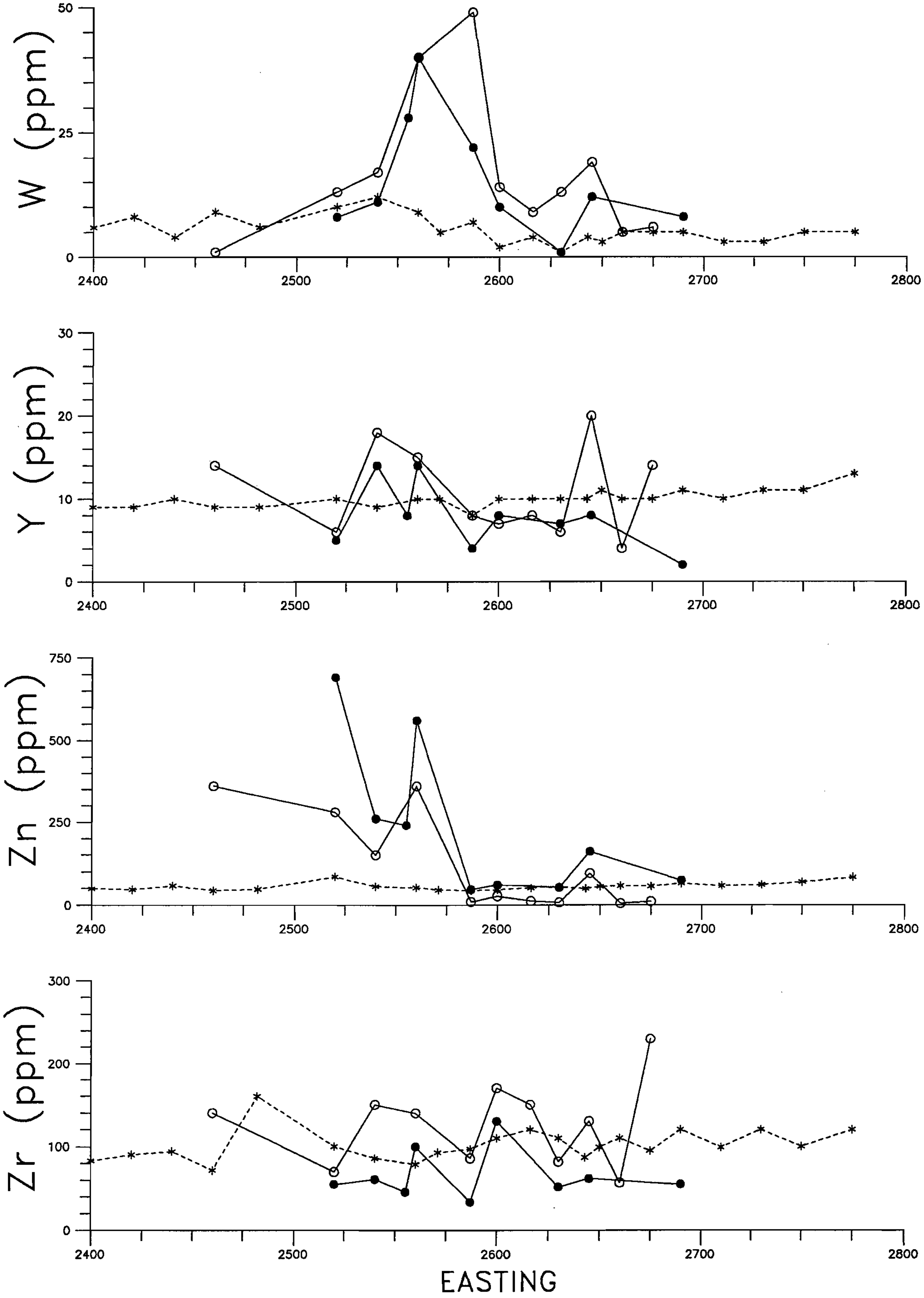
W (ppm)
50
25
0
Y (ppm)
30
20
10
0
Zn (ppm)
750
500
250
0
Zr (ppm)
300
200
100
0
2400
2500
2600
2700
2800
EASTING

3. Auger samples: Graphed data for 3700N

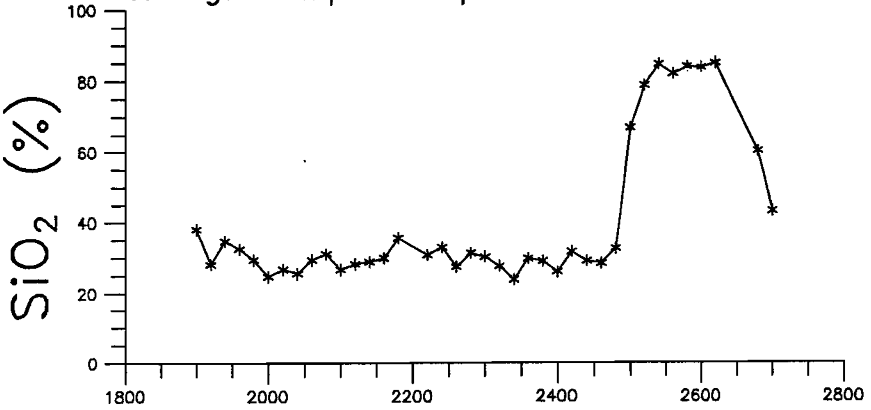

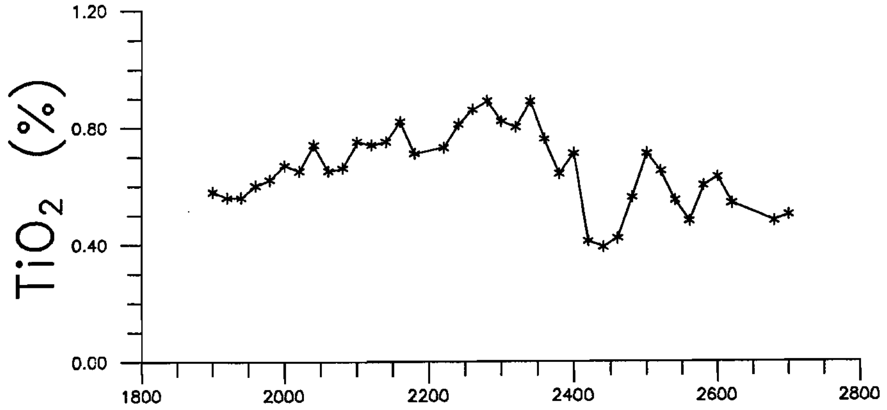

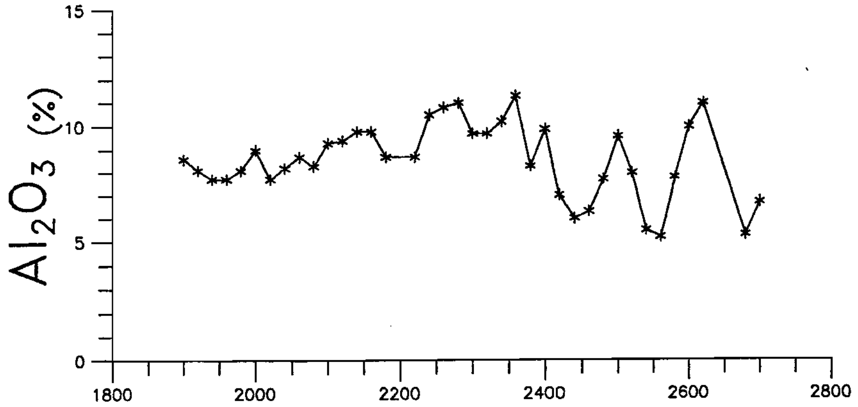

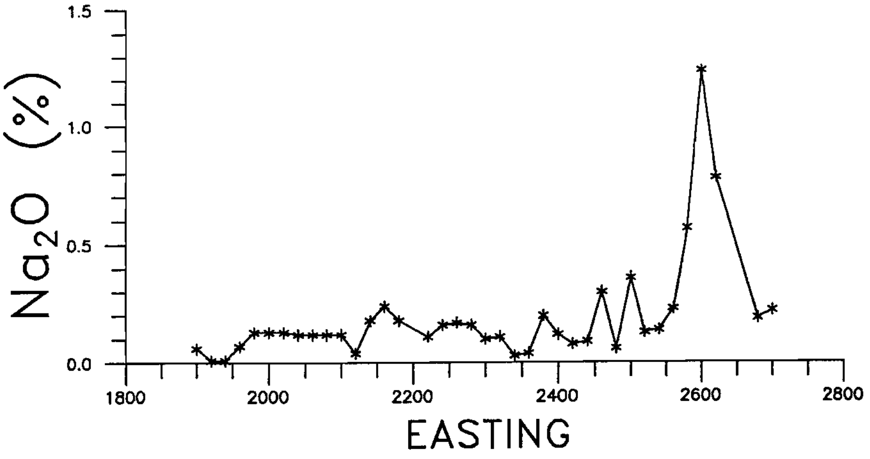

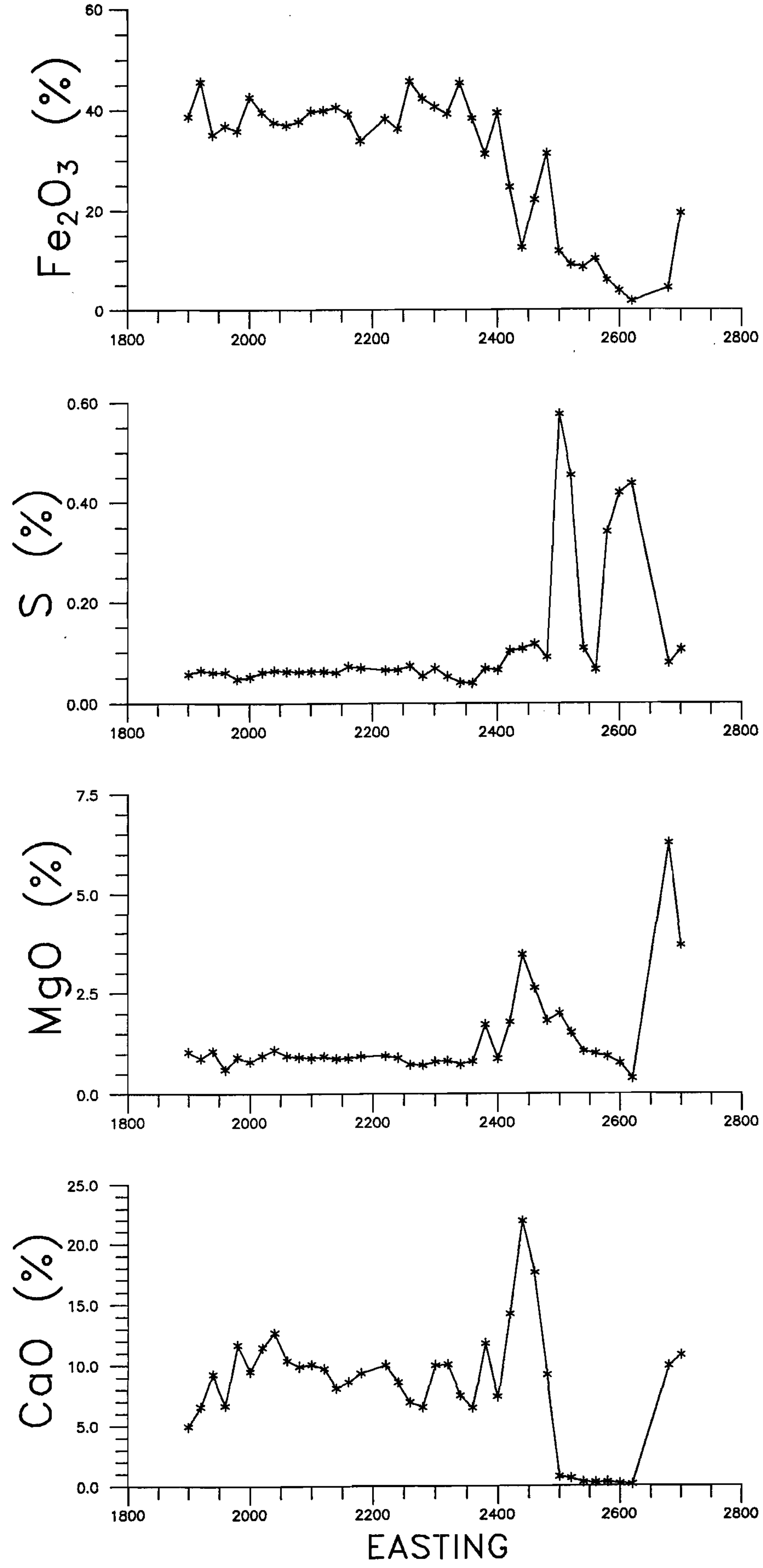
Fe2O3 (%)
60
40
20
0
S (%)
0.60
0.40
0.20
0.00
MgO (%)
7.5
5.0
2.5
0.0
CaO (%)
25.0
20.0
15.0
10.0
5.0
0.0
1800
2000
2200
2400
2600
2800
EASTING

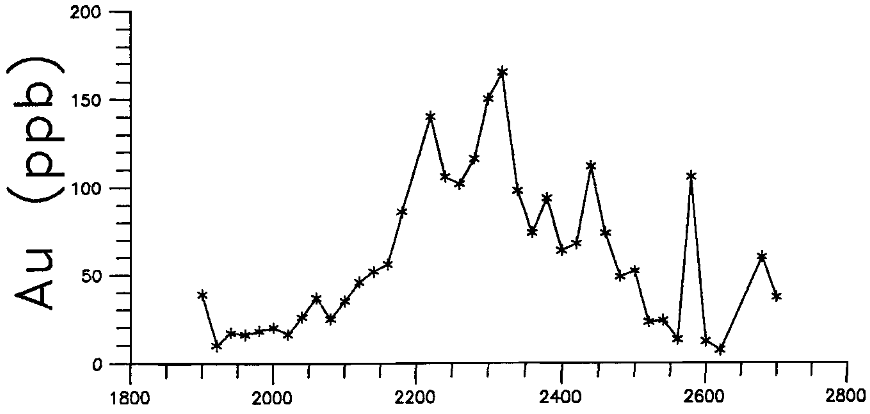
Au (ppb)
200
150
100
50
0
1800
2000
2200
2400
2600
2800

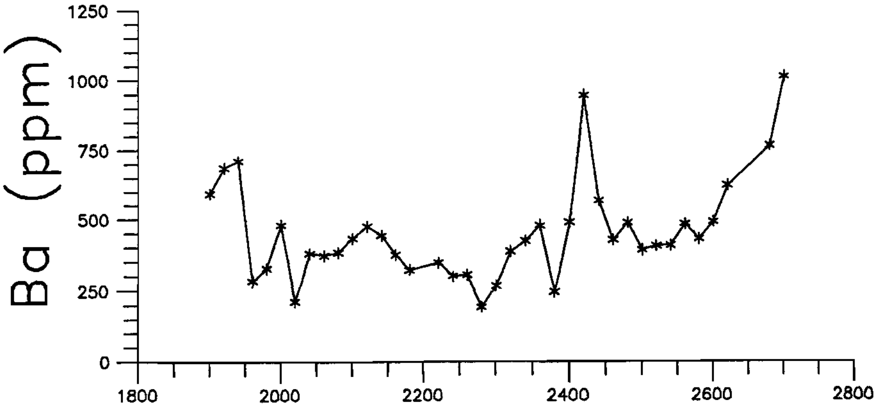
Ba (ppm)
1250
1000
750
500
250
0
1800
2000
2200
2400
2600
2800

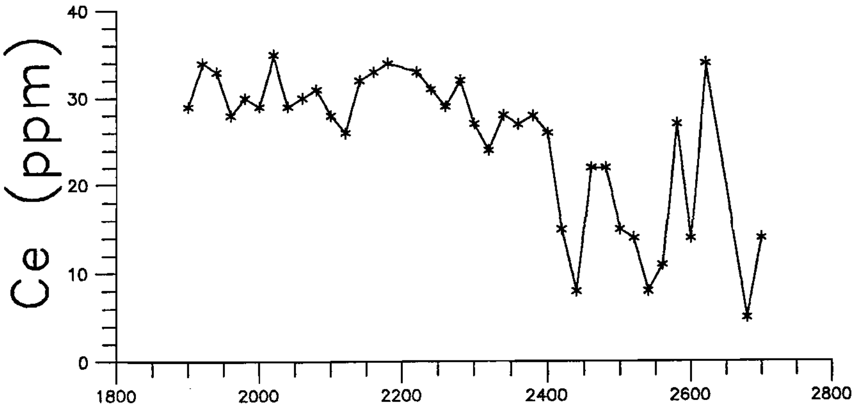
Ce (ppm)
40
30
20
10
0
1800
2000
2200
2400
2600
2800

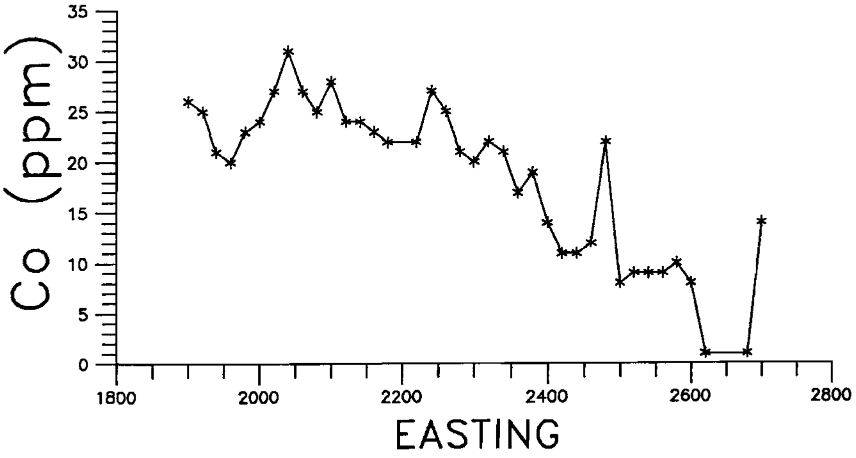
Co (ppm)
35
30
25
20
15
10
5
0
1800
2000
2200
2400
2600
2800
EASTING

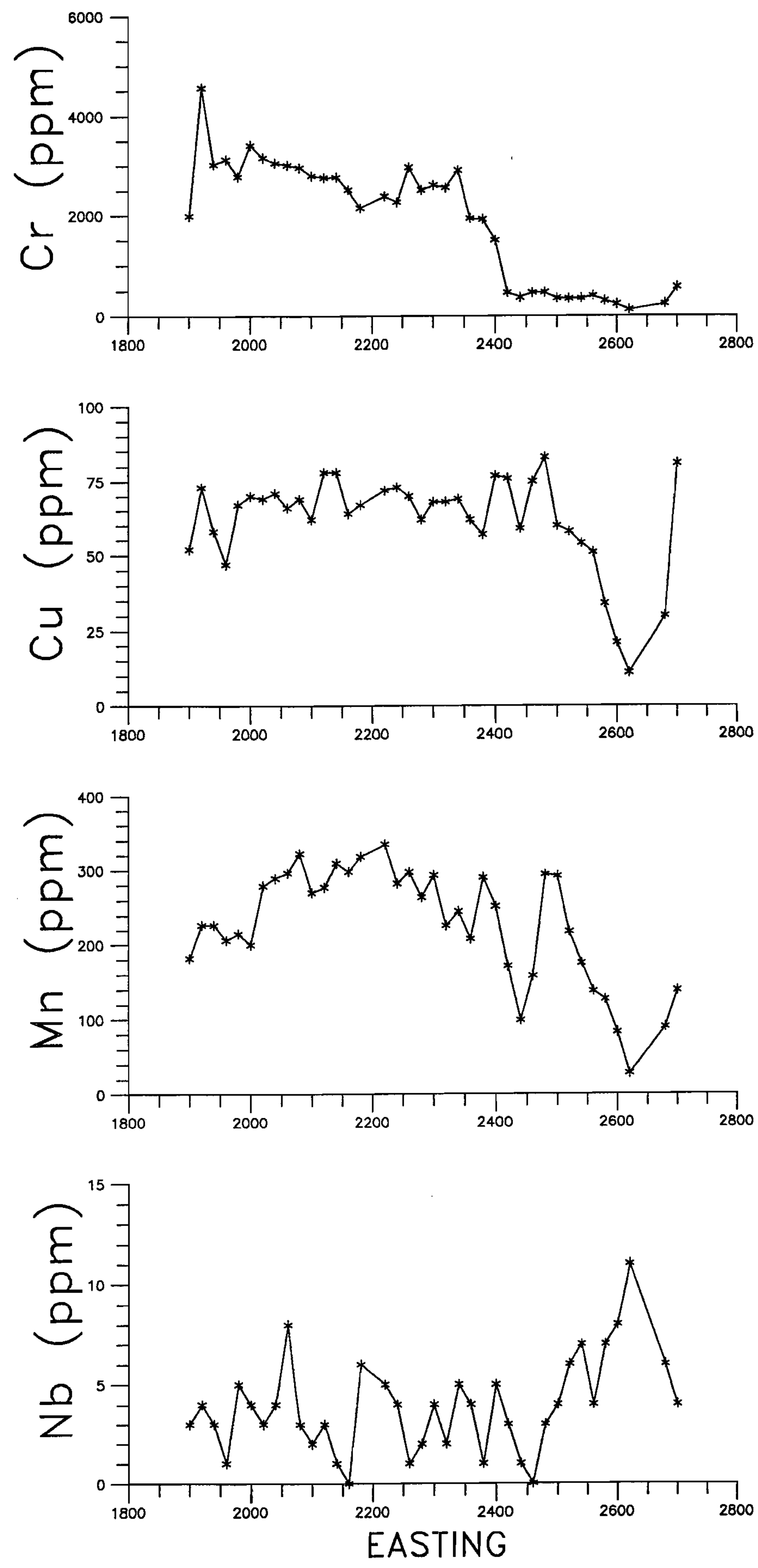
Cr (ppm)
6000
4000
2000
0
1800
2000
2200
2400
2600
2800
Cu (ppm)
100
75
50
25
0
1800
2000
2200
2400
2600
2800
Mn (ppm)
400
300
200
100
0
1800
2000
2200
2400
2600
2800
Nb (ppm)
15
10
5
0
1800
2000
2200
2400
2600
2800
EASTING

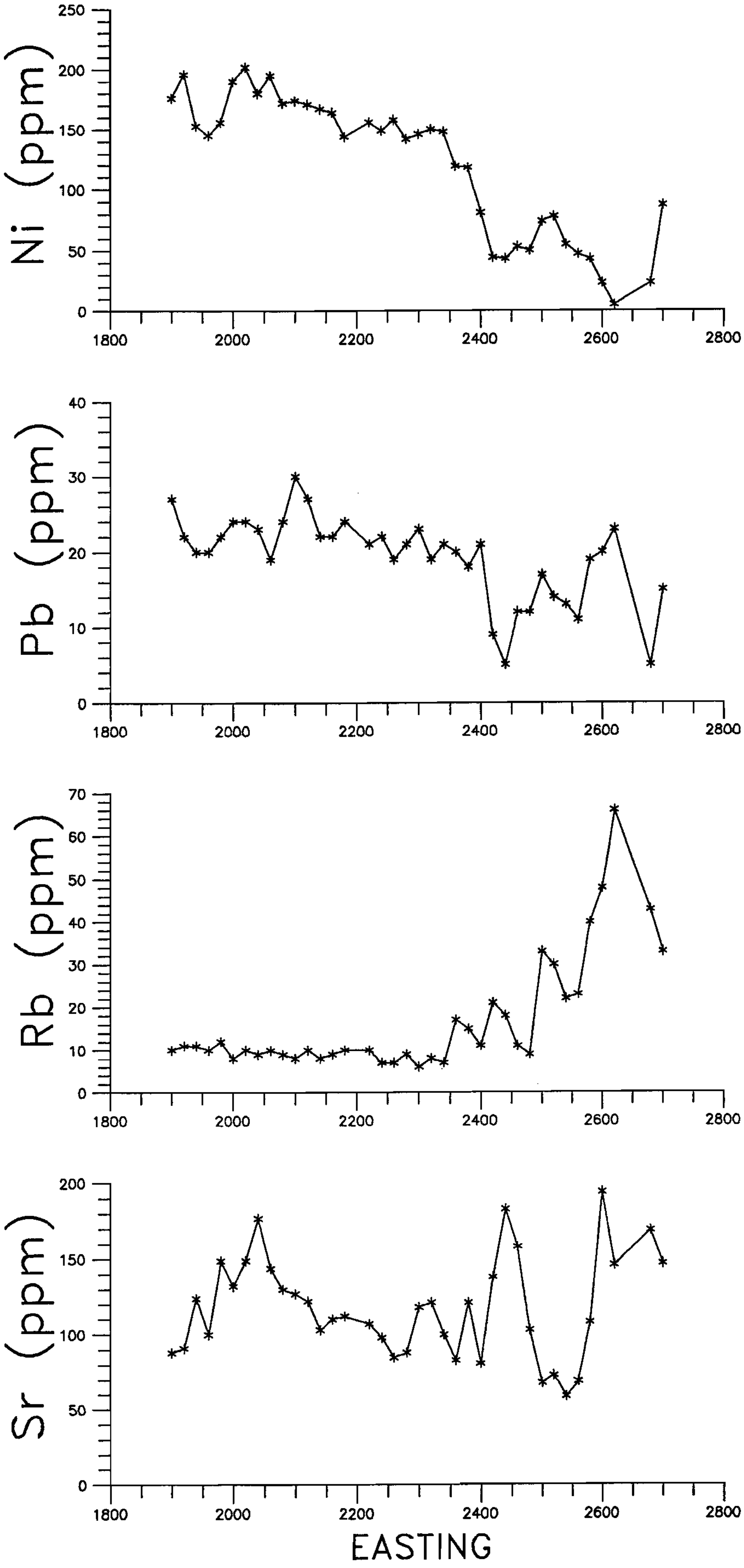
Ni (ppm)
250
200
150
100
50
0
1800
2000
2200
2400
2600
2800
Pb (ppm)
40
30
20
10
0
1800
2000
2200
2400
2600
2800
Rb (ppm)
70
60
50
40
30
20
10
0
1800
2000
2200
2400
2600
2800
Sr (ppm)
200
150
100
50
0
1800
2000
2200
2400
2600
2800
EASTING

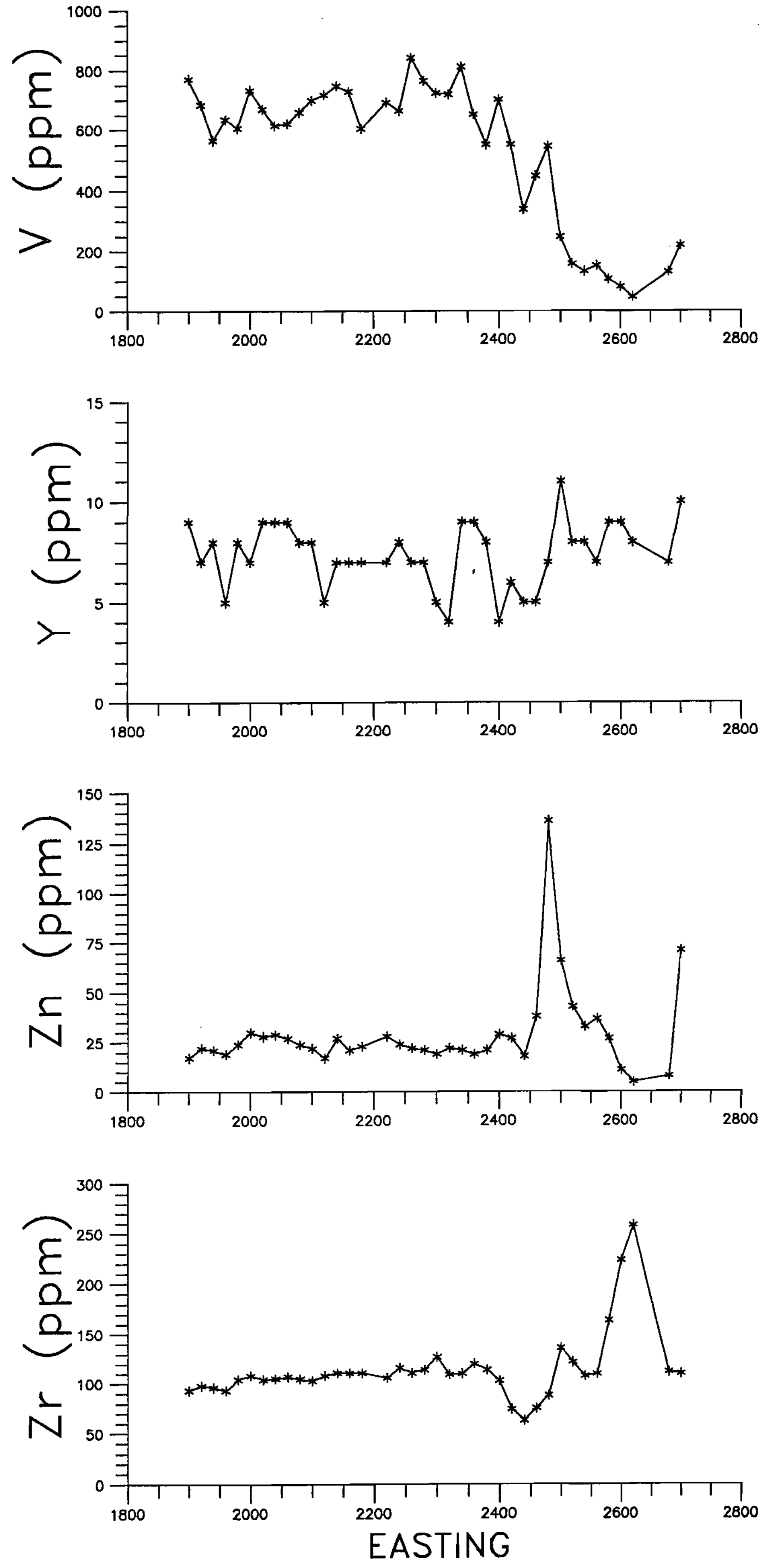
V (ppm)
1000
800
600
400
200
0
Y (ppm)
15
10
5
0
Zn (ppm)
150
125
100
75
50
25
0
Zr (ppm)
300
250
200
150
100
50
0
1800
2000
2200
2400
2600
2800
EASTING

EASTING				
FROM	TO	SAMPLE	Au (ppb)	As(ppm)
2232	2234	91564	20	250
2238	2240	91568	20	210
2242	2244	91570	10	260
2246	2248	91572	9	260
2250	2252	91574	2	260
2252	2254	91575	5	240
2256	2258	91578	10	200
2260	2262	91580	8	240
2264	2266	91582	20	230
2268	2270	91584	2	250
2272	2274	91586	2	250
2276	2278	91588	2	260
2280	2282	91590	2	270
2284	2286	91592	5	390
2288	2290	91594	2	340
2292	2294	91596	2	270
2296	2298	91598	2	230
2300	2302	91600	2	250
2302	2304	91601	2	280
2306	2308	91604	7	390
2310	2312	91606	20	480
2314	2316	91608	7	530
2320	2322	91612	10	490
2324	2326	91614	30	620
2328	2330	91616	10	650
2332	2334	91618	20	260
2336	2338	91620	30	280
2340	2342	91622	20	210
2344	2346	91624	30	190
2346	2348	91625	30	150
2350	2352	91628	60	160
2354	2356	91630	80	110
2358	2360	91632	70	260
2362	2364	91634	40	310
2366	2368	91636	40	210
2370	2372	91638	60	200
2374	2376	91640	70	250
2378	2380	91642	110	250
2382	2384	91644	60	250
2386	2388	91646	20	180
2390	2392	91648	70	220
2394	2396	91650	80	180
2400	2402	42350	20	80
2402	2404	42351	40	95
2404	2406	42352	20	130
2406	2408	42353	10	130
2408	2410	42354	170	120
2410	2412	42355	10	190
2412	2414	42356	10	75
2414	2416	42357	10	70
2416	2418	42358	10	110
2418	2420	42359	60	85
2420	2422	42360	20	60
2422	2424	42361	60	90
2424	2426	42362	10	65
2426	2428	42363	80	50
2428	2430	42364	910	100
2430	2432	42365	20	55
2432	2434	42366	10	90
2434	2436	42367	60	75
2436	2438	42368	40	95
2438	2440	42369	10	90
2440	2442	42370	20	60
2442	2444	42371	40	90
2444	2446	42372	80	140
2446	2448	42373	20	130
2448	2450	42374	80	35
2450	2452	42375	20	65
2452	2454	42376	80	90
2454	2456	42377	10	65
2456	2458	42378	10	90
2458	2460	42379	20	75
2460	2462	42380	10	80
2462	2464	42381	40	65
2464	2466	42382	10	50
2466	2468	42383	10	50
2468	2470	42384	10	110
2470	2472	42385	10	130
2472	2474	42386	60	35
2474	2476	42387	60	40
2476	2478	42388	10	7
2478	2480	42389	10	50
2480	2482	42390	130	60
2482	2484	42391	60	55
2484	2486	42392	10	40
2486	2488	42393	10	80
2490	2492	42395	10	20
2494	2496	42397	10	4
2498	2500	42399	10	45
2502	2504	42401	10	100

Appendix 4: Tabulated data for the trench samples along 3700N (see Figure 13)

SAMPLE	SPECIES	EASTING	NORTHING	ASH (%)	Ca (%)	Fe (%)	Mg (%)	Na (%)	P (%)	Al	As	Au	Ba
04-2001	Atriplex sp.	3300	4200	22.4	3.08	0.13	1.12	29.00	0.36	2025	<7	0.018	65
04-2002	Atriplex sp.	3273	4200	17.7	4.76	0.18	1.32	24.89	0.32	2051	<6	0.002	65
04-2003	Atriplex sp.	3246	4200	26.6	2.90	0.06	1.86	25.66	0.35	741	5	0.012	19
04-2004	Melaleuca sp.	3219	4200	6.2	24.45	0.42	2.68	9.06	0.95	4720	15	0.132	42
04-2005	Halosarcia sp.	3192	4200	23.8	1.67	0.41	1.40	34.91	0.14	3725	<5	0.004	26
04-2006	Melaleuca sp.	3165	4200	7.2	15.83	0.57	2.86	12.47	0.48	5838	18	0.018	45
04-2007	Melaleuca sp.	3138	4200	6.4	24.66	0.51	2.82	7.01	0.76	5391	14	0.040	44
04-2008	Melaleuca sp.	3111	4200	8.0	24.80	0.35	1.27	7.37	0.38	4071	29	0.029	32
04-2009	Lawrencia sp.	3084	4200	14.3	8.00	2.43	2.03	4.56	0.38	23162	51	0.005	58
04-2010	Melaleuca sp.	3057	4200	5.7	19.24	0.49	2.78	13.44	0.67	6473	19	0.038	68
04-2011	Halosarcia sp.	3005	4200	29.7	1.34	0.19	1.62	33.06	0.15	2363	6	0.008	21
04-2012	Halosarcia sp.	2978	4200	26.1	0.95	0.18	0.84	40.61	0.09	2280	<5	<0.001	20
04-2013	Dodonaea sp.	2951	4200	3.4	8.88	0.29	3.92	1.91	3.90	3310	<6	0.185	116
04-2014	Atriplex sp.	2924	4200	17.0	4.18	0.15	1.90	33.39	0.57	1899	<5	<0.001	220
04-2015	Halosarcia sp.	2897	4200	40.9	1.75	0.18	1.38	23.27	0.16	2188	<4	<0.001	18
04-2016	Atriplex sp.	2870	4200	20.0	3.39	0.11	1.16	29.29	0.43	1367	<5	0.002	76
04-2017	Eremophila sp.	2843	4200	4.4	10.37	0.23	2.41	1.28	3.22	3558	<5	0.016	52
04-2018	Eremophila sp.	2816	4200	4.4	10.16	0.26	2.28	1.25	3.81	3649	7	0.008	45
04-2019	Atriplex sp.	2789	4200	21.8	3.14	0.09	1.31	26.48	0.33	1392	<4	0.015	74
04-2020	Eremophila sp.	2767	4200	4.7	10.94	0.20	1.65	0.68	5.04	2727	<6	0.009	38
04-2021	Atriplex sp.	2735	4200	18.5	3.31	0.12	1.23	25.87	0.21	1830	<5	0.003	53
04-2022	Atriplex sp.	2708	4200	20.3	3.66	0.13	1.23	23.00	0.26	2404	<4	0.004	57
04-2023	Eremophila sp.	2681	4200	5.0	8.37	0.21	1.36	0.38	1.51	3200	10	0.014	49
04-2024	Atriplex sp.	2654	4200	22.9	2.56	0.08	1.13	28.52	0.22	1352	<4	0.003	75
04-2025	Halosarcia sp.	2613	4200	33.7	0.78	0.15	0.60	35.04	0.18	1981	8	<0.001	18
04-2026	Eremophila sp.	2590	4200	4.5	12.85	0.26	1.75	1.71	2.08	3362	24	0.016	65
04-2027	Atriplex sp.	2558	4200	23.9	2.51	0.08	1.00	24.18	0.22	925	<4	<0.001	71
04-2028	Eremophila sp.	2536	4200	4.5	8.58	0.44	1.61	1.59	2.33	3893	18	0.023	83
04-2029	Eremophila sp.	2479	4200	4.5	9.18	0.25	2.12	1.27	2.13	2914	11	0.017	96
04-2030	Atriplex sp.	2447	4200	26.6	1.78	0.07	0.81	31.08	0.28	966	<5	0.001	41
04-2031	Eremophila sp.	2425	4200	4.3	15.76	0.26	2.05	0.92	2.54	2624	12	0.024	181
04-2032	Atriplex sp.	2393	4200	27.8	2.14	0.07	0.79	28.31	0.32	780	<5	<0.001	51
04-2033	Eremophila sp.	2366	4200	4.5	13.41	0.37	2.43	0.94	1.42	2900	11	<0.001	96
04-2034	Atriplex sp.	2339	4200	20.8	3.18	0.08	1.41	28.39	0.24	1077	<5	<0.001	45
04-2035	Eremophila sp.	2307	4200	4.2	10.14	0.20	2.61	0.47	3.29	1600	<7	0.002	64
04-2036	Atriplex sp.	2285	4200	22.7	2.20	0.06	1.20	36.36	0.36	726	<5	<0.001	52
04-2037	Eremophila sp.	2253	4200	4.1	12.12	0.46	2.47	1.10	2.66	5315	<7	0.014	104
04-2038	Atriplex sp.	2226	4200	26.2	2.51	0.08	0.73	36.04	0.20	1113	<5	<0.001	59
04-2039	Eremophila sp.	2200	4200	3.9	9.08	0.21	1.87	0.98	2.40	2796	<8	0.024	58
04-2040	Eucalyptus sp.	1925	3700	4.5	13.03	0.24	2.84	8.34	1.90	1481	<7	<0.001	295
04-2041	Eremophila sp.	1940	3700	4.7	8.03	0.15	1.53	0.72	1.45	1077	<6	0.005	57
04-2042	Eucalyptus sp.	1950	3700	5.8	10.75	0.16	2.35	9.06	1.28	1201	<7	<0.001	216
04-2043	Eremophila sp.	1980	3700	4.5	11.39	0.23	2.65	0.46	1.34	2083	<9	0.007	31
04-2044	Eucalyptus sp.	2000	3700	5.0	14.42	0.18	2.57	8.20	1.88	1418	6	0.003	274
04-2045	Eremophila sp.	2010	3700	4.4	9.84	0.18	1.76	0.76	1.55	1667	9	<0.001	42
04-2046	Eremophila sp.	2038	3700	4.0	8.46	0.22	1.18	0.68	1.56	2166	<8	<0.001	40
04-2047	Eucalyptus sp.	2060	3700	3.1	9.38	0.31	3.32	12.89	2.35	2763	<13	<0.001	238
04-2048	Eremophila sp.	2075	3700	4.4	11.52	0.34	2.52	0.91	1.32	3152	<9	<0.001	51
04-2049	Eucalyptus sp.	2100	3700	5.2	11.00	0.21	2.07	6.76	1.65	1367	<6	<0.001	147
04-2050	Eremophila sp.	2133	3700	4.9	15.80	0.20	2.97	0.82	1.39	1846	<8	<0.001	48
04-2051	Eucalyptus sp.	2150	3700	5.0	14.57	0.23	2.17	8.04	1.37	1924	10	<0.001	235
04-2052	Eremophila sp.	2175	3700	4.9	13.87	0.17	2.48	0.38	2.59	1509	<8	<0.001	60
04-2053	Eucalyptus sp.	2220	3700	4.2	18.79	0.35	2.20	6.19	1.63	3079	12	0.003	304
04-2054	Eremophila sp.	2250	3700	4.7	11.33	0.34	2.09	0.89	1.45	4079	6	0.029	62
04-2055	Eremophila sp.	2275	3700	4.2	11.19	0.28	1.93	1.26	1.61	3679	9	0.011	53
04-2056	Eucalyptus sp.	2308	3700	4.8	15.31	0.27	2.71	9.58	1.20	3108	<6	0.003	465
04-2057	Eucalyptus sp.	2330	3700	5.0	14.29	0.31	2.29	10.92	1.03	2682	8	0.002	334
04-2058	Eremophila sp.	2345	3700	4.7	13.62	0.25	1.85	0.65	1.08	2394	6	0.009	60
04-2059	Eucalyptus sp.	2375	3700	4.8	10.51	0.32	2.90	9.33	1.46	2253	8	0.007	173
04-2060	Eremophila sp.	2400	3700	5.2	10.45	0.22	1.61	0.90	1.36	2224	12	0.016	59
04-2061	Eucalyptus sp.	2425	3700	3.9	12.01	0.38	3.16	11.20	1.18	3069	5	0.001	228
04-2062	Eremophila sp.	2450	3700	5.1	12.98	0.26	1.91	0.59	1.34	2676	12	0.049	53
04-2063	Eremophila sp.	2475	3700	4.4	16.77	0.24	2.99	1.25	1.47	2371	14	0.059	53
04-2064	Eremophila sp.	2500	3700	5.3	18.87	0.25	1.74	1.13	2.61	3634	11	0.007	68
04-2065	Atriplex sp.	2520	3700	16.2	3.80	0.14	1.27	24.70	0.33	1613	<4	<0.001	65
04-2066	Melaleuca sp.	2550	3700	7.1	31.49	0.33	2.77	3.91	0.96	3707	10	0.012	58
04-2067	Melaleuca sp.	2575	3700	8.5	22.36	0.18	1.79	4.75	0.52	1998	8	0.009	35
04-2068	Halosarcia sp.	2600	3700	31.3	2.21	0.11	1.46	32.26	0.13	1096	<3	<0.001	12
04-2069	Halosarcia sp.	2625	3700	24.8	2.04	0.23	1.80	31.42	0.12	2094	<4	0.003	29
04-2070	Halosarcia sp.	2650	3700	19.2	0.94	0.23	1.27	32.50	0.16	2967	6	<0.001	29
04-2071	Eucalyptus sp.	2680	3700	4.6	12.91	0.31	3.18	9.73	1.02	1913	11	0.009	277
04-2072	Eremophila sp.	2700	3700	4.4	12.16	0.27	1.96	0.77	1.40	2418	18	<0.001	49
04-2073	Eucalyptus sp.	2725	3700	5.0	11.11	0.39	2.18	12.69	1.19	3955	12	0.014	244
04-2074	Eremophila sp.	2750	3700	4.6	10.65	0.46	1.74	1.07	1.40	4906	15	0.027	50
04-2075	Eucalyptus sp.	2775	3700	4.7	12.08	0.38	2.70	9.10	1.66	2830	6	0.006	121
04-2076	Eremophila sp.	2805	3700	4.9	13.63	0.24	1.71	1.09	1.42	2291	16	0.010	38
04-2077	Eucalyptus sp.	2820	3700	4.0	13.63	0.48	2.73	14.04	0.86	4179	10	0.031	217
04-2078	Eremophila sp.	2850	3700	4.4	8.76	0.23	2.03	0.43	1.48	2210	<7	0.002	64
04-2079	Eucalyptus sp.	2875	3700	5.0	12.07	0.35	1.45	10.94	1.05	2790	<6	0.017	234
04-2080	Eremophila sp.	2905	3700	4.4	15.08	0.24	2.01	0.61	1.40	2148	<7	0.017	84
04-2081	Eremophila sp.	2925	3700	4.9	14.38	0.38	1.51	0.72	2.57	2486	6	0.009	47
04-2082	Eucalyptus sp.	2940	3700	3.8	13.61	0.25	2.92	11.14	1.38	2751	11	0.042	345
04-2083	Atriplex sp.	2975	3700	5.7	19.38	0.40	6.99	0.71	0.96	4208	7	0.019	761
04-2084	Eremophila sp.	3000	3700	4.5	14.03	0.28	1.71	0.67	1.21	2841	9	0.003	38
04-2130	Eucalyptus sp.	2280	3775	5.6	20.70	0.31	2.16	5.52	0.92	2779	<5	0.009	194
04-2131	Eremophila sp.	2280	3775	4.8	12.77	0.42	2.17	0.77	2.21	4167	8	0.026	42
04-2132	Eucalyptus sp.	2300	3792	4.4	12.22	0.37	2.89	8.69	0.99	3255	14	0.018	191
04-2133	Eremophila sp.	2300	3792	5.6	6.09	0.17	1.21	0.35	1.53	1850	5	<0.001	33
04-2135	Eremophila sp.	2410	3840	4.6	6.99	0.26	1.51	0.55	1.39	4008	17	0.015	67
04-2137	Eremophila sp.	2408	3770	3.9	16.27	0.53	3.39	1.54	1.46	5492	15	0.037	50
04-2138	Eucalyptus sp.	2375	3725	4.5	7.73	0.28	2.32	14.08	0.99	2453	11	0.003	121
04-2139	Eremophila sp.	2375	3725	5.2	11.73	0.24	1.68	0.64	1.38	2506	10	0.015	38
04-2140	Eucalyptus sp.	2250	4925	4.7	13.93	0.42	2.10	10.61	1.19	3145	<6	0.009	175
04-2141	Eremophila sp.	2250	4925	5.2	14.78	0.75	1.51	1.03	1.61	6781	8	0.033	68
04-2142	Eucalyptus sp.	2350	4900	5.0	13.81	0.43	2.72	13.28	0.99	2664	<6	0.015	167
04-2143	Eremophila sp.	2350	4900	5.8	18.11	0.56	2.33	0.39	1.70	4016	12	0.039	81

Appendix 5: Tabulated and graphed data for the vegetation samples.

SAMPLE	SPECIES	Be	Br	Co	Cr	Cu	Mn	Ni	Sb	Si	Ti	V	Zr
04-2001	Atriplex sp.	<1	1662	<1	20	57	476	6	<1	247	103	6	<1
04-2002	Atriplex sp.	<1	1749	<1	21	69	418	5	<1	679	101	7	<1
04-2003	Atriplex sp.	<1	2010	<1	9	41	95	32	<1	129	26	3	<1
04-2004	Melaleuca sp.	<1	486	<1	67	108	652	42	<1	858	222	14	<1
04-2005	Halosarcia sp.	<1	453	<1	25	73	206	8	<1	252	272	16	<1
04-2006	Melaleuca sp.	<1	229	<1	65	191	1226	24	<1	817	247	13	<1
04-2007	Melaleuca sp.	<1	192	<1	78	157	397	23	<1	578	189	17	<1
04-2008	Melaleuca sp.	<1	163	<1	46	98	257	14	<1	459	145	12	<1
04-2009	Lawrencia sp.	<1	137	<1	257	153	297	80	1	255	542	83	<1
04-2010	Melaleuca sp.	<1	391	<1	54	185	379	25	<2	1053	305	16	<1
04-2011	Halosarcia sp.	<1	539	<1	17	46	171	12	<1	97	185	7	<1
04-2012	Halosarcia sp.	<1	281	<1	20	88	861	14	<1	103	191	7	<1
04-2013	Dodonaea sp.	<1	158	<1	35	317	751	<1	<1	1786	183	10	<1
04-2014	Atriplex sp.	<1	393	<1	17	73	363	<1	<1	166	96	6	<1
04-2015	Halosarcia sp.	<1	445	<1	23	47	120	8	<1	51	116	7	<1
04-2016	Atriplex sp.	<1	493	<1	17	40	285	<1	<1	390	73	4	<1
04-2017	Eremophila sp.	<1	574	<1	34	380	484	<1	<1	1530	145	11	<1
04-2018	Eremophila sp.	<1	708	<1	38	454	508	<1	<1	1249	157	10	<1
04-2019	Atriplex sp.	<1	476	<1	14	48	396	<1	1	272	53	4	<1
04-2020	Eremophila sp.	<1	850	<1	31	422	520	<1	13	1309	107	7	<1
04-2021	Atriplex sp.	<1	670	<1	15	45	298	<1	<1	308	70	5	<1
04-2022	Atriplex sp.	<1	851	<1	16	48	1103	<1	<1	219	87	6	<1
04-2023	Eremophila sp.	<1	897	<1	15	270	470	<1	<1	1134	108	0	<1
04-2024	Atriplex sp.	<1	676	<1	8	44	259	<1	<1	208	52	3	<1
04-2025	Halosarcia sp.	<1	573	<1	10	37	187	9	<1	242	141	6	<1
04-2026	Eremophila sp.	<1	796	5	39	436	774	55	<1	1700	106	9	3
04-2027	Atriplex sp.	<1	687	<1	11	25	169	7	<1	915	44	4	<1
04-2028	Eremophila sp.	<1	692	<1	49	376	768	42	<1	1506	159	11	1
04-2029	Eremophila sp.	<1	938	<1	33	486	667	42	<1	1241	114	8	<1
04-2030	Atriplex sp.	<1	843	<1	9	40	201	4	<1	477	39	2	<1
04-2031	Eremophila sp.	<1	537	<1	41	328	1134	13	<1	2661	105	6	<1
04-2032	Atriplex sp.	<1	994	<1	11	28	364	11	<1	855	30	3	<1
04-2033	Eremophila sp.	<1	813	1	46	281	578	28	<1	2743	100	7	<1
04-2034	Atriplex sp.	<1	657	<1	13	27	181	9	<1	733	44	3	1
04-2035	Eremophila sp.	<1	1124	<1	36	331	502	33	<1	5628	72	3	<1
04-2036	Atriplex sp.	<1	611	<1	9	30	216	6	<1	276	33	2	<1
04-2037	Eremophila sp.	<1	722	<1	70	379	466	33	<1	1497	180	11	<1
04-2038	Atriplex sp.	<1	1077	<1	13	34	261	3	<1	263	46	3	<1
04-2039	Eremophila sp.	<1	767	<1	35	325	515	34	<1	1709	106	5	<1
04-2040	Eucalyptus sp.	<1	437	4	77	131	416	65	<1	1449	73	5	6
04-2041	Eremophila sp.	<1	1227	<1	34	500	278	6	<1	1286	67	3	<1
04-2042	Eucalyptus sp.	<1	432	4	64	132	260	68	<1	1260	60	4	6
04-2043	Eremophila sp.	<1	1481	<1	44	310	505	26	<1	3292	112	5	<1
04-2044	Eucalyptus sp.	<1	567	<1	53	112	485	52	<1	1180	68	2	<1
04-2045	Eremophila sp.	<1	976	<1	42	376	294	19	<1	4040	85	3	2
04-2046	Eremophila sp.	<1	1167	2	58	412	462	36	<1	2060	101	5	<1
04-2047	Eucalyptus sp.	<1	1254	<1	78	234	536	96	2	1907	163	7	6
04-2048	Eremophila sp.	<1	1678	<1	54	603	562	39	<1	1805	139	10	<1
04-2049	Eucalyptus sp.	<1	499	<1	68	149	328	56	<1	1694	73	4	<1
04-2050	Eremophila sp.	<1	1585	<1	36	360	412	29	8	2642	64	4	<1
04-2051	Eucalyptus sp.	<1	493	5	62	107	640	81	<1	2248	91	6	4
04-2052	Eremophila sp.	<1	1400	<1	39	383	864	58	<1	1155	49	4	<1
04-2053	Eucalyptus sp.	<1	602	5	104	129	1023	89	<1	1628	146	8	2
04-2054	Eremophila sp.	<1	741	<1	55	444	356	52	<1	1279	201	8	<1
04-2055	Eremophila sp.	<1	919	<1	42	306	555	45	<1	1184	150	6	<1
04-2056	Eucalyptus sp.	3	422	<1	42	137	631	39	<1	1523	145	7	<1
04-2057	Eucalyptus sp.	2	344	<1	65	210	443	50	<1	1599	139	8	<1
04-2058	Eremophila sp.	<1	1117	<1	48	256	246	54	<1	1858	102	7	<1
04-2059	Eucalyptus sp.	<1	316	<1	106	163	1372	81	<1	1352	100	7	<1
04-2060	Eremophila sp.	<1	812	<1	42	402	661	36	<1	1322	105	6	<1
04-2061	Eucalyptus sp.	<1	439	<1	97	154	1277	60	<1	2962	148	7	2
04-2062	Eremophila sp.	<1	691	<1	44	390	618	43	<1	1574	109	7	<1
04-2063	Eremophila sp.	3	745	<1	42	170	211	57	<1	1940	186	6	1
04-2064	Eremophila sp.	2	221	<1	53	599	572	46	<1	1677	79	7	<1
04-2065	Atriplex sp.	1	159	<1	17	44	308	15	<1	594	96	6	2
04-2066	Melaleuca sp.	<1	99	2	54	73	822	55	<1	1112	157	12	2
04-2067	Melaleuca sp.	<1	98	3	32	52	324	55	<1	700	75	6	4
04-2068	Halosarcia sp.	1	218	<1	14	35	113	13	<1	318	83	4	<1
04-2069	Halosarcia sp.	1	179	<1	21	36	178	14	<1	1427	165	7	<1
04-2070	Halosarcia sp.	1	179	<1	24	67	1100	35	<1	285	266	10	<1
04-2071	Eucalyptus sp.	4	322	<1	83	86	1398	67	<1	1732	108	6	<1
04-2072	Eremophila sp.	5	711	<1	44	257	322	42	<1	3721	109	7	<1
04-2073	Eucalyptus sp.	3	291	<1	59	145	648	66	<1	1507	191	11	1
04-2074	Eremophila sp.	2	608	3	56	221	360	68	<1	1367	232	13	3
04-2075	Eucalyptus sp.	<1	391	<1	103	168	570	55	<1	1669	137	7	3
04-2076	Eremophila sp.	<1	699	10	42	253	381	44	<1	1674	82	7	7
04-2077	Eucalyptus sp.	<1	416	1	100	96	583	90	<1	1843	212	11	3
04-2078	Eremophila sp.	<1	726	6	50	210	404	39	<1	5031	110	6	<1
04-2079	Eucalyptus sp.	<1	374	11	96	141	569	67	<1	1221	154	6	2
04-2080	Eremophila sp.	<1	827	7	38	461	689	27	<1	1624	99	3	<1
04-2081	Eremophila sp.	<1	913	6	97	524	854	111	<1	1772	121	8	3
04-2082	Eucalyptus sp.	<1	656	5	64	104	998	75	<1	1734	148	5	4
04-2083	Atriplex sp.	<1	443	<1	79	81	487	53	<1	2394	289	10	9
04-2084	Eremophila sp.	<1	924	13	45	378	664	54	<1	1320	123	6	<1
04-2130	Eucalyptus sp.	<1	302	8	65	113	428	67	1	1100	108	6	<1
04-2131	Eremophila sp.	<1	778	2	58	417	625	41	<1	1152	189	9	<1
04-2132	Eucalyptus sp.	<1	467	3	85	145	649	59	17	1580	160	9	4
04-2133	Eremophila sp.	<1	539	<1	27	448	561	31	<1	2916	118	5	<1
04-2135	Eremophila sp.	<1	761	7	39	383	346	44	<1	1488	198	7	<1
04-2137	Eremophila sp.	<1	406	5	70	290	520	43	9	1656	434	15	1
04-2138	Eucalyptus sp.	1	411	7	38	196	2826	66	17	1847	192	7	2
04-2139	Eremophila sp.	<1	1005	3	38	241	937	29	<1	1214	130	8	1
04-2140	Eucalyptus sp.	<1	452	9	123	205	500	100	12	1782	247	10	2
04-2141	Eremophila sp.	<1	872	14	128	376	651	87	<1	1482	362	19	2
04-2142	Eucalyptus sp.	<1	419	<1	103	130	586	92	<1	1049	202	4	<1
04-2143	Eremophila sp.	<1	1107	<1	78	278	531	60	8	520	125	9	<1

Appendix 5 (continued): Tabulated and graphed data for the vegetation samples.

5. Vegetation sample data: Graphed data for 3700N.

ooooo	Eucalyptus spp.
*****	Eremophila spp.
Me	Melaleuca spp.
Ha	Halosarcia spp.
At	Atriplex spp.

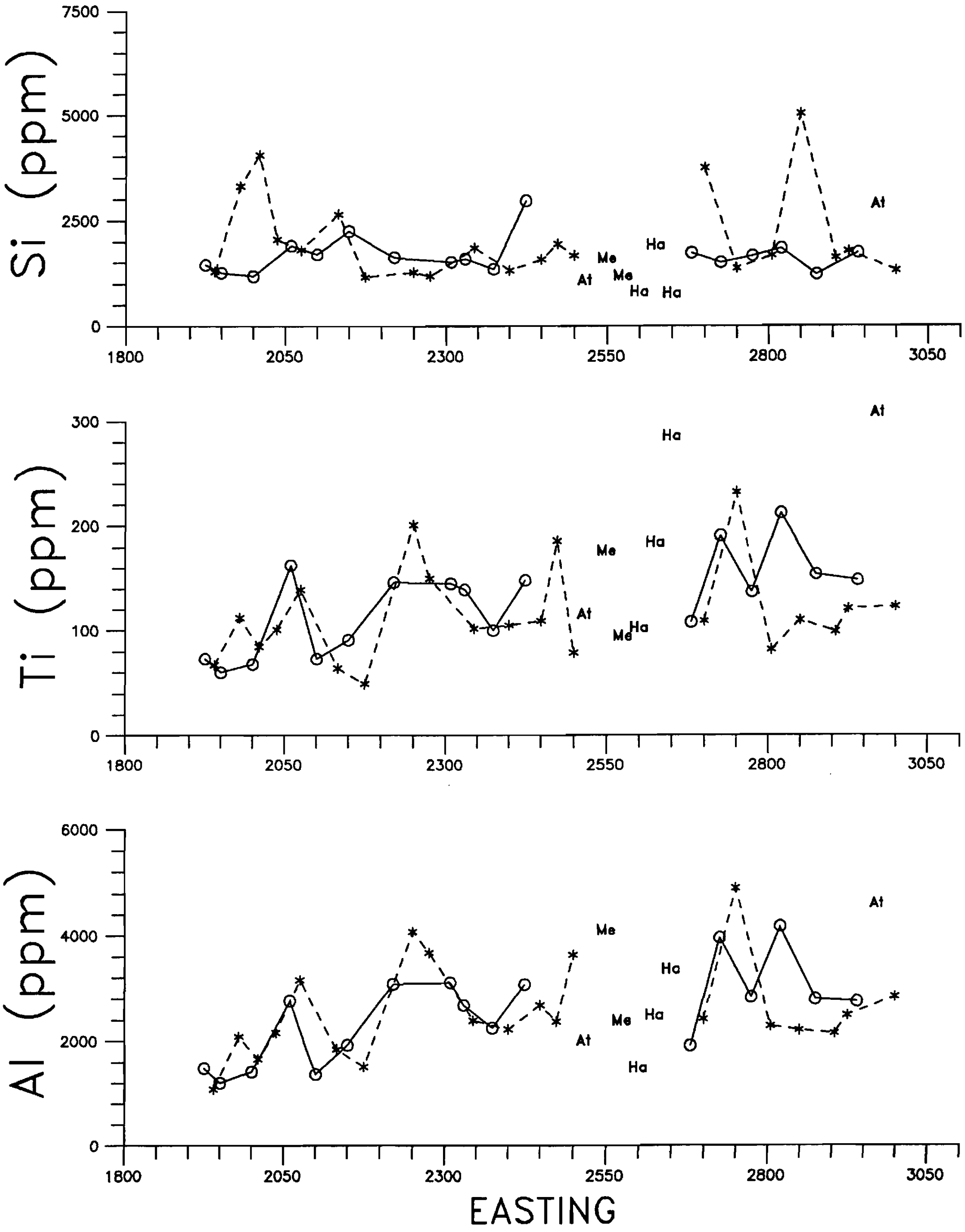

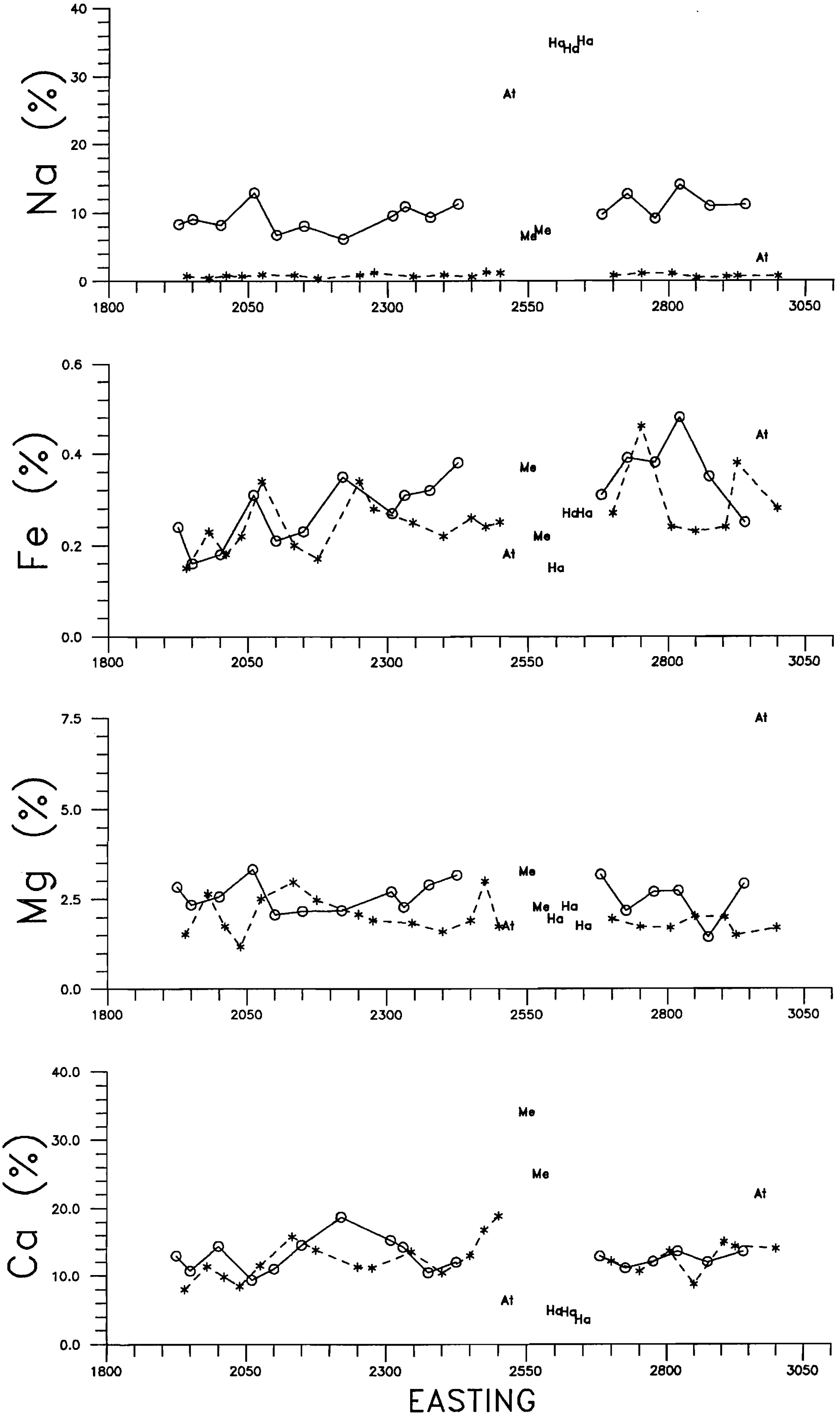
Na (%)
40
30
20
10
0
HaHdHa
At
MeMe
At
1800
2050
2300
2550
2800
3050
Fe (%)
0.6
0.4
0.2
0.0
At
Me
HdHa
Me
At
Ha
1800
2050
2300
2550
2800
3050
Mg (%)
7.5
5.0
2.5
0.0
At
Me
Me Ha
Ha
Ha
At
1800
2050
2300
2550
2800
3050
Ca (%)
40.0
30.0
20.0
10.0
0.0
Me
Me
At
At
HaHaHa
1800
2050
2300
2550
2800
3050
EASTING

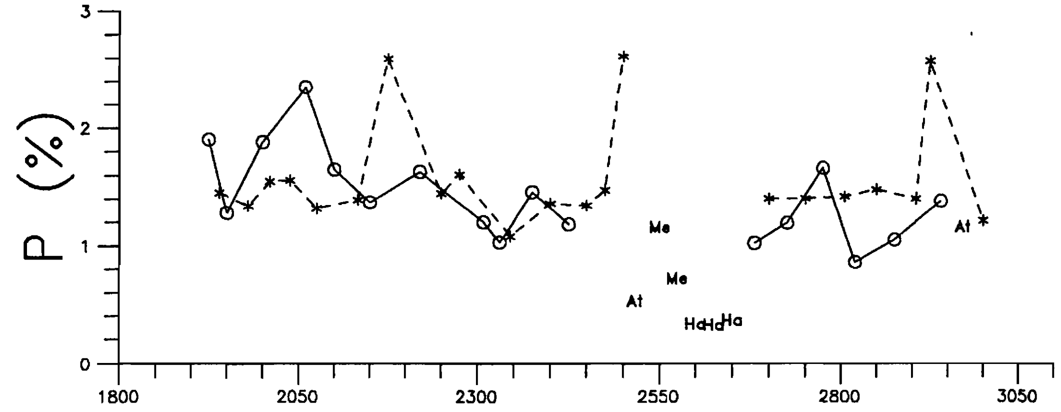
P (%)
3
2
1
0
Me
Me
At
HaHaHa
At
1800
2050
2300
2550
2800
3050

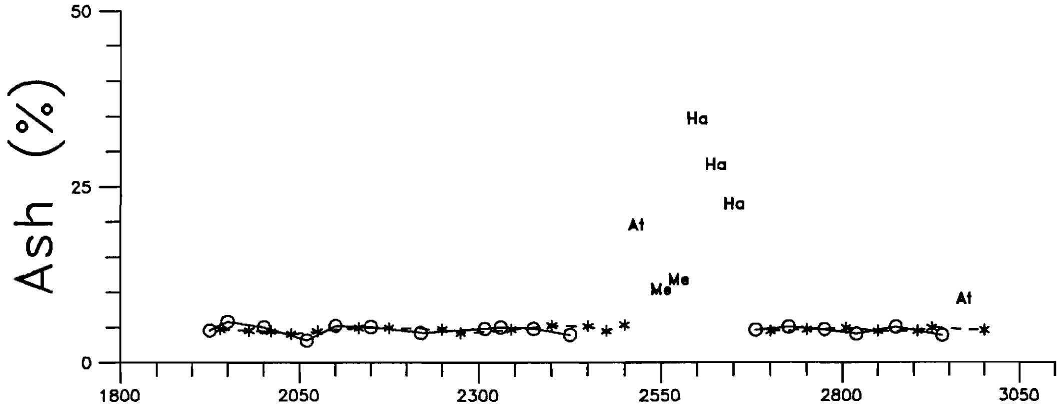
Ash (%)
50
25
0
Ha
Ha
Ha
At
MeMeMe
At
1800
2050
2300
2550
2800
3050

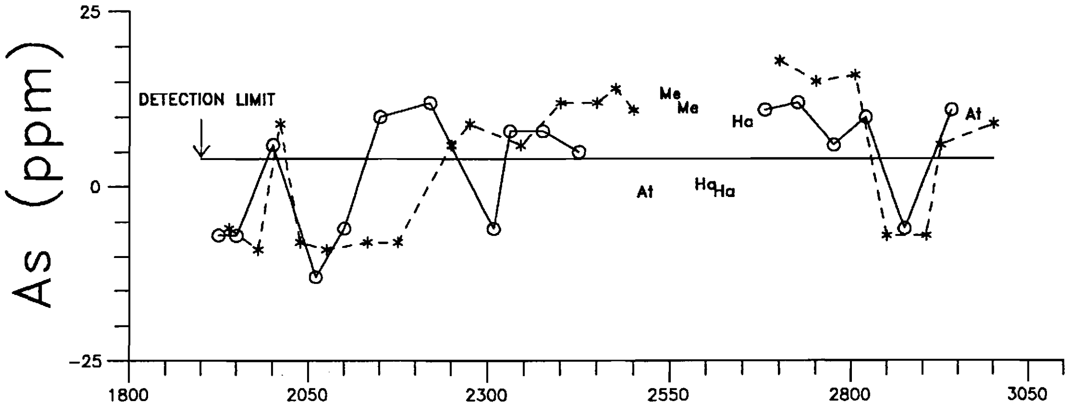
As (ppm)
25
0
-25
DETECTION LIMIT
MeMe
Ha
At
HaHa
At
1800
2050
2300
2550
2800
3050

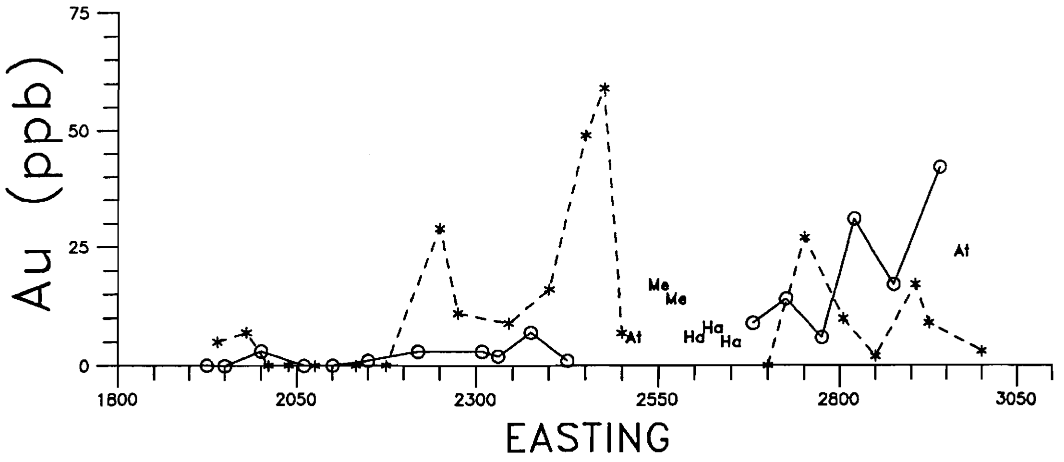
Au (ppb)
75
50
25
0
MeMe
At
HaHaHa
At
1800
2050
2300
2550
2800
3050
EASTING

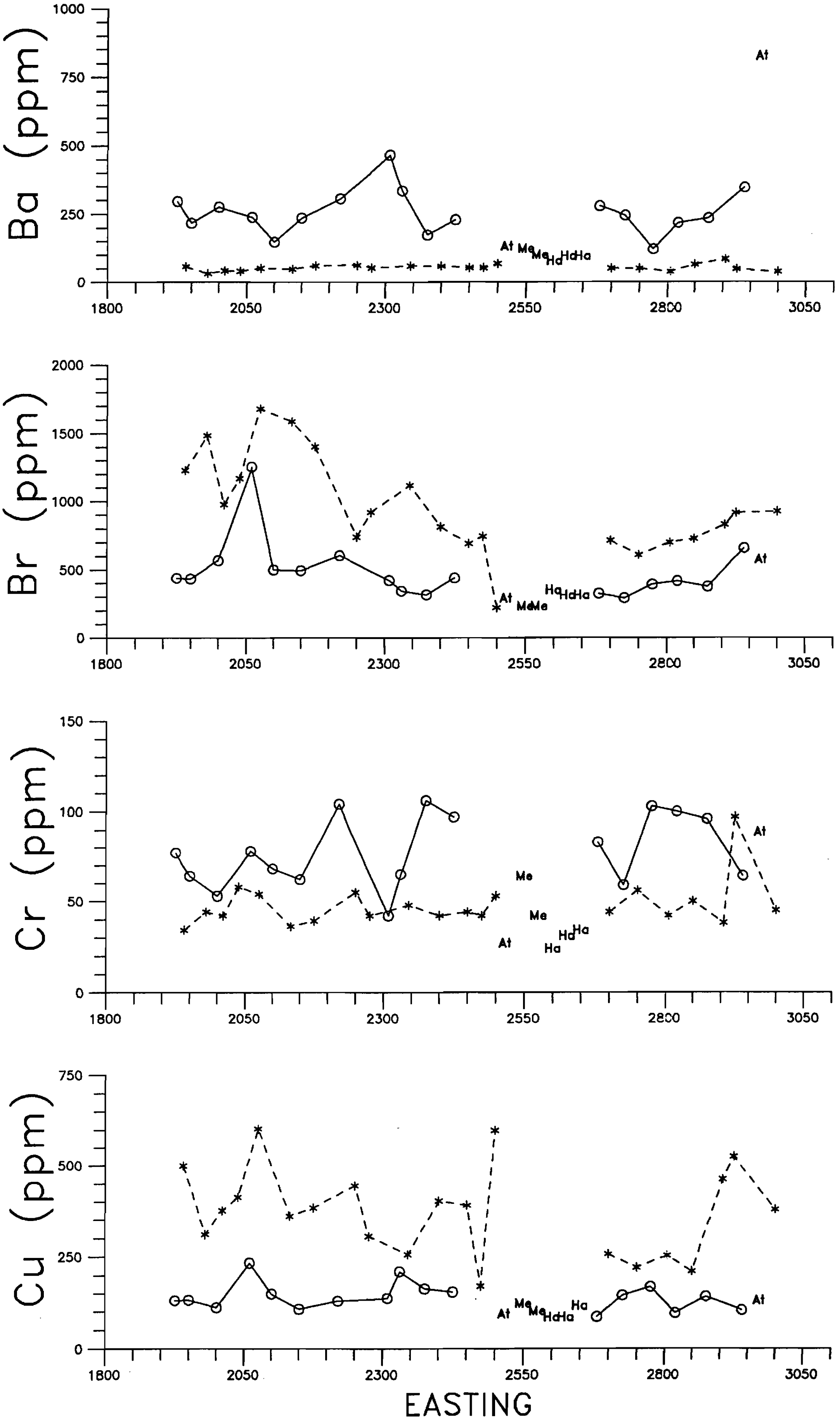
Ba (ppm)
1000
750
500
250
0
At
At Me Me Ha Ha Ha
1800
2050
2300
2550
2800
3050
Br (ppm)
2000
1500
1000
500
0
At
At MeMe
HaHaHa
1800
2050
2300
2550
2800
3050
Cr (ppm)
150
100
50
0
At
Me
Me
Ha Ha
At
Ha
1800
2050
2300
2550
2800
3050
Cu (ppm)
750
500
250
0
At Me Me Ha Ha Ha
At
1800
2050
2300
2550
2800
3050
EASTING

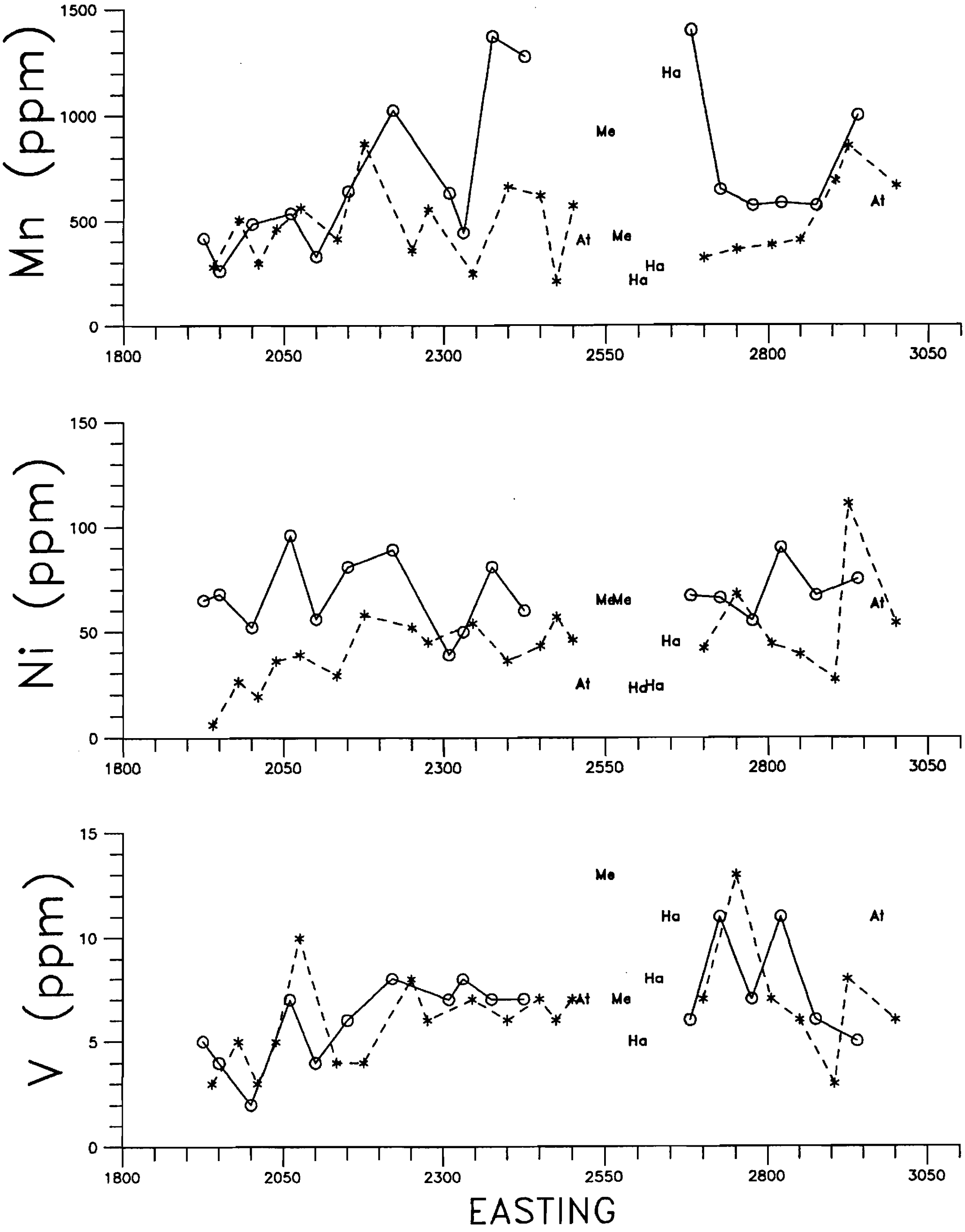
Mn (ppm)
1500
1000
500
0
Ha
Me
At
Me
Ha
Ha
At
Ni (ppm)
150
100
50
0
MeMe
Ha
At
HaHa
At
V (ppm)
15
10
5
0
Me
Ha
At
Ha
At
Me
Ha
1800
2050
2300
2550
2800
3050
EASTING

5. Vegetation sample data: Graphed data for 4200N.

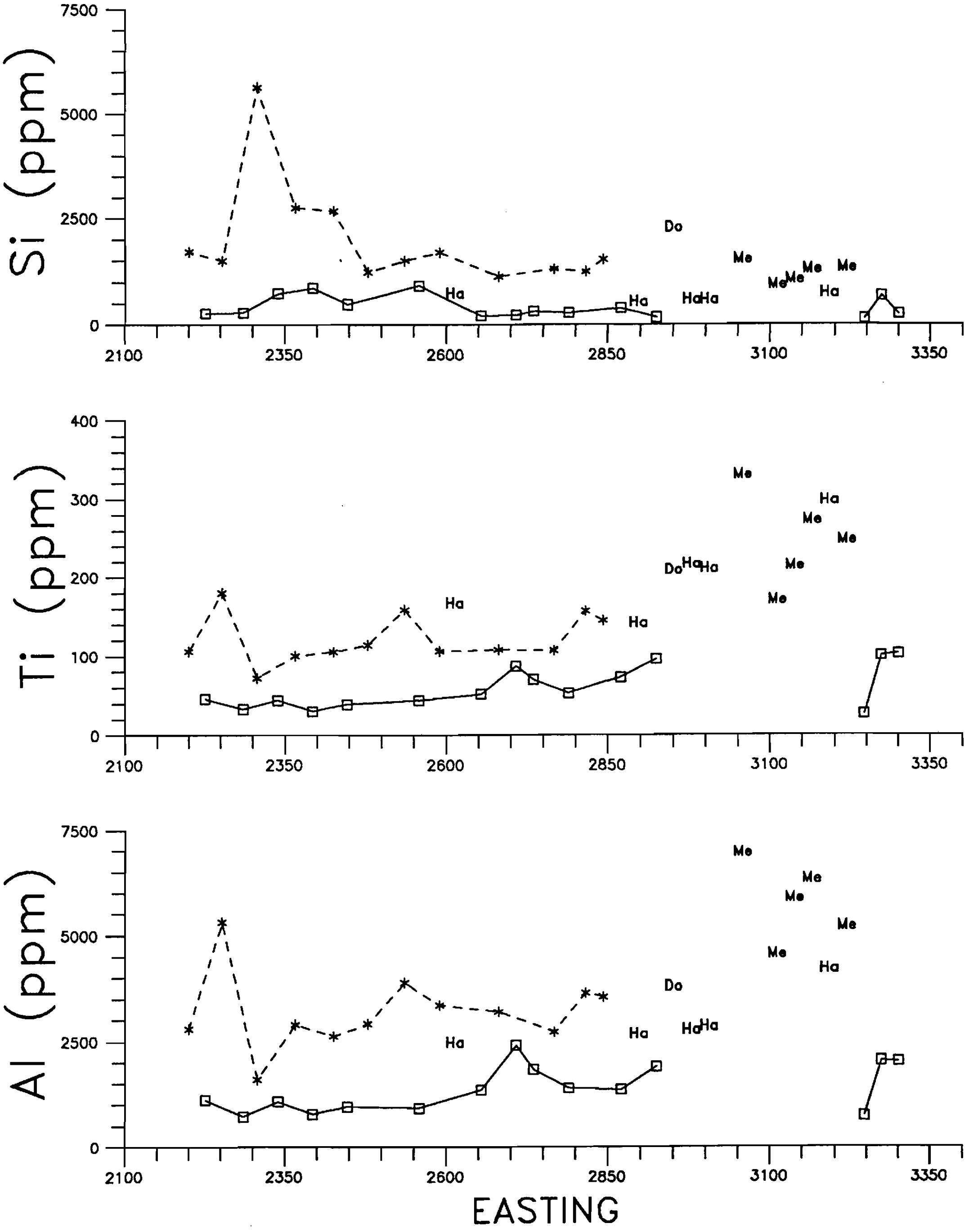

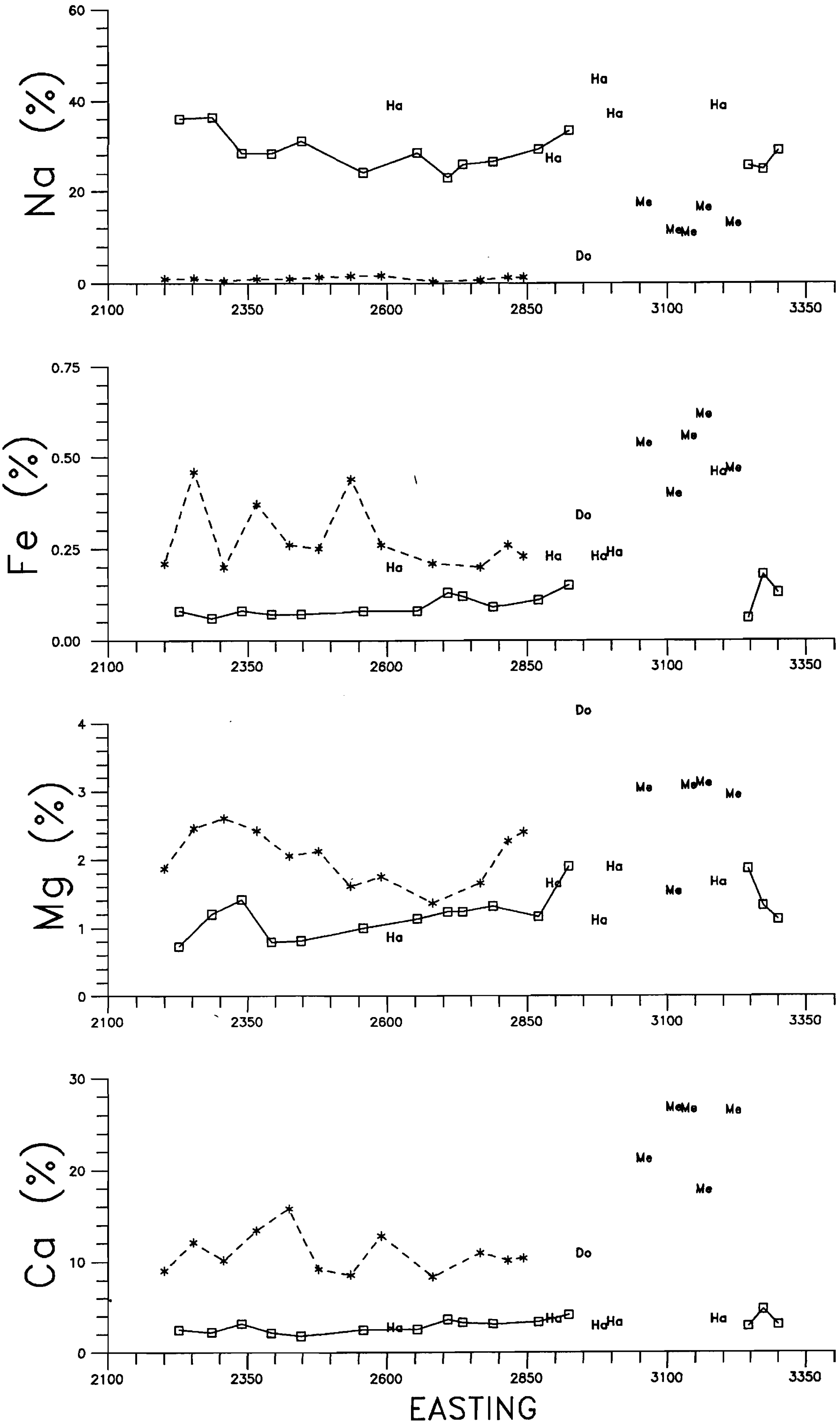
Na (%)
60
40
20
0
Fe (%)
0.75
0.50
0.25
0.00
Mg (%)
4
3
2
1
0
Ca (%)
30
20
10
0
2100
2350
2600
2850
3100
3350
Ha
Me
Do
EASTING

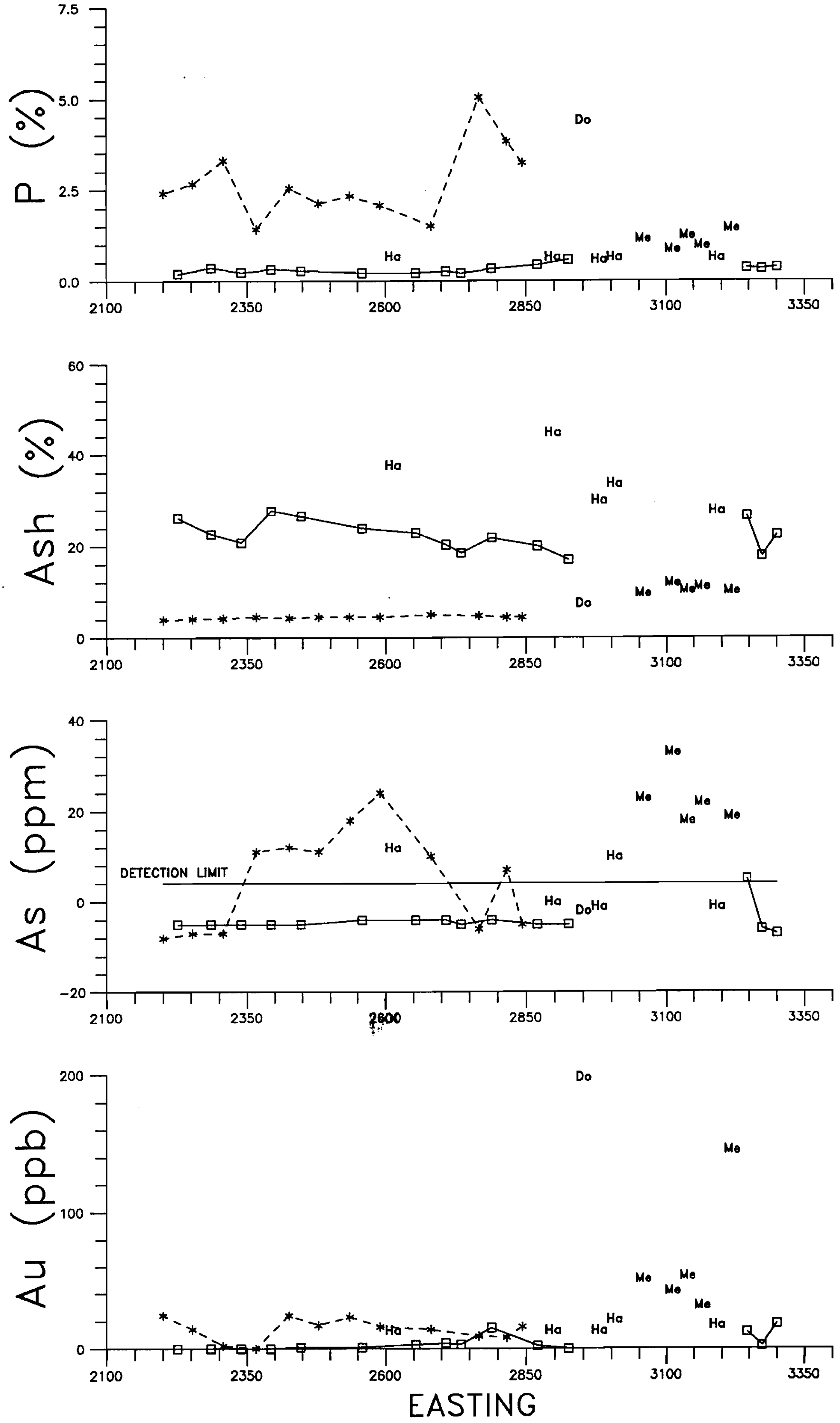
P (%)
7.5
5.0
2.5
0.0
Do
Me
Ha
Ash (%)
60
40
20
0
As (ppm)
40
20
0
-20
DETECTION LIMIT
Au (ppb)
200
100
0
2100
2350
2600
2850
3100
3350
EASTING

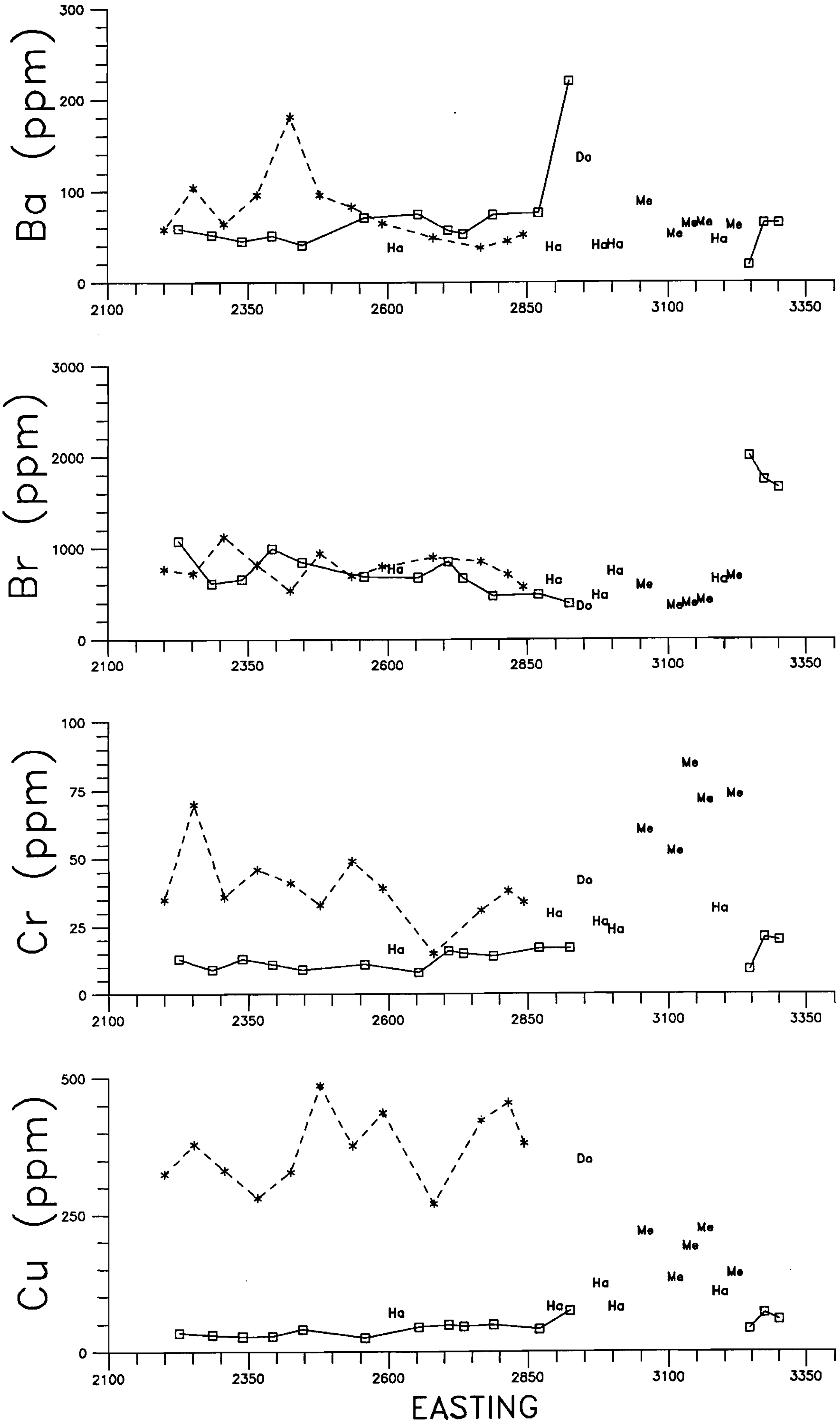
Ba (ppm)
300
200
100
0
Do
Me
Me
MeMe
Me
Ha
Ha
HaHa
Ha
Br (ppm)
3000
2000
1000
0
Ha
Ha
Ha
Ha
Ha
Me
MeMeMe
Do
Cr (ppm)
100
75
50
25
0
Me
Me
Me
Me
Me
Do
Ha
Ha
HaHa
Ha
Cu (ppm)
500
250
0
Do
Me
Me
Me
Me
Me
Ha
Ha
Ha
Ha
Ha
2100
2350
2600
2850
3100
3350
EASTING

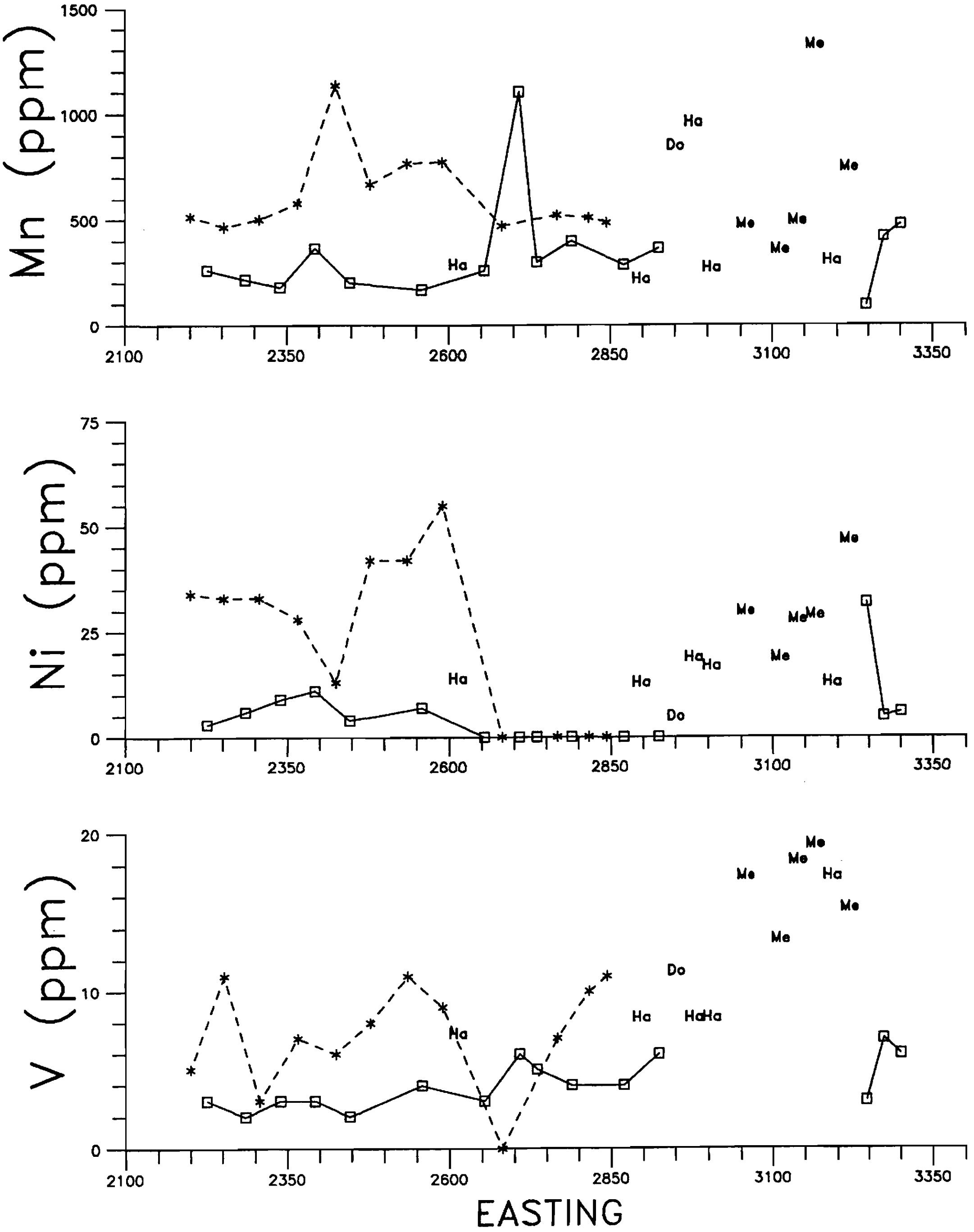
Mn (ppm)
1500
1000
500
0
Ni (ppm)
75
50
25
0
V (ppm)
20
10
0
2100
2350
2600
2850
3100
3350
EASTING
Ha
Do
Me

SAMPLE	TYPE	SiO2	Al2O3	Fe2O3	MgO	CaO	Na2O	TiO2	P2O5	Au(ppm)
04-2112	Whole	27.30	9.40	43.80	0.40	2.63	<0.01	0.38	<0.01	0.099
04-2129	Whole	36.60	11.29	36.50	0.44	2.06	0.22	0.66	<0.01	0.267
04-2150	Carbonate	11.44	2.17	1.15	3.85	39.48	<0.01	0.13	0.03	0.062
04-2151	White saprolite	60.30	16.72	0.65	0.68	6.72	0.05	0.90	0.03	<0.002
04-2152	Red saprolite	43.70	12.30	32.37	0.16	0.15	0.13	0.75	<0.01	<0.002
04-2153	Carbonate	11.70	2.21	2.09	2.86	36.81	<0.01	0.12	0.08	0.157
04-2154	Carbonate	18.90	3.37	4.67	3.38	32.12	<0.01	0.20	0.06	0.210
04-2155	Red saprolite	36.97	12.93	36.66	0.48	0.37	0.11	0.70	<0.01	0.002
04-2156	Carbonate	18.57	3.24	3.63	3.42	33.22	0.15	0.20	0.06	0.173
04-2157	Carbonate	17.81	3.37	2.94	3.46	33.13	0.15	0.19	0.02	0.199
04-2158	Red saprolite	34.55	12.63	37.91	0.50	0.41	0.10	0.69	<0.01	0.012

SAMPLE	TYPE	Ba	Be	Co	Cr	Cu	Mn	Ni	V	Zr
04-2112	Whole	1089	1	2	771	82	47	52	460	71
04-2129	Whole	686	<1	<1	417	39	120	28	579	111
04-2150	Carbonate	889	1	13	62	35	43	17	25	25
04-2151	White saprolite	55	2	13	42	26	3	47	32	99
04-2152	Red saprolite	9	<1	15	397	<5	38	37	413	128
04-2153	Carbonate	13385	<1	18	88	26	79	41	35	27
04-2154	Carbonate	1392	<1	13	163	42	139	51	73	51
04-2155	Red saprolite	207	<1	4	492	21	12	34	397	135
04-2156	Carbonate	4814	3	10	155	45	87	39	76	45
04-2157	Carbonate	4903	1	5	129	46	83	40	47	60
04-2158	Red saprolite	313	<1	7	592	24	21	39	458	132

SAMPLE	TYPE	S	Ce	Ga	Ge	Mo	Nb	Pb	Rb	Sr	Y	Zn
04-2112	Whole	0.06	9	19	4	4	2	4	18	64	8	28
04-2129	Whole	0.05	18	18	<1	2	3	6	1	69	5	54

Appendix 6: Tabulated data for the grab samples.

SAMPLE	DEPTH (m)	WEIGHT MINUS 0.2mm	WEIGHT PLUS 0.2mm	Au MINUS 0.2mm	Au PLUS 0.2mm	Au MINUS (mg)	Au PLUS (mg)
2113	0.025	386.3	104.3	31	3	11.98	0.31
2114	0.075	292.3	199.2	29	13	8.48	2.59
2115	0.125	302.2	193.2	18	1	5.44	0.19
2116	0.175	355.9	136.5	27	1	9.61	0.14
2117	0.250	403.1	87.7	47	2	18.95	0.18
2118	0.350	421.7	67.0	32	2	13.49	0.13
2119	0.450	400.6	85.6	52	10	20.83	0.86
2120	0.550	380.8	105.8	75	43	28.56	4.55
2121	0.650	350.1	136.5	76	31	26.61	4.23
2122	0.750	356.5	152.7	223	54	79.50	8.25
2123	0.850	406.9	86.2	160	73	65.10	6.29
2124	0.950	420.0	66.9	137	66	57.45	9.16
2125	1.100	206.2	289.9	123	15	35.66	4.35
2126	1.300	140.2	359.0	105	16	14.72	5.74
2127	1.500	286.3	199.6	39	28	11.17	5.59
2128	1.700	393.0	103.1	7	7	2.75	0.72

APPENDIX 7: Tabulated data for Profile C samples showing Au distribution analysis on two size fractions.